

1967

Numerical techniques applied to the investigation of the dynamic response of a four layer diode

Ronald John Schmitz
Iowa State University

Follow this and additional works at: <https://lib.dr.iastate.edu/rtd>

 Part of the [Electrical and Electronics Commons](#)

Recommended Citation

Schmitz, Ronald John, "Numerical techniques applied to the investigation of the dynamic response of a four layer diode " (1967).
Retrospective Theses and Dissertations. 3212.
<https://lib.dr.iastate.edu/rtd/3212>

This Dissertation is brought to you for free and open access by the Iowa State University Capstones, Theses and Dissertations at Iowa State University Digital Repository. It has been accepted for inclusion in Retrospective Theses and Dissertations by an authorized administrator of Iowa State University Digital Repository. For more information, please contact digirep@iastate.edu.

This dissertation has been
microfilmed exactly as received 68-5983

SCHMITZ, Ronald John; 1934-
NUMERICAL TECHNIQUES APPLIED TO THE
INVESTIGATION OF THE DYNAMIC RESPONSE
OF A FOUR LAYER DIODE.

Iowa State University, Ph.D., 1967
Engineering, electrical

University Microfilms, Inc., Ann Arbor, Michigan

NUMERICAL TECHNIQUES APPLIED TO
THE INVESTIGATION OF THE DYNAMIC RESPONSE
OF A FOUR LAYER DIODE

by

Ronald John Schmitz

A Dissertation Submitted to the
Graduate Faculty in Partial Fulfillment of
The Requirements for the Degree of
DOCTOR OF PHILOSOPHY

Major Subject: Electrical Engineering

Approved:

Signature was redacted for privacy.

In Charge of Major Work

Signature was redacted for privacy.

Head of Major Department

Signature was redacted for privacy.

Dean of Graduate College

Iowa State University
Of Science and Technology
Ames, Iowa

1967

TABLE OF CONTENTS

	Page
INTRODUCTION	1
Theory of Operation	1
Lateral Effects in Gated P-N-P-N Devices	8
Turn-On and Turn-Off Gain	10
Structures	10
Spread of "On" Region	14
DESCRIPTION OF THE PROPOSED MATHEMATICAL MODEL	15
Factors Effecting Gate Controlled Devices	15
Overall View of the Problem	17
Base Bias Calculations	26
Continuity Equation Solution	36
PERFORMANCE OF THE MATHEMATICAL MODEL	56
Comparison to Experimental Results	58
SUMMARY AND CONCLUSIONS	68
LITERATURE CITED	70
ACKNOWLEDGMENTS	72
APPENDIX A: DEFINITION OF COMPUTER PROGRAM VARIABLES	73
APPENDIX B: COMPUTER PROGRAM	79

INTRODUCTION

Active devices that possess inherent negative resistance hold an important place in the field of electronics. A device that has this characteristic will ordinarily have two stable states and will be able to be switched from one to the other. There has been a good deal of work done on a variety of two and three terminal p-n-p-n semiconductor devices that fall into the above category. The three terminal device that is controllable for both turn-on and turn-off by means of gate current I_g will be the type of device that is to be considered here. This type of device has various names such as thyristor, GTO (gate turn-off), and GCS (gate controlled switch) depending on the reference or manufacturer being considered. The purpose of this thesis will be to present a mathematical model, using numerical techniques to set up a computer solution, of the gate controllable device that will permit the exploration of the behavior of the device during the time of switching from one stable state to the other and that will allow exploration of the dependence of this behavior on the device geometry and fabrication. The computer model results will be compared to the actual behavior of a commercial device.

Theory of Operation

Some of the basic concepts involved in the two terminal device as shown in Figure 1a are presented by Moll et al. (17). This type of device is fairly amenable to analysis and has been given a good deal of attention in the literature. Mackintosh (14) and Aldrich and Holonyak (1)

have discussed some aspects of the three terminal version of the p-n-p-n switch as shown in Figure 1b. As pointed out in these papers, this type device usually has transverse base currents and so will present a two-space dimensional problem which will be more difficult to handle than the two terminal case.

The process of switching from the "off" state to the "on" state for the two terminal device is ordinarily done by increasing the value of anode-to-cathode voltage to a point where avalanching occurs across the center junction of the device. To switch from the "on" state to the "off" state, the device current I is interrupted in some manner until the change has been accomplished.

The three terminal device as shown in Figure 1b can be turned on by applying a current pulse I_g of appropriate polarity to the gate terminal. Some three terminal devices must be turned off by interruption of the device current I_A by some manner while other three terminal devices can be turned off by a current pulse I_g of the appropriate polarity at the gate terminal.

Referring to Figures 1a and 1b the two outer regions both act as emitters so that the outer junctions will be referred to as J_{E1} and J_{E2} . The center junction J_C acts as a collector and the two inner regions both act as base regions. The P_1 region will be referred to as base 1 and the N_2 region as base 2. The static fraction of the emitter current at emitter J_{E1} into base 1 that is collected at J_C will be called α_1 . The static fraction of the emitter current at emitter J_{E2} into base 2 that is collected at J_C will be called α_2 . When a low value

of voltage V of polarity shown in Figures 1a and 1b is applied, the junctions J_{E1} and J_{E2} will be forward biased, and J_C will be reverse biased. This corresponds to the high impedance, or "off", state shown as Region 1 in Figure 2.

For the two terminal device of Figure 1 the device current I will be

$$I = \alpha_1 I + \alpha_2 I + I_{CO} \quad (1)$$

where I_{CO} is the collector junction saturation current. If this equation is solved for I the result is

$$I = \frac{I_{CO}}{1 - \alpha_1 - \alpha_2} \quad (2)$$

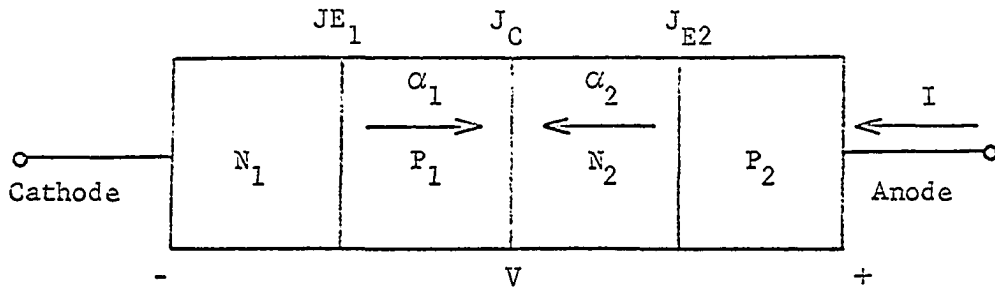
Thus if I_{CO} is small and $(\alpha_1 + \alpha_2)$ is small, the current I will be small, so that the "off" state corresponds to the condition

$$\alpha_1 + \alpha_2 < 1 \quad (3)$$

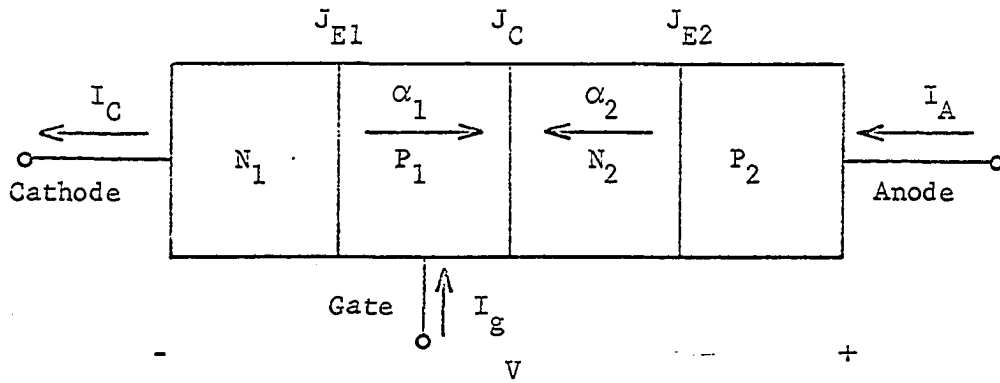
If the values of α_1 and α_2 increase for some reason, and the condition

$$\alpha_1 + \alpha_2 \geq 1 \quad (4)$$

exists, then Equation 2 is no longer valid and the device current is limited only by the external circuit. In order for the collector current to be limited to the value of current flowing in the external circuit, the center junction becomes forward biased thereby emitting electrons and holes back into the base layers causing the base layers to become saturated with minority carriers. Under the condition of Equation 4, the device has all three junctions forward biased and is now in its low impedance, or "on" state corresponding to Region 2 of Figure 2 and will remain in this state until some external signal is applied to force a change. It has been shown that the alpha value increases with emitter



(a)



(b)

Figure 1. Four layer devices
 (a) Two terminal device and
 (b) three terminal device.

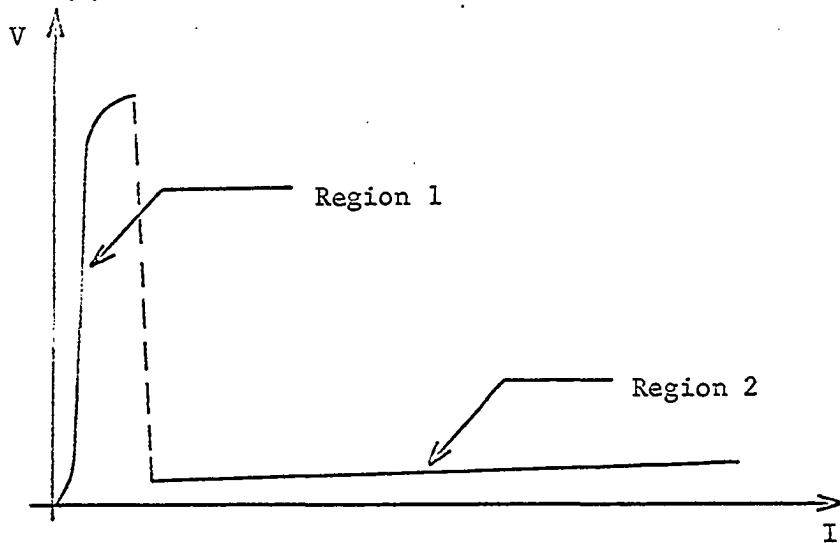


Figure 2. Idealized V-I curve of a p-n-p-n device

current as discussed by Moll et al. (17), Aldrich and Holonyak (2), Jonscher (11a), and others. Figure 3 gives the approximate behavior of the alphas for a four layer device under the assumption that the maximum value of α_1 is near unity while the maximum value of α_2 is considerably less. At very low values of emitter current alpha is very small because much of the current across the emitter junction is caused by recombination taking place inside the space depletion region of the junction causing the emitter injection efficiency to be low for low values of emitter current according to Sah et al. (22b). As the emitter current increases the recombination centers in the space depletion region tend to become saturated so that diffusion of carriers across the region increases causing the emitter injection efficiency, and thus alpha, to increase. The value of alpha will tend to drop off somewhat at high values of emitter current due to conductivity modulation of the base region causing the emitter efficiency, and thus alpha, to decrease.

To turn on the two terminal device of Figure 1a, the voltage V is increased to a level where avalanche breakdown at J_C causes an increase in the emitter currents causing α_1 and α_2 to increase. If the condition of Equation 4 is reached, the device will change from the high impedance to the low impedance state as J_C changes from a reverse to a forward bias. The device will remain in this low impedance state even if V is no longer held at the switching level. To return the device to the "off" state, the usual method of turning off the two terminal device is to reduce the device current below a certain minimum value, called the holding current, causing the device to change from the low impedance to

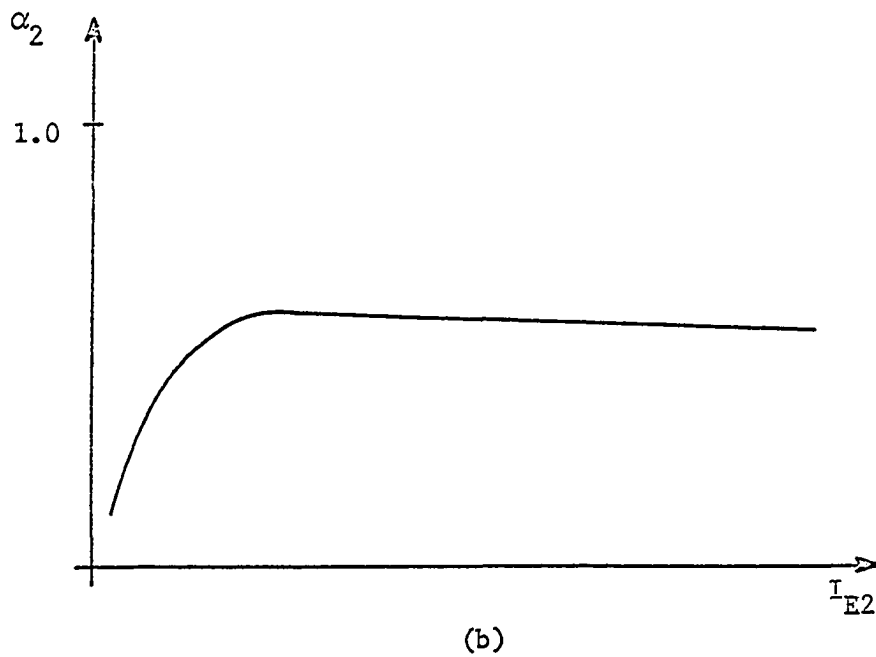
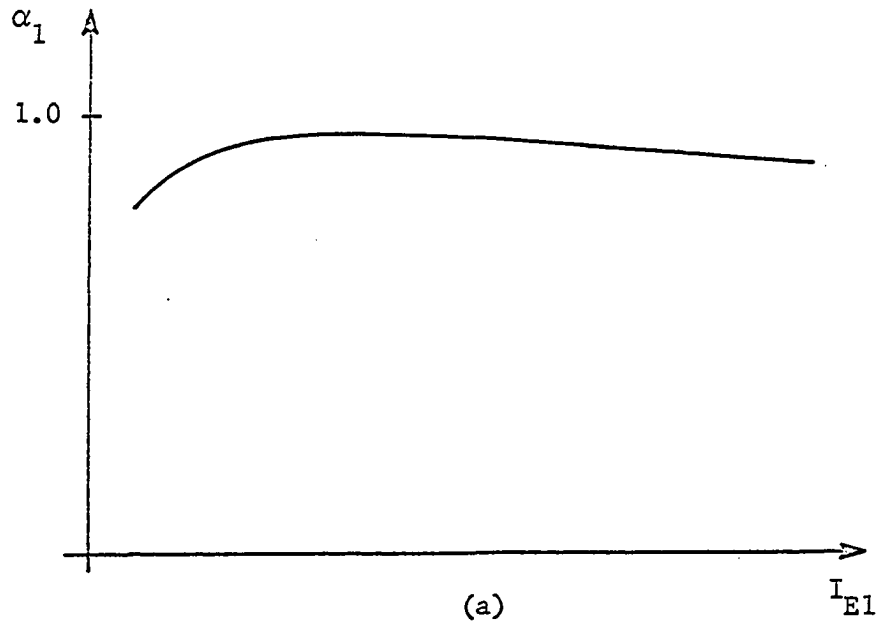


Figure 3. Approximate alpha behavior for a p-n-p-n device for (a) the high alpha base and (b) the low alpha base

the high impedance state as the center junction goes back to the reverse bias condition.

The behavior of the three terminal device can be discussed in a similar way. The anode current is

$$I_A = \alpha_2 I_A + \alpha_1 (I_A + I_g) + I_{CO} \quad (5)$$

If this equation is solved for I_A the result is

$$I_A = \frac{\alpha_1 I_g + I_{CO}}{1 - \alpha_1 - \alpha_2} \quad (6)$$

where I_{CO} is again the collector junction saturation current. Again, if I_g , I_{CO} , and $(\alpha_1 + \alpha_2)$ are small, I_A will be small and the device will be in the "off" state. If $(\alpha_1 + \alpha_2) \geq 1$ now becomes the case, the device current will be limited by the external circuit and the device will be "on". For the three terminal device switching can be accomplished by increasing the emitter currents, and hence the alpha sum, by supplying a gate current at one of the bases. For turn-off, if the three terminal device is properly designed, charge can be withdrawn from the gate base which will reduce the emitter currents and the alpha sum causing the center junction to return to a reverse bias, high impedance condition when the two bases come out of saturation.

The definition of turn-on time will be taken as the length of time from the application of a gate pulse until saturation of the base regions occur which will be when the device current begins to be limited by the external circuit. The turn-off time will be the length of time from when the control pulse is applied until the device current is small enough so that the device will again act as a high impedance device with

the control pulse ended.

Lateral Effects in Gated P-N-P-N Devices

Fletcher (5) has pointed out an effect in power transistors that must also be considered in devices with a gated base region. Because of the narrow base region and the finite resistivity of the base layer of a device such as in shown in Figure 1b, the base current flowing in a transverse direction in the base region to supply the necessary charge for volume recombination, junction capacitance charging, losses due to emitter efficiencies less than unity, and any other necessary charge will cause transverse voltage differences along the base region. Thus when base current is being supplied to base 1 to turn the device on, the injected carriers along the emitter junction will be a maximum nearest the base lead and will fall off due to the drop in emitter forward bias caused by the ohmic voltage gradient along the base. Thus for a narrow base region with relatively high resistivity, the effective emitter area will be limited to a region close to the gate contact. Figure 4 illustrates the case during the time the device is being turned on.

The turn-off operation is also complicated by the transverse base resistance. For turn-off, the entire emitting area must essentially be turned off when withdrawal of charge through the gate terminal is stopped or the device will still be in the low impedance condition. With charge being removed from the gate, there will be an ohmic voltage gradient that will cause the emitter voltage forward bias to be lowest next to the gate terminal and higher at points more remote from the gate. Figure 5 illustrates the case for charge being withdrawn from the base.

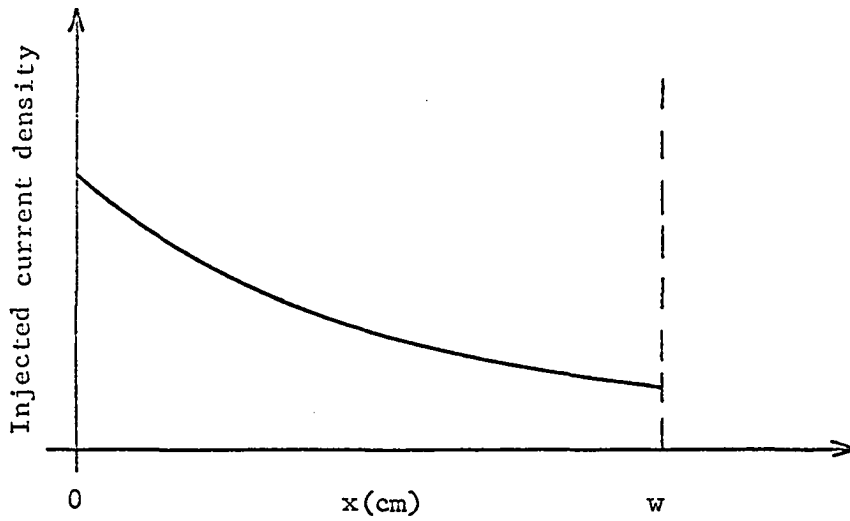


Figure 4. Fall off of injected emitter current density as a function of transverse distance along base. Charge is being supplied to gate at $x = 0$. Base edges are at 0 and at w .

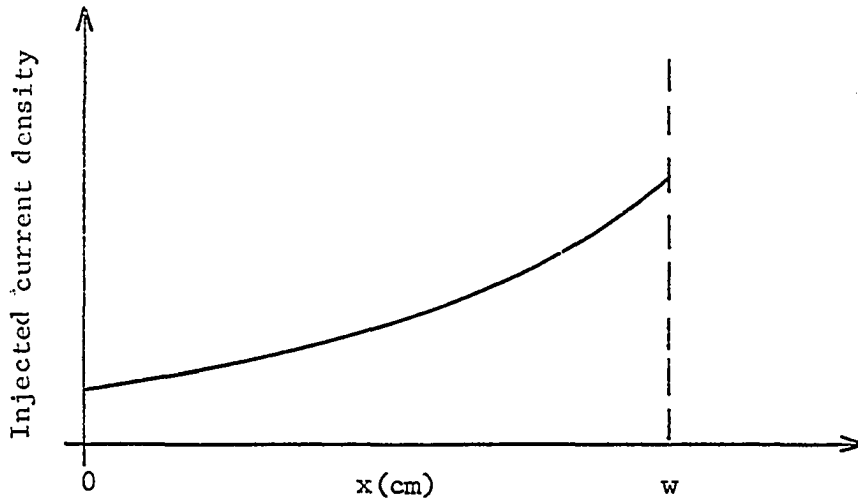


Figure 5. Increase in injected emitter current density as a function of transverse distance along base. Charge is being withdrawn from gate at $x = 0$. Base edges are at 0 and at w .

Turn-On and Turn-Off Gain

Turn-on gain is the ratio of load current after the device is on to the necessary value of gate current to turn it on. Likewise, turn-off gain is the ratio of the load current before turn-off is started to the gate current necessary to cause the device to turn off. Goldey et al. (9) have discussed some of the factors influencing gain. In order for the gate current to have maximum effect during turn-on, the alpha of the gated base should be large so that a given gate current will cause a large increase in emitter currents which in turn will increase the alpha sum causing turn-on if said increase is great enough. Once the device is "on", the center junction limits the device current and the alpha sum to approximately unity. If the device current were not limited, the alpha sum would approach some maximum value. The amount that this maximum value of the alpha sum exceeds unity essentially determines how much excess minority carrier charge is stored in the base regions. To keep this excess stored charge at a minimum, the alpha of the ungated base should be kept low. Thus the physical design of the device should be such as to give a high α_1 for the gated base, and a low α_2 for the ungated base.

Structures

A necessary condition for the operation of the p-n-p-n semiconductor device is the variable alpha sum. This is true for both the two-terminal and the three-terminal device. The avalanche process at junction J_C is the means for increasing the alpha sum in the case of the two-terminal device. The consideration of turn-off gain for the gated three terminal

devices of Figures 6 and 7 puts the additional boundary condition of wanting the gated base alpha to be high and the ungated base alpha to be low. Consideration must be given to how the magnitude and variation in alpha can be controlled.

The quantity α_1 of the gated base is desired to be fairly high. The design of the device for this purpose is done using well known techniques, e.g. narrow base width, high injection efficiency, low volume recombination rate, etc. The controlled low α_2 structure can be achieved by reducing either the emitter efficiency γ_2 of J_{E2} or the transport factor β_2 of base 2 to low values. A general discussion of the ideas involved here are given in Gentry et al. (6).

If the transport factor β_2 of a device such as that shown in Figure 6 is to be controlled, this may be done by employing a wide base region for base 2. The same purpose would be accomplished if the lifetime were lowered by having a high density of recombination centers. As injection levels increase, and saturation of recombination centers enter into consideration, the lifetime would increase and tend to raise α_2 . This effect might not be desirable if α_2 is to be kept at a low value to minimize saturation minority-carrier densities. Still another way that the minority-carrier transport can be varied is by an electric field in a wide base region due to majority carrier current flow. This effect is dependent on device current and thus gives a variable α_2 . This method of control is discussed by Lesk (12), Aldrich and Holonyak (1), and Gentry et al. (6).

If the emitter efficiency of J_{E2} is to be the controlling variable,

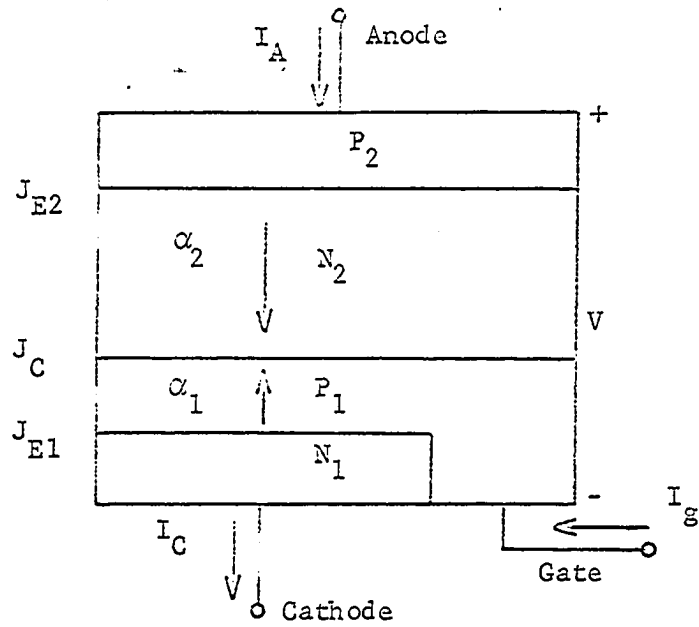


Figure 6. Low α_2 is controlled by causing emitter efficiency or transport factor of base 2 to be low

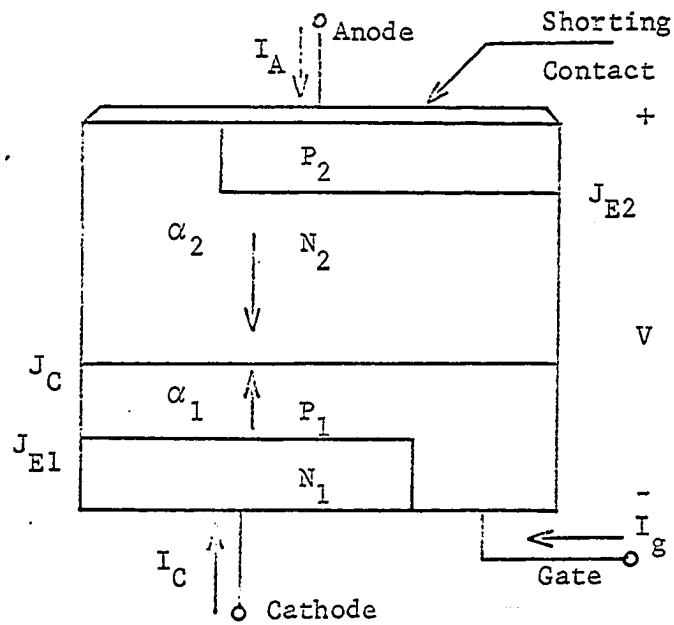


Figure 7. Low α_2 is controlled by shorting emitter 2 and base 2 together giving a variable emitter injection efficiency

there are at least two techniques that will allow this. The absolute magnitude of γ_2 may be restricted to low values by designing emitter 2 to have a high sheet resistivity with respect to the value of the sheet resistivity of base 2. The value of γ as shown in Goldey et al. (9) is

$$\gamma \approx \frac{R_b}{R_e + R_b} \quad (7)$$

where R_b is the sheet resistance of the base layer and R_e is the sheet resistance of the emitter layer. To obtain a low γ the quantity $R_e \gg R_b$. If the emitter layer is made very thin and highly doped giving a high R_e , conductivity modulation of the emitter will not occur. If conductivity modulation occurred an increase in emitter injection efficiency would occur and cause a corresponding increase in α_2 . Another way to gain the variability and control of size for γ_2 is by using a shorting contact to short together emitter 2 and base 2. Aldrich and Holonyak (2) discussed this technique in some detail and further discussion of this idea can be found in Gentry et al. (6, 7). As device current begins to flow in this type of device, as in Figure 7, there is a transverse flow of charge in base 2 under the shorted emitter toward the shorting contact causing a transverse voltage along base 2 which will forward bias the junction J_{E2} and cause injection of holes into base 2. At low device current, the junction J_{E2} is nearly inoperative as an emitter so that γ_2 is very nearly zero. As device current increases the forward bias on J_{E2} will increase and the emitter will begin injecting more charge with a corresponding increase in γ_2 . If γ_2 increases sufficiently to cause the alpha sum to reach unity, the device

will switch to the low impedance, or "on", state. For turn-off, the preceding routine is reversed. If enough gate charge is withdrawn so that the transverse voltage drop in base 2 is insufficient to maintain heavy injection at J_{E2} , γ_2 will decrease enough to cause a drop in the alpha sum and the device will switch to the "off" state. The relative widths of the emitter layers are important and will effect the sizes of holding current and gate current for turn-on or turn-off. It should be especially noted that the shorting contact introduces further very important transverse considerations.

Spread of "On" Region

Because of the transverse biasing effect in a gated four-layer diode as discussed in the section on lateral effects, the region of the p-n-p-n switch that will be "on" first will be that part of the emitter closest to the gate terminal. If the device anode current is greater than the holding current when the gate current is discontinued after local turn-on has taken place, the device will remain on and there will be a gradual spreading of the "on" region due to the lateral diffusion of carriers in the base region so that the "on" state will spread. This phenomenon has been discussed by Longini and Melngailis (13). They have discussed this in terms of a "velocity of propagation" of the "on" state. Dodson (4a) did a good deal of experimental work on devices of the general form shown in Figure 6 that demonstrated how the "on" state spreads after local turn-on has taken place next to the gate region.

DESCRIPTION OF THE PROPOSED MATHEMATICAL MODEL

The two types of devices that will be considered in this proposed mathematical model will be the devices shown in Figures 6 and 7. Both these devices have transverse base currents that strongly influence their behavior. The controlling quantity in both devices will be considered to be the gate current I_g for both turn-on and turn-off. The voltage applied across the device will be assumed to be less than that required for avalanching to become important at junction J_C .

Factors Effecting Gate Controlled Devices

The gated p-n-p-n switch has high level effects that arise due to the base biasing effects causing the emitter current density at the gated emitter to be quite high at regions near the gate and to fall off rapidly at more remote parts of the emitter. The collector junction J_C becomes forward biased in the "on" state and this also must be accounted for. For devices of the sort shown in Figures 6 and 7 with α_2 of the ungated base being designed to have a low value with a relatively wide base region of high resistivity, electric fields due to majority carrier current flow may also be important.

The results of the considerations entering into the design of the devices of Figures 6 and 7 that will be important in the considerations for a mathematical model are:

1. Transverse voltage gradient along base 1 and base 2 due to transverse current flow

2. Two-dimensional minority carrier concentration in base 1 and base 2 due to transverse base currents
3. Injected minority carrier concentration may be large enough to cause conductivity modulation to occur
4. Emitter injection efficiency may be low enough in some cases so that carrier injection into the emitter may become important
5. Collector junction J_C becomes forward biased as the device turns on
6. Electric field due to ohmic voltage drop in the low wide base region may become important.

Some of these factors will be more important than others. The first of these factors has been discussed in the sections on lateral effects and on structures. This factor is very important and certainly must be included. The importance of the first factor leads directly to the reason why factor 2 must be included. Factor 3 is important since some parts of the gated p-n-p-n will be conducting heavily and will be turned on while other parts will be conducting very lightly. If the injected minority carrier concentration becomes sufficiently high, the transverse voltage along the effected base would be correspondingly changed and the emitter injection efficiency would change due to its dependence on the relative size of the base and emitter sheet resistivities as discussed in the section on turn-on and turn-off gain. Factor 4 must be considered since low emitter injection efficiency will result in the injection of charge from the base into the emitter and will increase the amount of base current necessary to drive the effected base. Factor 5 must be

taken into consideration because as the four-layer device changes from a high impedance to a low impedance state the center junction J_C must change from a reverse to a forward bias in order to limit the device current. This points out that the criteria for the device being "on" depends on whether or not the center junction is reverse biased. The final factor is important because an electric field can cause more charge to be transported across the base thus effectively varying the alpha of the corresponding base and also can effect the transit time of carriers on base 2. Since the four-layer device is dependent on changing values of alphas for its behavior, this electric field must be considered.

Overall View of the Problem

The analysis of the devices of Figures 6 and 7 is complicated by their two-dimensional nature arising from transverse effects caused by variation in the emitter junction voltage from the transverse base current flow through the transverse base resistance and from transverse effects caused by the shorting contact of the device of Figure 7. Further complications arise due to the way the base regions are coupled so that they furnish drive to each other. Other factors discussed in the preceding section also cause complications. All these considerations make it extremely difficult, if not impossible, to get any sort of an exact mathematical solution. If a reasonably accurate analysis is desired, it becomes necessary to go to numerical techniques. The necessary equations will now be obtained and discussed, and then the overall approach to the use of these equations for the analysis of the problem will be discussed.

Equations needed for the solution

The basic relation that governs the flow of the charged particles through semiconductor material is the equation of continuity. This equation completely describes the behavior of either electrons or holes in semiconductor material for both time and space variations. If an incremental volume $dx dy dz$ centered at (x, y, z) in a cartesian coordinate system is considered within the semiconductor material, the continuity equation requires that the time rate of increase in the number of carriers within this incremental volume is equal to the excess of generation over recombination plus the net inward flow of carriers across the surface of the volume. The method used here for the development of the continuity equation parallels that of Shockley (23). If an N-type material is considered, the time rate of change of holes in the incremental volume is

$$\frac{\partial p}{\partial t} dx dy dz \quad (8)$$

The excess rate of generation over recombination in the incremental volume is

$$(g - r) dx dy dz \quad (9)$$

where g is the net rate of generation of holes per unit volume and r is the net rate of recombination of holes per unit volume. The current density in the x -direction and into the middle of the $dy dz$ face of the volume is

$$i_{px}(x, y, z) - \frac{\partial i_{px}(x, y, z)}{\partial x} \frac{dx}{2} \quad (10)$$

The current flow out of the middle of the other $dy dz$ face will be of

exactly the same form with the negative sign replaced by a positive sign. Thus the net inward flow of holes for the dydz faces will be

$$- \left[\frac{1}{q} (i_{px}(x,y,z) - \frac{\partial i_{px}(x,y,z)}{\partial x} \frac{dx}{2}) - \frac{1}{q} (i_{px}(x,y,z) + \frac{\partial i_{px}(x,y,z)}{\partial x} \frac{dx}{2}) \right] dydz = - \frac{1}{q} \frac{\partial i_{px}(x,y,z)}{\partial x} dx dy dz \quad (11)$$

The net inward flow of holes for the dx dy and dx dz faces can also be found in an exactly similar manner resulting in an equation for the net inward flow of holes being

$$- \frac{1}{q} \left(\frac{\partial i_{px}}{\partial x} + \frac{\partial i_{py}}{\partial y} + \frac{\partial i_{pz}}{\partial z} \right) dx dy dz = - \frac{1}{q} \vec{\nabla} \cdot \vec{i}_p dx dy dz \quad (12)$$

Again referring to Shockley (23), if the assumption is made that the number of excess holes decay with the characteristic lifetime τ_p , the average lifetime of a hole before recombination with an electron, the following relation is obtained:

$$(g - r) dx dy dz = \frac{p_n - p'}{\tau_p} dx dy dz = - \frac{p}{\tau_p} dx dy dz \quad (13)$$

Here p_n is the equilibrium value of concentration, p' is the total concentration, and p is the excess concentration of the holes in the N-type material. The complete continuity equation obtained by putting these results together after noting that the dx dy dz dependence will cancel out of each term gives

$$\frac{\partial p}{\partial t} = - \frac{p}{\tau_p} - \frac{1}{q} \vec{\nabla} \cdot \vec{i}_p \quad (14)$$

After a similar development is gone through for P-type material the

resulting equation for the minority electron concentration is

$$\frac{\partial n}{\partial t} = -\frac{n}{\tau_n} + \frac{1}{q} \vec{\nabla} \cdot \vec{i}_n \quad (15)$$

The difference in sign on the divergence term results from the fact that, due to the opposite sign on the charge of holes and electrons, hole diffusion current flows in the direction of decreasing density while electron diffusion current flows in the direction of increasing density.

In order to have the continuity equation strictly in terms of the minority carrier concentration, the relation between current density and this concentration is needed. For current density due to hole flow in an N-type region this relation is

$$\vec{i}_p = q\mu_p \vec{E}(p + p_n) - qD_p \vec{\nabla} p \quad (16)$$

The analogous expression for current density due to electron flow in a P-type region is

$$\vec{i}_n = q\mu_n \vec{E}(n + n_p) + qD_n \vec{\nabla} n \quad (17)$$

In both Equation 16 and 17, the first term on the right is a drift current due to an electric field and the second is diffusion due to a density gradient in the excess minority carrier concentration. For these equations, μ_n and μ_p are mobilities of electrons and holes in $\text{cm}^2/\text{volt sec}$, D_n and D_p are diffusion constants for electrons and holes in cm^2/sec , \vec{E} is the electric field vector, q is the magnitude of the charge on an electron, and \vec{i}_n and \vec{i}_p are current density vectors.

If one of the continuity equations is to be applied to the analysis of a base region, it is necessary that the relation between the excess

minority carrier density at the edge of the transition region of a junction and the voltage across that junction be known. For an N-type region, the excess hole concentration at the edge of the transition region is

$$p = p_n (\exp(qv/kT) - 1) \quad (18)$$

For a P-type region, the excess electron concentration at the edge of the transition region is

$$n = n_p (\exp(qv/kT) - 1) \quad (19)$$

Here k is Boltzmann's constant, T is absolute temperature, and v is the voltage across the junction which will be a function of position and time. Equations 18 and 19 give the boundary conditions at both the emitter and the collector for either base region being investigated. Boundary conditions at exposed base surfaces will be determined by assuming a recombination velocity of some value, Middlebrook (15). The equation of this boundary condition for an N-type material expresses the fact that the rate of hole diffusion to the surface is proportional to the excess carrier density at the surface

$$D_p \frac{\partial p}{\partial n} = -S \cdot p \quad (20)$$

where $\frac{\partial p}{\partial n}$ is the component of excess hole density gradient normal to the surface and S is the effective surface recombination velocity with dimensions of cm/sec.

Organization of the solution

The base current for the ungated base N_2 will be electrons collected at the center junction from base P_1 . Conversely, the holes collected at

J_C from base N_2 will provide drive for the gated base P_1 . The gated base can also receive base current from the gate terminal. Since the gated base for either of the devices of Figures 6 or 7 is a P-type region, the gate current I_g to base 1 for switching from the high to the low impedance state will consist of positive carriers into the gate terminal. For this reason the gate current for the defined direction shown in Figures 6 and 7 will be a positive pulse of current for turn-on. For turn-off, positive charge will have to be withdrawn from the gated base so that I_g will then be a negative pulse of current. The current pulse in both cases will be of finite length. For turn-on or for turn-off, if the magnitude or the time duration of the pulse is insufficient, the device will fail to change its state. The total base current furnished to the gated base will be the sum of the hole current collected at J_C from region N_2 plus the gate current I_g .

During turn-on, the base current for either base must supply several needs. For the emitter voltage to increase to a forward bias value, charge must be furnished to the emitter junction capacitance. At the start of turn-on the center junction is reverse biased, when turn-on has been achieved the center junction is forward biased. The base current must furnish the charge for this change in voltage for J_C . The excess of recombination over generation within the base must also be supplied as well as having to supply the majority carrier charge that will offset the increase in minority carriers present as required for space-charge equilibrium as the minority carrier concentration builds up during turn-on.

The current density equations shown as Equations 16 and 17 allow the total device current to be calculated when applied at the center junction J_C if the electric field and the excess minority carrier concentration is known. These equations allow the base current into base 1 and base 2 to be calculated if the value of I_g is assumed known. The minority carrier concentration in either base can be found from the continuity equations if the boundary conditions specified as Equations 18, 19, and 20 are known. Equations 18 and 19 allow the excess minority carrier concentration to be calculated if the appropriate junction voltages are known. The circuit of Figure 9 will be used for both turn-on and turn-off. With the device in the "off" state, the center junction J_C will be reverse biased with essentially the full voltage E . The two junctions J_{E1} and J_{E2} will have a very low forward bias which will be considered to be zero to give a distinct starting point. The device current I_A will be essentially the saturation current of the center junction. The initial value of the excess minority carrier concentration in both base 1 and base 2 can then be approximated to get a starting point for the analysis. The starting point of the turn-on process occurs at the time when the positive pulse of current I_g as shown in Figure 8 is applied. The continuity equations for base 1 and base 2 will be approximated over as fine a grid as desired with finite difference approximations to Equations 14 and 15 after combining these with Equations 16 and 17 so that the continuity equations are wholly in terms of excess minority carrier concentrations. The behavior of the device can now be analyzed for the turn-on period by stepping forward in time using a finite time increment

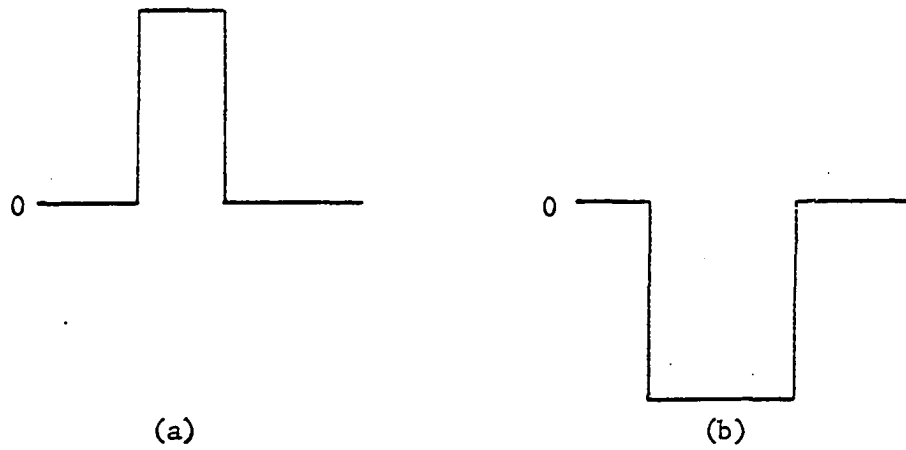


Figure 8. Values of I_g are (a) positive for turn-on and (b) negative for turn-off

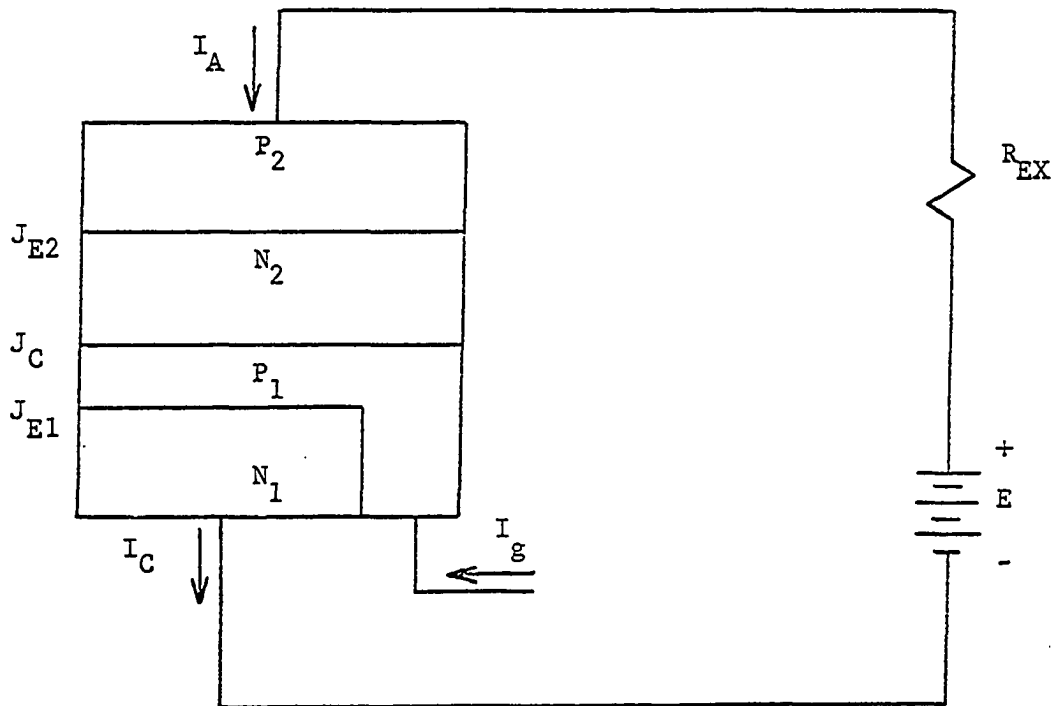


Figure 9. Assumed circuit for transient analysis of device

and going through the following steps:

1. Calculate currents at junction J_C to get total base drives into either base 1 or base 2 at one particular point in time. Base 1 also has I_g supplying drive current.
2. To step forward a specified time increment, the base drive current is assumed constant over the time increment thus giving the total charge supplied to the base during this time step. Knowing the total charge supplied and the junction voltages at the beginning of the time step will allow calculation of the new junction voltages at the end of the time step by consideration of the necessary charge needed for capacitance charging, volume recombination etc., and comparing it to the actual amount supplied. These junction voltages are calculated only at discrete points.
3. The finite difference form of the continuity equations will be solved by an iterative technique to get the values of the excess minority carrier concentration at the end of the time step at the intersections of the specified mesh.
4. Return to step 1 and step forward another increment in time. Continue until solution is completed.

The starting values of junction voltages, minority carrier concentration, and device currents for the beginning of the turn-off period will be known from the end results of the turn-on calculations just described. The beginning of turn-off will be at the time when the negative pulse of current I_g as shown in Figure 8 is applied. The solution for the

turn-off process follows the same pattern just described. The excess minority carrier concentration of the bases will be decaying during the turn-off process in contrast to turn-on when they will be building up. The logical flow of the computer program used for the modeling of the devices of Figures 6 and 7 is shown in Figure 10. More detail will be gone into on some of the individual blocks shown on this figure.

Base Bias Calculations

More detail will now be gone into in regard to the two blocks shown on Figure 10 for base 1 and base 2 bias calculations. Each of the two base regions is divided into finite sized increments by constructing a network of variably spaced grid lines completely covering both base regions. The device shown is the shorted emitter device of Figure 7. To avoid overcrowding the sketch only base 1 is shown covered by a grid of horizontal and vertical lines. Exactly the same type of grid is placed over base 2. To simplify the computer program, both regions were made rectangular as shown by the two dashed lines on Figure 11. The two omitted regions should not have a significant effect on the analysis. The methods used in the various parts of the computer program are nowhere dependent on having exact rectangular regions. The assumed position of gate contact shown on Figure 11 is a consequence of neglecting the resistance of base 1 in regions away from the active base region between the N_1 and the P_1 regions. The vertical grid lines divide the horizontal width up into $(IM-1)$ finite increments where IM is a variable integer. The horizontal grid lines divide the vertical height up into $(JMT-1)$ finite increments where JMT is a variable integer. Base 2 has

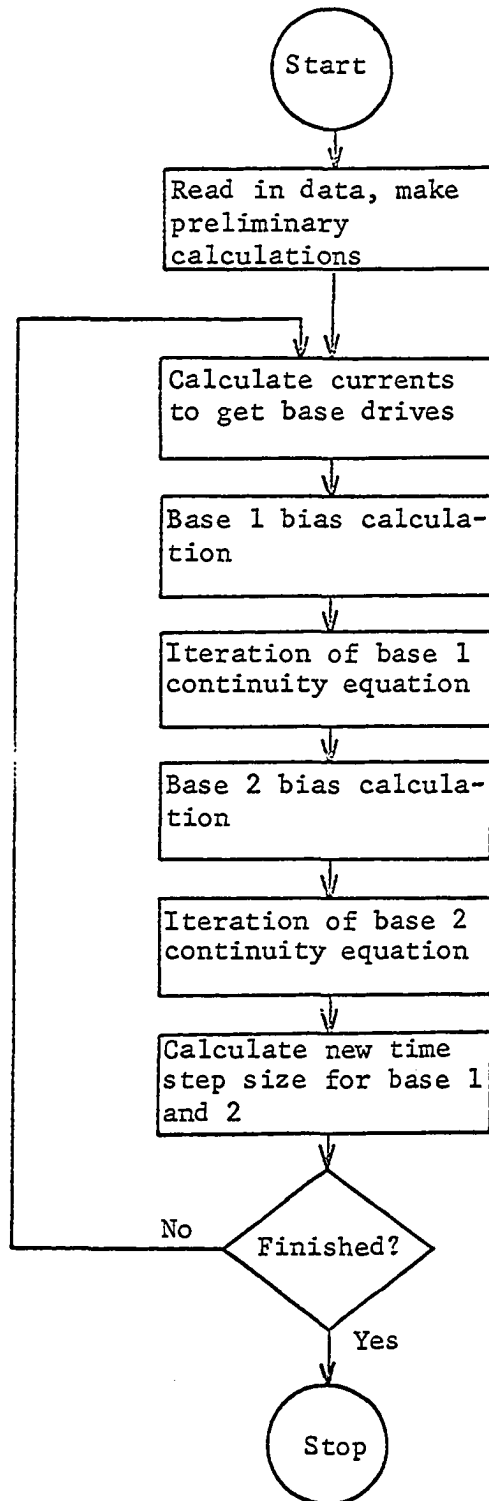


Figure 10. Flow diagram of overall computer program

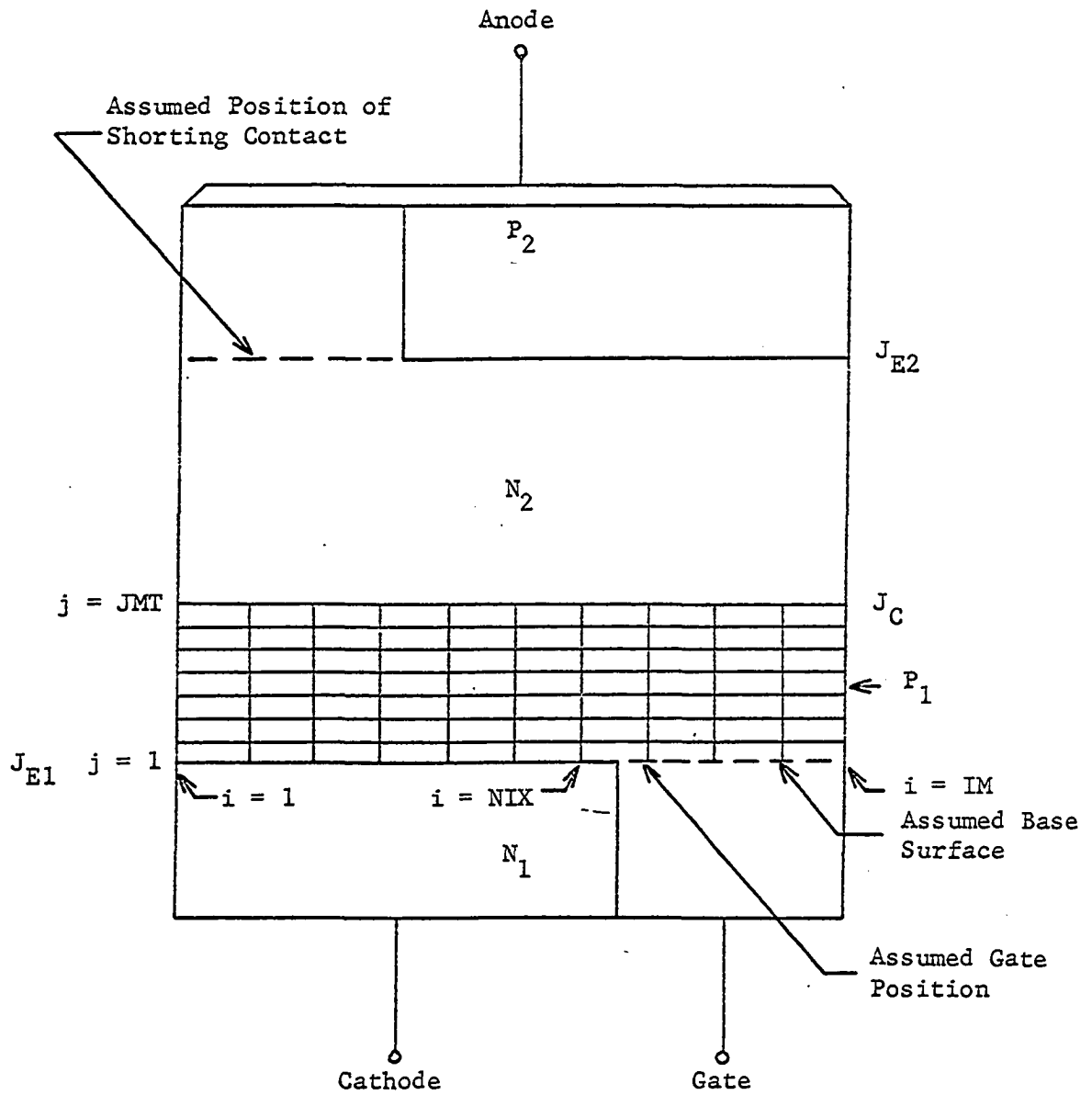


Figure 11. Shorted emitter device shown with grid over base 1 and with assumed rectangular base regions for the mathematical analysis

(IM-1) horizontal and (JM2T-1) vertical finite increments. The assuming of base 2 to be a rectangle does not arise for the device of Figure 6 since base 2 is rectangular as it stands.

To enable calculation of the excess minority carrier concentration along J_{E1} , J_C , and J_{E2} from Equations 19 and 20, the voltages along these junctions must be known at the points defined by the vertical grid lines. As explained in the last section, the drive current for base 1 will consist of hole current collected at J_C and whatever gate current is supplied. The drive current for base 2 will consist of electron current collected at the center junction. The equation that expresses the needs that must be supplied for either base by the base current in incremental form is

$$I_b = \frac{Q}{\tau} + \frac{\Delta V_c}{\Delta t} C_c + \frac{\Delta V_e}{\Delta t} C_e + \frac{\Delta Q}{\Delta t} + I_{e \text{ loss}} \quad (21)$$

during a specific time increment Δt . If Δt is chosen sufficiently small then to a good approximation the base current I_b being supplied to the base will be constant over that time increment. The term $I_{e \text{ loss}}$ is due to emitter efficiency being less than unity. The term Q/τ is the recombination current. The second and third term represent the amount of current needed to supply the charge to the collector and emitter capacitance to have a change in voltage of ΔV_c and ΔV_e during the time increment Δt . The term $\Delta Q/\Delta t$ is a measure of the base current needed to supply or remove majority carriers to maintain space-charge equilibrium as the excess minority carriers stored in the bulk base region changes. The capacitance terms C_c and C_e both are a function of the voltage across their respective junctions. For a step junction, an expression

for capacitance from Gibbons (8) is

$$C = \frac{C(0)}{(1 - v/\phi)^{\frac{1}{2}}} \quad (22)$$

where v is the junction bias voltage, ϕ is the contact potential, and $C(0)$ is the capacitance of the junction for a voltage bias of zero. An expression for $C(0)$ is

$$C(0) = \frac{\epsilon A}{l_1 + l_2} \quad (23)$$

where ϵ is the permittivity, A is the junction area, and l_1 and l_2 are the voltage dependent space charge layer widths into the two regions on either side of the junction for a voltage bias of zero. When the transverse variation of junction voltage of v is noted, the junction capacitance is seen to be both time and space dependent.

A slice of either base 1 or 2 is now considered that is Δx wide, where Δx is the distance between two vertical grid lines, and centered on a vertical grid line. To effect a change in the old values of junction voltages at either end of this slice after an incremental step Δt forward in time, this slice of base must have an amount of base current furnished to, or carried away from, it as determined by consideration of Equation 21. In any given slice, there will be a certain amount of base current flow into the slice due to collection at J_C from the other base. If the amount of base drive needed for this slice is more than the amount supplied from the second base, the difference must be supplied by a transverse flow through the active base region. If the amount of base drive needed for this slice is less than that

supplied from the second base, the excess must be carried away by a transverse flow through the active base region. In either case the transverse flow of base current will cause a voltage variation along the base region since the transverse resistance of any slice is

$$R_T = \frac{\rho \Delta x}{D \cdot BW} \quad (24)$$

where ρ is the average resistivity of the base, D is the depth of the device into the paper, and BW is the distance from emitter to collector of the base being considered. Transverse flow in base 1 will be very important during turn-on or turn-off when I_g is being applied. Base 2 will always have a great deal of transverse flow in the shorted emitter type of device. Even in the non-shorter emitter device, transverse flow in base 2 will occur due to the collection of drive current into base 2 being heaviest at areas under high injection levels for emitter 1, which occur over an area close to the gate for turn-on and remote from the gate for turn-off.

One other factor of importance here is the conductivity modulation that occurs when and if the minority carrier concentration reaches the same order of magnitude as the doping concentration. When this happens the increase of majority carrier concentration in the base to maintain charge neutrality will be a significant amount with respect to the magnitude of the doping concentration. Using the P-type base as an example, the equation for resistivity assuming low injection levels is

$$\rho \approx \frac{1}{q\mu_p N_A} \quad (25)$$

where μ_p is the mobility of holes and N_A is the acceptor impurity density. The case where the injection level becomes high can be handled by noting that for charge neutrality the minority carrier buildup in the base is matched by an equal buildup of majority carriers to give a new value of resistivity of

$$\rho' \approx \frac{1}{q\mu_p(n + N_A)} = \rho \frac{1}{1 + n/N_A} \quad (26)$$

where n is the excess minority carrier density. It is noted that for $N_A \gg n$ ρ' and ρ are approximately the same. When this condition is no longer true ρ' becomes less than ρ .

The anode-to-cathode voltage across the device can be calculated as the voltage E minus the drop due to the current I_A flowing through the resistor R_{EX} . The voltage across the center junction can then be calculated by noting that along any chosen longitudinal path through the device the anode-to-cathode voltage must exactly equal the sum of all junction voltages, with proper regard to sign, and all voltage drops due to majority carrier flow through the bulk material of the various regions.

The routine to step forward in time by Δt for a given base assuming that junction voltages and currents across J_C at the beginning of the time step are known for that base will be discussed. Before going into the calculation for new bias conditions the values of resistivity are computed for regions where conductivity modulation has become important and the values of junction capacitances are calculated using the known junction voltages that exist at the beginning of the time step. The

values of resistivity and capacitances are assumed to be fixed at these calculated values for the entire incremental time step. What is needed at the end of the time step are the new values of junction voltages and, in the case where the junction voltage across J_C has become positive, new values of currents across J_C .

To proceed for the step forward in time for base 1, a value of minority carrier concentration is assumed at $i = NIX$, giving a corresponding value of voltage for the emitter junction at this point. The voltage across the center junction is then calculated and the total base drive needed for this slice is found using Equation 24. The starting value of a variable called GIR for base 1 that represents the total transverse current flow at any point is found by taking the sum of the gate drive and the base current into base 1 from the second base for all slices to the right of and including the slice centered at $i = NIX$, and subtracting the base drive needed for all slices to the right of and including the slice centered at $i = NIX$. This starting value of GIR will be the transverse current flow through the slice centered at $i = NIX$ causing the emitter voltage at $(NIX-1)$ to differ from that at NIX by the product of GIR and R_T where R_T is for base 1. The base drive needed for the strip centered at $(NIX-1)$ is subtracted from, and the amount of base current into this strip is added to, the running value of GIR. This process is continued slice by slice until the extreme left edge of base 1 is reached. If the value assumed for minority carrier concentration at $i = NIX$ were exactly correct, GIR would be precisely zero after all base strips have been accounted for. The residue of GIR is checked and an

appropriate change is made in the assumed value of minority carrier concentration at $i = NIX$. The entire process is repeated until the residue of GIR at the left edge of the base region is as small as necessary for the desired accuracy.

When new bias conditions are being calculated for base 2, the assumed value for the shorted emitter base is the amount of transverse current flowing out from under the shorted emitter while the assumed value for the non-shorter emitter is the value of minority carrier concentration at emitter J_{E2} at $i = 1$. The running variable for the transverse current flow in base 2 at any point is called RUNT. The procedure in base 2 is to start at the left edge and go through analogous calculations slice by slice until the right edge is reached where the residue of RUNT is compared to zero. The assumed value is changed and the calculations are repeated until the residue of RUNT becomes sufficiently small at the right edge.

A general flow chart of the computer program for the bias routine for either base is shown in Figure 12, though in actuality two different programs were used for the two separate bases. Base 2 differs somewhat in that it is assumed that majority carrier flow is great enough due to the low α_2 so that longitudinal voltage drops, and hence electric fields, must be accounted for. The shorted emitter device will also have transverse electric fields due to the transverse flow of current to the shorting contact.

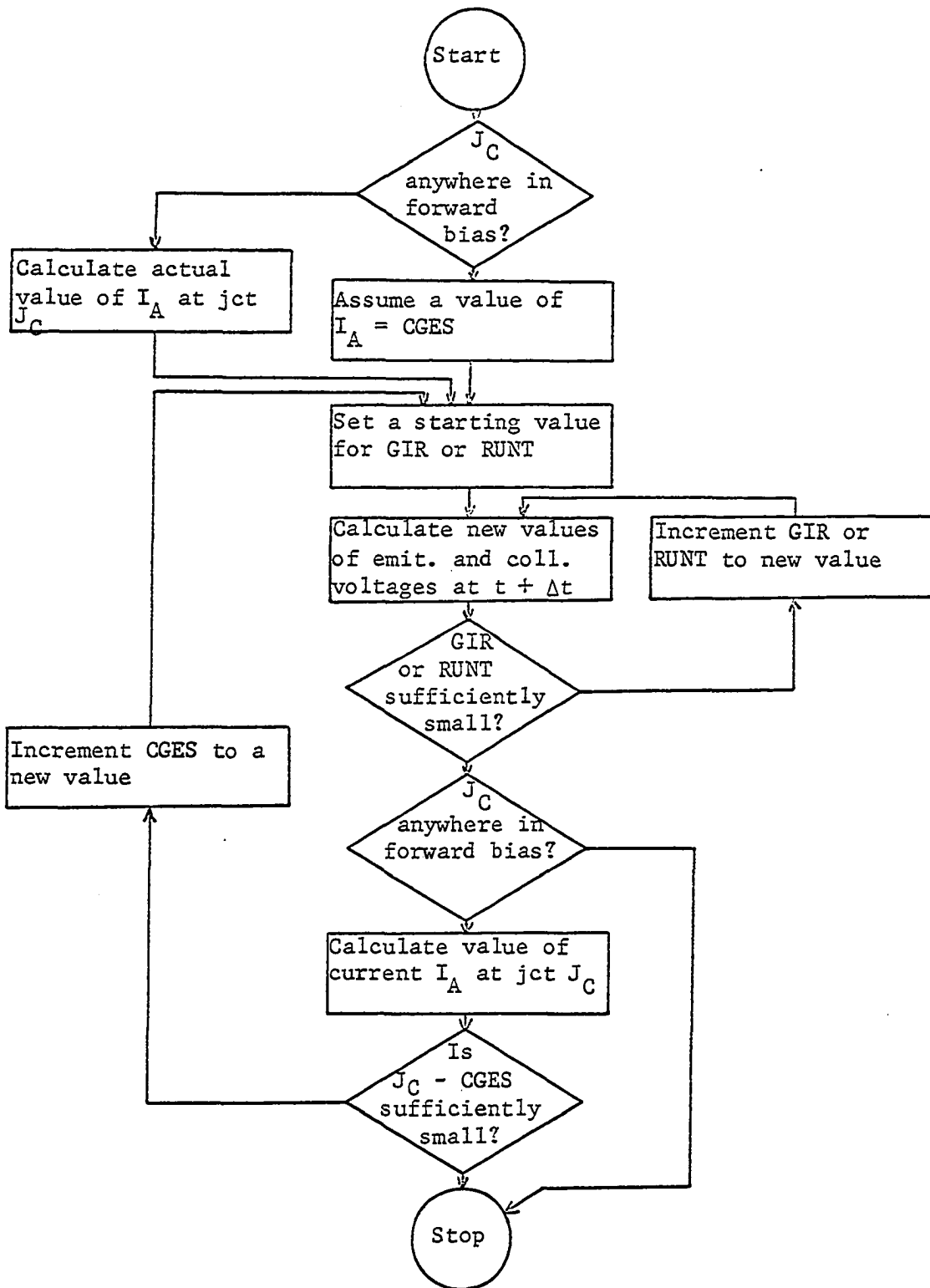


Figure 12. Flow diagram of base bias computer program

Continuity Equation Solution

After the junction voltages are known for $(t_0 + \Delta t)$ the values of excess minority carrier concentration at the junctions at this new time are known. This gives the boundary conditions for the continuity equation for either base at $(t_0 + \Delta t)$ and the new values of excess minority carrier concentration at points interior to the base regions can now be found by stepping forward in time to $(t_0 + \Delta t)$ for the solution of the continuity equation. Due to the variations in the boundary conditions at the junctions, the continuity equation must be handled in terms of two space dimensions. Because of the many complicating factors such as the two dimensional nature of the problem, conductivity modulation of parts of the base region, etc., the solution of the continuity equation is, for all practical purposes, impossible to obtain in closed form. The continuity equation will be put into finite difference form. A stepwise solution of this finite difference form of the continuity equation will then be used to get numerical approximations to the values of excess minority carrier concentrations at finite points inside the base region being considered.

Survey of iterative techniques

Basically, there are two types of finite difference equations that could be considered for the type of problem discussed here. The first of these is the explicit method in which the value of the variable sought at a particular point at time $(t_0 + \Delta t)$ can be expressed completely in terms of known values of the variable at this point and surrounding points at time t_0 . The solution of this type of difference scheme is

quite simple. The second type of difference equation is the implicit method which results in large systems of simultaneous equations to be solved at each time step which is fairly difficult.

A basic difficulty with the explicit difference method is that when stability criteria for the explicit difference method is applied, O'Brien et al. (20) has shown that the size of the time step is severely restricted so that an uneconomically large number of time steps must be made in order to insure stability. This same paper points out that for an implicit difference scheme stability is present without having to restrict the time step. In the book by Varga (24), the material of Chapter 8 is on parabolic partial differential equations which is the class in which the continuity equation fits. Several possible approaches to the solution of this type of equation are discussed, and the conclusion is that the most widely used methods in practice are variants of the alternating-direction implicit method mainly because of their inherent unconditional stability.

Alternating-direction implicit method

The alternating-direction implicit method is attributed to Peaceman and Rachford (21) and requires the line-by-line solution of small sets of simultaneous equations that can be solved in a non-iterative way. Basically the step Δt forward in time is divided into two half steps each $\Delta t/2$ in length. First a finite difference form of the partial differential equation is written in which the partials with respect to x are replaced in terms of the unknown values of excess minority carrier concentration at $(t_0 + \Delta t/2)$ and the partials with respect to y are

replaced by known values of excess minority carrier concentration at t_0 . This results in an expression that is implicit in the x direction for a given row. Each row results in a set of simultaneous equations that are solved row-by-row over the entire region of interest. Second a finite difference form of the partial differential equation is written in which the partials with respect to y are replaced in terms of the unknown values of excess minority carrier concentration at $(t_0 + \Delta t)$ and the partials with respect to x are replaced by known values of excess minority carrier concentration at $(t_0 + \Delta t/2)$. This results in an expression that is implicit in the y direction for a given column. Each column results in a set of simultaneous equations that are solved column-by-column over the entire region of interest. These two steps taken together complete one step Δt forward in time. This results in a procedure that is alternately implicit on rows for one half time step and implicit on columns for the next half time step, hence the name alternating-direction implicit method.

Many of the symbols and techniques in the following work are similar to those used by Burley (3) who worked out a solution for a heat flow problem in terms of the alternating-direction implicit method. The continuity equation for a P-type base will be considered first so the excess minority carrier concentration will be n. With reference to Figure 11, the two difference equations referred to in the above discussion will be

$$An'_{i-1,j} - Bn'_{i,j} + Cn'_{i+1,j} = -An_{i,j-1} + Bn_{i,j} - Cn_{i,j+1} \quad (27)$$

for the x-implicit half step and

$$A n'_{i,j-1} - B M n'_{i,j} + C n'_{i,j+1} = - A n_{i-1,j} + B M n_{i,j} - C n_{i+1,j} \quad (28)$$

for the y-implicit half step where Equation 27 and 28 must be applied alternately with equal sized steps. The coefficients defined in these two equations are singly subscripted variables since a set of equations is written for each row for the x-iteration and for each column for the y-iteration. For simplicity, the singly subscripted nature of these coefficients is not indicated in the equations. Here the primed value implies that this is the unknown value at the starting time plus a time increment while the unprimed values are the known values at the starting time. Application of Equation 27 to a row or Equation 28 to a column will result in a set of N simultaneous equations in terms of N unknowns that form a tri-diagonal matrix which can be solved by use of the algorithm given by Peaceman and Rachford (21). For $r = 1, 2, \dots, N$ being the N nodes that appear along a given row or column the system of equations that result are shown below, with the subscripts shown being values of r.

$$\begin{aligned} B_1 n'_1 + C_1 n'_2 &= D_1 \\ A_r n'_{r-1} + B_r n'_r + C_r n'_{r+1} &= D_r \quad (2 \leq r \leq N - 1) \\ A_N n'_{N-1} + B_N n'_N &= D_N \end{aligned} \quad (29)$$

The constant A_r is A or A1, C_r is C or C1, B_r is either (- B) or (- BM) depending on which equation is being applied, and D_r is equal to the entire right hand side of whichever equation is being applied. The

algorithm for solution of the system of Equations 29 follows.

$$w_1 = B_1$$

$$w_r = B_r - A_r b_{r-1} \quad (2 \leq r \leq N) \quad (30)$$

$$b_r = C_r / w_r \quad (1 \leq r \leq N - 1) \quad (31)$$

$$g_1 = D_1 / w_1$$

$$g_r = (D_r - A_r g_{r-1}) / w_r \quad (2 \leq r \leq N) \quad (32)$$

The solution is

$$n'_N = g_N$$

$$n'_r = g_r - b_r n'_{r+1} \quad (1 \leq r \leq N - 1) \quad (33)$$

Equations 30 through 32 are calculated in order of increasing r and Equation 33 in order of decreasing r . One complete iteration consists of two equal half steps where the first is the x -implicit half step for which Equation 29 is written and solved by the given algorithm row-by-row over the entire region of interest, and the second is the y -implicit half step for which Equation 29 is written and solved column-by-column over the entire region of interest. The general flow diagram for the iteration program for either base 1 or base 2 is shown in Figure 13, though in actuality two different programs were used due to the differences in coefficients for the two bases.

Finite difference form of the continuity equation

The mesh points formed by the horizontal and vertical grid lines shown in Figure 11 will be the points at which the approximation to the exact solution of the continuity equation will be found. For each mesh

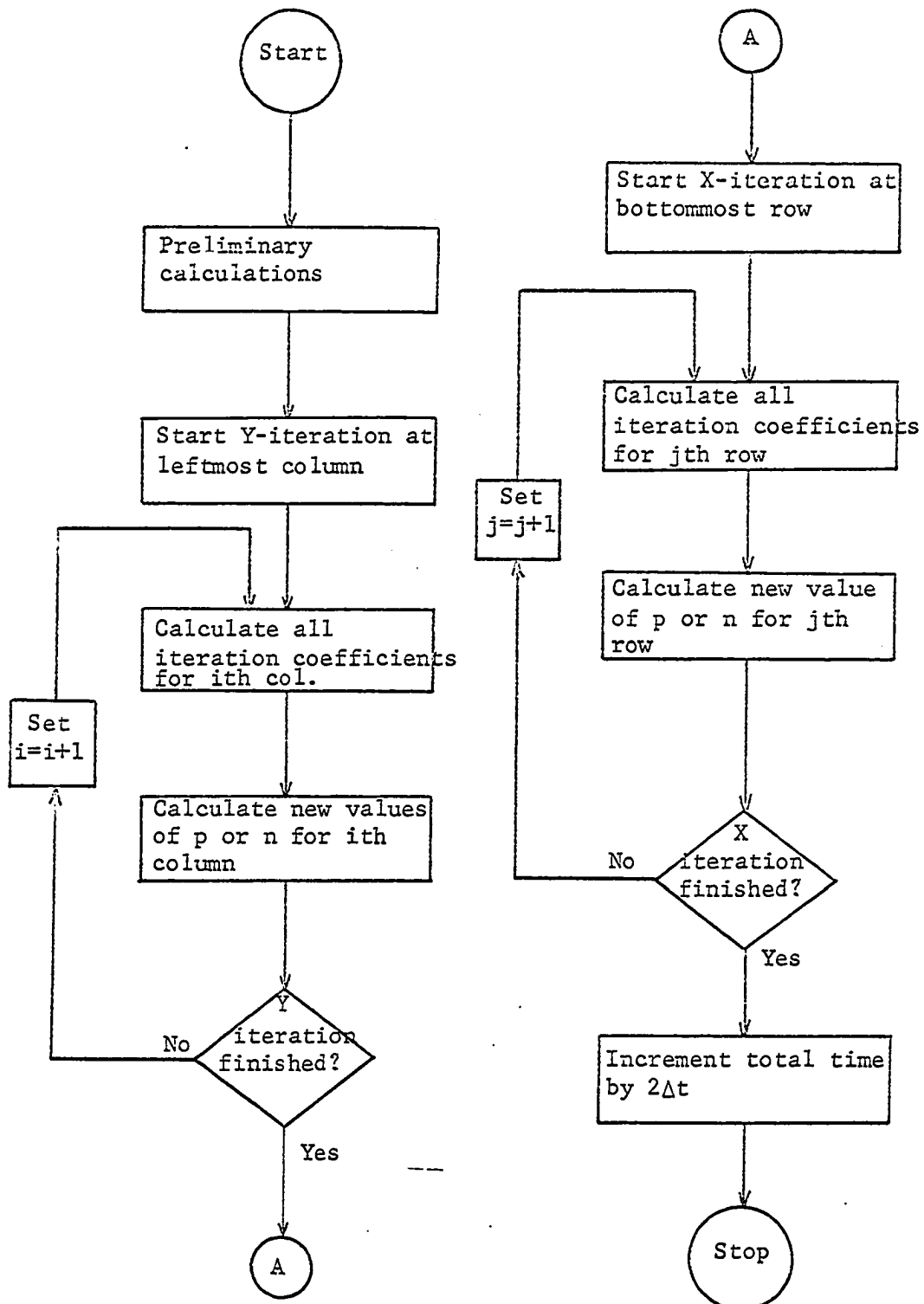


Figure 13. Flow diagram of continuity equation iteration program

point there is an associated mesh region $r_{i,j}$ with a width of Δx and a height of Δy as shown in Figure 14 for an interior mesh point. In Figure 14, Δx and Δy are shown divided into two equal parts. This results when assuming a uniform mesh spacing that is a convenient, but not necessary, assumption. For each mesh point at which the value of $n_{i,j}$ for base 1 or $p_{i,j}$ for base 2 is unknown, the continuity equation is integrated over the mesh region $r_{i,j}$. The excess minority carrier concentration will be known along the junctions as a result of the base bias calculations.

The region of P-type base 1 will be considered first. In this region there is in general a concentration of minority carriers that is high at the emitter and low at the collector. The majority carriers that must be supplied to the base to maintain approximate space charge neutrality will also have a gradient from base to emitter tending to set up a diffusion flow of holes from emitter to base which would carry the holes away from the emitter and destroy the space charge neutrality. Equilibrium is reached when there is a small unbalance of charge density that sets up an electric field tending to cause holes to move from collector to emitter, and the diffusion of majority carriers in one direction is just canceled by the drift of majority carriers in the opposite direction. The small electric field is in such a direction as to aid the diffusion flow of minority carriers. If the majority carrier current density i_p is taken as zero, and the electric field is eliminated between Equations 16 and 17, the value of minority carrier current density is

$$\vec{i}_n = q \left(1 + \frac{n}{n + N_A} \right) D_n \vec{\nabla} n \quad (34)$$

The quantity inside the bracket is seen to be unity for $n \ll N_A$ and to be two for values of $n \gg N_A$. Thus the result of the small electric field that arises due to the causes just discussed is to cause the effective diffusion constant to double for very high injection levels. This effect is important only at high injection levels. The value inside the brackets is defined as

$$g = 1 + \frac{n}{n + N_A} \quad (35)$$

where g is a function of time and position.

The result of the combination of the continuity equation and the minority current density equation with g present to account for high injection levels for base 1 is

$$\frac{\partial n}{\partial t} = - \frac{n}{\tau_n} + D_n \vec{\nabla} \cdot (g \vec{\nabla} n) \quad (36)$$

Here g takes care of the variation of the effective diffusion constant between D_n and $2D_n$ so that D_n itself can be considered a constant. If the following relationships are defined

$$x = LX, \quad y = LY, \quad t = L^2 T / D_n, \quad \text{and} \quad \lambda = L^2 / \tau_n D_n \quad (37)$$

where L is the width of the device and X, Y , and T are nondimensional variables, the continuity equation can now be rewritten as

$$\frac{\partial n}{\partial T} = - \lambda n + \vec{\nabla}' \cdot (g \vec{\nabla}' n) \quad (38)$$

where $\vec{\nabla}'$ has partials with respect to X and Y . In order to get the finite difference approximation for Equation 38, integration over a given

mesh region $r_{i,j}$ is given as

$$\iint_{r_{i,j}} \frac{\partial n}{\partial T} dXdY = \iint_{r_{i,j}} (-\lambda n) dXdY + \iint_{r_{i,j}} \vec{\nabla}' \cdot (g \vec{\nabla}' n) dXdY \quad (39)$$

If Green's theorem in the plane is applied to the final term in Equation 39 the result is

$$\begin{aligned} \iint_{r_{i,j}} \vec{\nabla}' \cdot (g \vec{\nabla}' n) dXdY &= \iint_{r_{i,j}} \left[\frac{\partial}{\partial X} \left(g \frac{\partial n}{\partial X} \right) + \frac{\partial}{\partial Y} \left(g \frac{\partial n}{\partial Y} \right) \right] dXdY \\ &= \int_C \left[g \frac{\partial n}{\partial X} dY - g \frac{\partial n}{\partial Y} dX \right] \end{aligned} \quad (40)$$

The final form is a line integral to be taken around the contour of $r_{i,j}$ in such a direction that the region $r_{i,j}$ is on the left as advance in the positive direction along the curve is made.

As an illustration of the derivation of the finite difference equation from Equation 39, the necessary details for an internal node as shown in Figure 14 for the X-implicit half time step will be worked out for base 1. The partial with respect to time term can be approximated as

$$\iint_{r_{i,j}} \frac{\partial n}{\partial T} dXdY = \frac{n'_{i,j} - n_{i,j}}{\Delta T} \Delta X \Delta Y \quad (41)$$

where the primed value is the unknown value at $(T_0 + \Delta T)$ and the unprimed value is the known value at T_0 . The term representing volume recombination can be approximated by using the average value of $n_{i,j}$ over the time increment ΔT .

$$\iint_{r_{i,j}} (-\lambda n) dXdY = -\lambda \left(\frac{n'_{i,j} + n_{i,j}}{2} \right) \Delta X \Delta Y \quad (42)$$

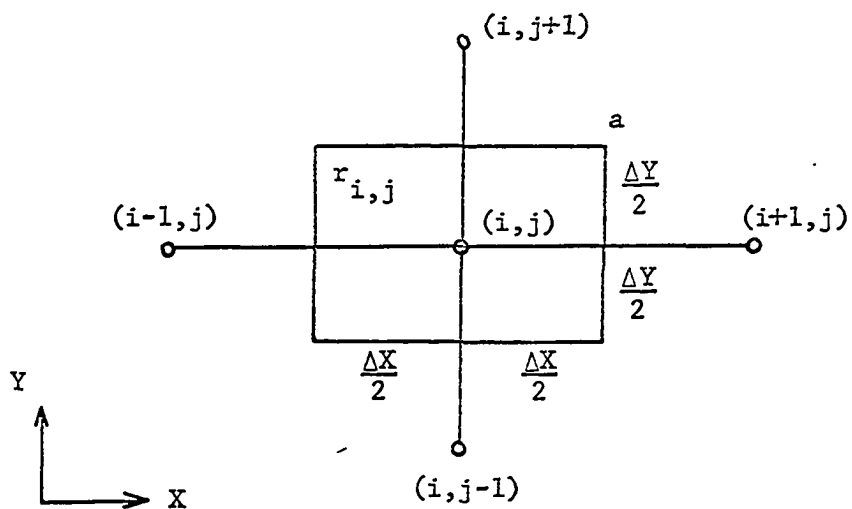


Figure 14. An interior grid point (i,j) surrounded by four grid points

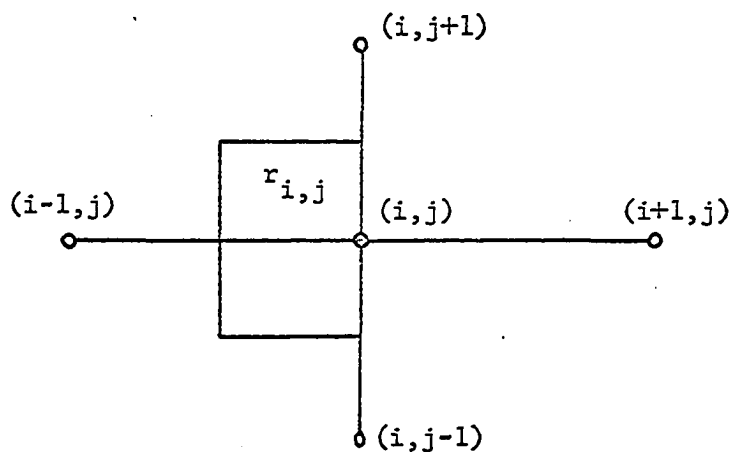


Figure 15. A grid point on the exterior base surface

The contour integral starting at "a" and going in a counterclockwise direction around $r_{i,j}$ gives

$$\begin{aligned}
 \oint_C \left(g \frac{\partial n}{\partial X} dY - g \frac{\partial n}{\partial Y} dX \right) &= g_{i,j} \left(\frac{n_{i,j+1} - n_{i,j}}{\Delta Y} \right) \Delta X \\
 &+ g_{i,j} \left(\frac{n'_{i-1,j} - n'_{i,j}}{\Delta X} \right) \Delta Y \\
 &+ g_{i,j} \left(\frac{n_{i,j-1} - n_{i,j}}{\Delta Y} \right) \Delta X \\
 &+ g_{i,j} \left(\frac{n'_{i+1,j} - n'_{i,j}}{\Delta X} \right) \Delta Y
 \end{aligned} \tag{43}$$

If all the terms of Equations 41, 42, or 43 are gathered into the form shown in Equation 27, the results for the coefficients are

$$A = g_{i,j} \frac{\Delta Y}{\Delta X}, \quad B = 2g_{i,j} \frac{\Delta Y}{\Delta X} + \frac{\Delta X \Delta Y}{\Delta T} + \frac{\lambda \Delta X \Delta Y}{2}, \quad C = g_{i,j} \frac{\Delta Y}{\Delta X} \tag{44}$$

$$A1 = g_{i,j} \frac{\Delta X}{\Delta Y}, \quad B1 = 2g_{i,j} \frac{\Delta X}{\Delta Y} - \frac{\Delta X \Delta Y}{\Delta T} + \frac{\lambda \Delta X \Delta Y}{2}, \quad C1 = g_{i,j} \frac{\Delta X}{\Delta Y}$$

The details on the Y-implicit difference equation for the internal node for base 1 will be found in Table 1.

The X-implicit finite difference equation for base 1 will now be considered for a node that is on the right external surface of the base as shown in Figure 15. The partial with respect to time term will be simply

$$\iint_{r_{i,j}} \frac{\partial n}{\partial T} dXdY = \left(\frac{n'_{i,j} - n_{i,j}}{\Delta T} \right) \frac{\Delta X \Delta Y}{2} \tag{45}$$

The next term to be considered is the volume recombination term. The result for this term is

$$\iint_{r_{i,j}} (-\lambda n) dXdY = -\lambda \left(\frac{n'_{i,j} + n_{i,j}}{2} \right) \frac{\Delta X \Delta Y}{2} \quad (46)$$

The contour integral is the term that is effected by the boundary condition at the external surface as given by Equation 20 in terms of the appropriate minority carrier concentration for base 1.

$$\begin{aligned} \int_C \left(g \frac{\partial n}{\partial X} dY - g \frac{\partial n}{\partial Y} dX \right) &= g_{i,j} \left(\frac{n_{i,j+1} - n_{i,j}}{\Delta Y} \right) \frac{\Delta X}{2} \\ &+ g_{i,j} \left(\frac{n'_{i-1,j} - n'_{i,j}}{\Delta X} \right) \Delta Y \\ &+ g_{i,j} \left(\frac{n_{i,j-1} - n_{i,j}}{\Delta Y} \right) \frac{\Delta X}{2} \\ &- \frac{S}{D_n} n'_{i,j} \Delta Y \end{aligned} \quad (47)$$

If all the coefficients of the various terms are gathered together, the values for A, B, C, A1, B1, and C1 for this particular type of node are

$$A = g_{i,j} \frac{\Delta Y}{\Delta X}, \quad B = g_{i,j} \frac{\Delta Y}{\Delta X} + \frac{\Delta X \Delta Y}{2\Delta T} + \frac{\lambda \Delta X \Delta Y}{4} + \frac{S \Delta Y}{D_n}, \quad C = 0 \quad (48)$$

$$A1 = g_{i,j} \frac{\Delta X}{2\Delta Y}, \quad B1 = g_{i,j} \frac{\Delta X}{\Delta Y} - \frac{\Delta X \Delta Y}{2\Delta T} + \frac{\lambda \Delta X \Delta Y}{4}, \quad C1 = g_{i,j} \frac{\Delta X}{2\Delta Y}$$

The details on the y-implicit difference equation for this type of surface node will be found in Table 1.

For base 1 of the devices shown in Figures 6 and 7 there are various types of nodal points to handle, and the different types are assigned identification numbers. Table 1 shows the assigned numbers and gives a description either in words or a node picture, in which an area labeled

Table 1. Node identification and values for iteration coefficients for base 1

Node ID No.	Node Description	A	C	A1	C1	M	N	B	B1
1	$\begin{array}{c c} 0 & 1 \\ \hline 0 & 1 \end{array}$	0	TYOX	XOY	XOY	$\frac{1}{2} M_1$	$\frac{1}{2} N_1$	B+S ₃	B1
2	First 1 node below center junction	X-Iteration: Node 1 equation as it stands Y-Iteration: Node 1 equation, C1 $n'_{i,j+1}$ included in H as a known quantity							
3	First 1 node above J _{e1} junction	X-Iteration: Node 1 equation as it stands Y-Iteration: Node 1 equation, A1 $n'_{i,j-1}$ included in H as a known quantity							
4	$\begin{array}{c c} 1 & 0 \\ \hline 1 & 0 \end{array}$	TYOX	0	XOY	XOY	$\frac{1}{2} M_1$	$\frac{1}{2} N_1$	B+S ₃	B1
5	First 4 node below center jct.	X-Iteration: Node 4 equation as it stands Y-Iteration: Node 4 equation, C1 $n'_{i,j+1}$ included in H as a known quantity							
6	$\begin{array}{c c} 1 & 0 \\ \hline 0 & 0 \end{array}$	YOX	0	0	XOY	$\frac{1}{4} M_1$	$\frac{1}{4} N_1$	B+ $\frac{1}{2}$ S ₃	B1+ $\frac{1}{2}$ S ₁
7	$\begin{array}{c c} 1 & 1 \\ \hline 0 & 0 \end{array}$	YOX	YOX	0	TXOY	$\frac{1}{2} M_1$	$\frac{1}{2} N_1$	B	B1+S ₁
8	First 7 node right of center jct.	X-Iteration: Node 7 equation, A $n'_{i-1,j}$ included in H as a known quantity Y-Iteration: Node 7 equation as it stands							
9	First 10 node above J _{e1} junction	X-Iteration: Node 10 equation as it stands Y-Iteration: Node 10 equation, A1 $n'_{i,j-1}$ included H as a known quantity							

Table 1 (Continued)

Node ID No.	Node Description	A	C	A1	C1	M	N	B	B1
10	$\begin{array}{c c} 1 & 1 \\ \hline 1 & 1 \end{array}$	TYOX	TYOX	TXOY	TXOY	M_1	N_1	B	B1
11	First 10 node below center jct.	X-Iteration: Node 10 equation as it stands Y-Iteration: Node 10 equation, C1 $n'_{i,j+1}$ included in H as a known quantity							

1 is inside the base region while an area labeled 0 is outside, for the necessary node types of base 1. For the X-iteration

$$H = A n_{i,j-1} - B n_{i,j} + C n_{i,j+1} \quad (49)$$

and for the Y-iteration

$$H = A n_{i-1,j} - B m_{i,j} + C n_{i+1,j} \quad (50)$$

The coefficients of Equations 27 and 28 are defined in Table 1 for base 1 in terms of the following defined parameters:

$$\begin{aligned} S_1 &= S \Delta X / D_n, \quad S_3 = S \Delta Y_1 / D_n, \quad M_1 = \Delta X \Delta Y_1 / \Delta T, \quad N_1 = \Delta X \Delta Y_1 / 2 \\ YOX &= g_{i,j} \Delta Y_1 / 2 \Delta X, \quad XOY = g_{i,j} \Delta X / 2 \Delta Y_1, \quad TYOX = 2 YOX, \quad TXOY = 2 XOY \end{aligned} \quad (51)$$

$$B = A + C + M + N, \quad BM = B - 2M, \quad B1 = A1 + C1 - M + N,$$

$$BM1 = B1 + 2M$$

For base 2, the result of the combination of the continuity equation and the minority carrier current density equations is

$$\frac{\partial p}{\partial t} = - \frac{p}{\tau_p} - \mu_p \vec{E} \cdot \vec{\nabla} (p + p_n) + D_p \vec{\nabla} \cdot (\vec{\nabla} p) \quad (52)$$

If non-dimensional variables are again defined

$$\begin{aligned} x &= LX, \quad y = LY, \quad t = L^2 T / D_n, \quad \lambda_1 = L^2 / D_p \tau_p, \\ \lambda_2 &= L \mu_p / D_p, \quad A_T = D_n / D_p \end{aligned} \quad (53)$$

and the continuity equation is rewritten, the result is

$$A_T \frac{\partial p}{\partial T} = - \lambda_1 p - \lambda_2 \vec{E} \cdot \vec{\nabla}' p + \vec{\nabla}' \cdot (\vec{\nabla}' p) \quad (54)$$

where the ∇' operator has partials with respect to X and Y. The A_T constant is necessary so that the time variable T is the same for both base regions.

When base 2 of the device is considered, the electric field present cannot be handled in terms of the g parameter since the majority carrier current flow cannot be considered negligible in this relatively low alpha base. The only type of term for the continuity equation for the base 2 region given as Equation 54 that is different from the types of terms handled for the base 1 region is the one containing the electric field. This term can be rewritten in the form

$$\iint_{r_{i,j}} (-\lambda_2 \vec{E} \cdot \vec{\nabla}' p) dXdY = -\lambda_2 \iint_{r_{i,j}} [\vec{E} \cdot \vec{\nabla}' (p + p_n) + (p + p_n) \vec{\nabla}' \cdot \vec{E}] dXdY \quad (55)$$

Now, when $\vec{\nabla}' \cdot \vec{E}$ is of appreciable size, it is reasonable to assume that the excess minority carrier concentration p is much greater than the equilibrium minority carrier concentration p_n . Equation 55 can then be rewritten as

$$\iint_{r_{i,j}} (-\lambda_2 \vec{E} \cdot \vec{\nabla}' p) dXdY = -\lambda_2 \iint_{r_{i,j}} [E_x \frac{\partial p}{\partial X} + E_y \frac{\partial p}{\partial Y} + p \frac{\partial E_x}{\partial X} + p \frac{\partial E_y}{\partial Y}] dXdY \quad (56)$$

When this term is written in its finite-difference form for an internal node for the x -iteration the result is

$$\begin{aligned}
\iint_{r_{i,j}} (-\lambda_2 \vec{E} \cdot \vec{\nabla}' p) dXdY = & p'_{i-1,j} \left(\frac{\lambda_2 \Delta Y_2}{4} \right) (E_{x_{i,j}} + E_{x_{i,1,j}}) \\
& - p'_{i,j} \left(\frac{\lambda_2 \Delta X}{4} \right) (E_{y_{i,j+1}} - E_{y_{i,j-1}}) \\
& - p'_{i+1,j} \left(\frac{\lambda_2 \Delta Y_2}{4} \right) (E_{x_{i+1,j}} + E_{x_{i,j}}) \\
& + p_{i,j-1} \left(\frac{\lambda_2 \Delta X}{4} \right) (E_{y_{i,j}} + E_{y_{i,j-1}}) \\
& - p_{i,j} \left(\frac{\lambda_2 \Delta Y_2}{4} \right) (E_{x_{i+1,j}} - E_{x_{i-1,j}}) \\
& - p_{i,j+1} \left(\frac{\lambda_2 \Delta X}{4} \right) (E_{y_{i,j+1}} + E_{y_{i,j}}) \quad (57)
\end{aligned}$$

The details of handling all the other terms is exactly the same as was done earlier for the base 1 region and will not be repeated here.

The general form of the finite difference equations for base 2 is exactly the same as Equations 27, 28, 49, and 50 with n replaced by p since the excess minority carriers are holes in base 2. As in base 1, there are various types of nodes to be handled so identification numbers are assigned to these nodes. The coefficients of the finite difference equations are defined in Equation 58 and in Table 2 in terms of the following defined parameters:

$$S2_3 = S\Delta Y_2 / D_p, M_2 = A_T \Delta X \Delta Y_2 / \Delta T, N_2 = \lambda_1 \Delta X \Delta Y_2 / 2$$

$$YOX_2 = \Delta Y_2 / 2\Delta X, XOY_2 = \Delta X / 2\Delta Y_2, TYOX_2 = 2YOX_2, TXOY_2 = 2XOY_2$$

$$FYOX_2 = 4YOX_2, FXOY_2 = 4XOY_2, BM = B - 2M, BM1 = B1 + 2M$$

Table 2. Node identification and values for iteration coefficients for base 2

Node ID No.	Node Description	A	C	A1	C1	M	N	B	B1
1	$\begin{array}{c c} 0 & 1 \\ \hline 0 & 1 \end{array}$	0	TYOX2 -C11	XOY2 -SCJL/2	XOY2 -SCJT/2	$M_2/2$	$N_2/2$	TYOX ₂ +S2 ₃ +M+N +(SCJT-SCJL)/2	TXOY ₂ -M+N +CM ₁₁
2	First 1 node below S.C. or J _{e1}	X-Iteration:	Node 1 equation as it stands						
		Y-Iteration:	Node 1 equation, Clp' _{i,j+1} included in H as a known quantity						
3	First 1 node above center jct.	X-Iteration:	Node 1 equation as it stands						
		Y-Iteration:	Node 1 equation, Alp' _{i,j-1} included in H as a known quantity						
4	$\begin{array}{c c} 1 & 0 \\ \hline 1 & 0 \end{array}$	TYOX ₂ +A11	0	XOY ₂ +SCJL/2	XOY ₂ -SCJT/2	$M_2/2$	$N_2/2$	TYOX ₂ +S2 ₃ +M+N +(SCJT-SCJL)/2	TXOY ₂ +S2 ₃ -M+N+AM ₁₁
5	First 4 node below J _{e2} junction	X-Iteration:	Node 4 equation as it stands						
		Y-Iteration:	Node 4 equation, Clp' _{i,j+1} included in H as a known quantity						
6	First 4 node above center jct	X-Iteration:	Node 4 equation as it stands						
		Y-Iteration:	Node 4 equation, Alp' _{i,j-1} included in H as a known quantity						
7	First 10 node left of known node	X-Iteration:	Node 10 equation, Cp' _{i+1,j} included in H as a known quantity						
		Y-Iteration:	Node 10 equation as it stands						
8	First 10 node below left of known	X-Iteration:	Node 10 equation, Cp' _{i+1,j} included in H as a known quantity						
		Y-Iteration:	Node 10 equation, Clp' _{i,j+1} included in H as a known quantity						

Table 2 (Continued)

Node ID No.	Node Description	A	C	A1	C1	M	N	B	B1	
9	First 10 node above center jct.	X-Iteration:	Y-Iteration:	Node 10 equation as it stands						Node 10 equation, $Alp'_{i,j-1}$ included in H as a known quantity
10	$\frac{1}{1} \mid \frac{1}{1}$	$TYOX_2 + A_{11}$	$TYOX_2 - C_{11}$	$TXOY_2 + SCJL$	$TXOY_2 - SCJT$	M_2	N_2	$FYOX_2 + M + N + SCJT - SCJL$	$FXOY_2 - M + N + C_{11} - A_{11}$	
11	First 10 node below a known node	X-Iteration:	Y-Iteration:	Node 10 equation as it stands						Node 10 equation, $C1p'_{i,j+1}$ included in H as a known quantity

$$\begin{aligned}
A_{11} &= (\lambda_2 \Delta Y_2 / 4) (E_{x_{i,j}} + E_{x_{i-1,j}}), \quad C_{11} = (\lambda_2 \Delta Y_2 / 4) (E_{x_{i+1,j}} \\
&\quad + E_{x_{i,j}}) \\
AM_{11} &= A_{11} - \lambda_2 \Delta Y_2 E_{x_{i-1,j}} / 2, \quad CM_{11} = C_{11} - \lambda_2 \Delta Y_2 E_{x_{i,j}} / 2 \\
SCJL &= (\lambda_2 \Delta X / 4) (E_{y_{i,j}} + E_{y_{i,j-1}}), \\
SCJT &= (\lambda_2 \Delta X / 4) (E_{y_{i,j+1}} E_{y_{i,j}}) \quad (58)
\end{aligned}$$

The terms A_{11} , AM_{11} , C_{11} , and CM_{11} are singly subscripted variables while $SCJL$ and $SCJT$ are doubly subscripted variables. It has been assumed that the electric field in the x-direction does not vary as a function of y, but to take into account the effects of volume recombination in a wide base region the electric field in the y-direction is assumed to be a function of both x and y.

PERFORMANCE OF THE MATHEMATICAL MODEL

The accuracy of the finite difference solution to the partial differential equation is of interest and must be considered. The performance of this model can be discussed in terms of the convergence and stability of the finite difference method used. As defined in the paper by O'Brien et al. (20), the question of convergence is concerned with whether or not the exact solution of the finite difference equation approaches the exact solution of the partial differential equation while the question of stability is concerned with whether or not the numerical solution of the finite difference equation approaches the exact solution of the finite difference equation. In this same paper truncation error is defined as the difference between the exact solution of the finite difference and the partial differential equations while numerical error is defined as the difference between the exact solution and the numerical solution of the finite difference equation. Thus the question of the convergence of a particular iteration scheme is related to truncation error caused by the finite distance between mesh points while the question of stability is related to the numerical errors such as round-off errors.

O'Brien et al. (20) has demonstrated unconditional stability for the alternating direction implicit method for the general parabolic partial differential equation assuming constant boundary conditions and constant coefficients. Lees (11b) has demonstrated unconditional stability for the very general parabolic partial differential equation

$$\frac{\partial u}{\partial t} = \frac{\partial}{\partial x}(a(x,y,t)\frac{\partial u}{\partial x}) + \frac{\partial}{\partial y}(b(x,y,t)\frac{\partial u}{\partial y}) + f(x,y,u,t,\frac{\partial u}{\partial x},\frac{\partial u}{\partial y}) \quad (59)$$

for the alternating direction implicit method. Douglas (4b) has shown that unconditional stability of an iteration method also implies the convergence of that method with proper choice of space and time mesh increments. The continuity equation being worked with is of the general form shown as Equation 59 and thus the alternating direction implicit method used for the continuity equation should be both stable and convergent. Thus the question of convergence and accuracy will depend on the choice of space and time mesh increments.

Once a particular choice of spatial mesh size is made, the accuracy is dependent on the time increment size. In general, for that part of the solution where the quantity being solved for is far from steady state and is varying rapidly the time increment size should be small for best accuracy. When the quantity being solved for is approaching its steady state value the time increment size can be made considerably larger. A precise best choice for the time increment size is very difficult to make, Varga (24). A convenient way to check the accuracy for a particular time increment at any time in the solution is to use a new time increment half, or some other fraction, as large as the old time increment and check the results obtained for both new and old time increments at the same point in time. This approach was used to select the values of the array TM(L), TMAX, and TMAX2 that was used in the computer program for the calculation of the time increment size for the

succeeding step. The rate of change of n in base 1 or p in base 2 was calculated and used as a basis for choosing a particular value of $TM(L)$ which was then used as a multiplier for $TMAX$ or $TMAX2$ as shown in Figure 16. The minimum size of the time increment will ordinarily be limited by consideration of the amount of computer time needed. The cost of greater accuracy as the minimum time increment becomes smaller will be an increase in computer time needed to carry out the solution.

Comparison to Experimental Results

In order to test the capability of the model to predict device behavior, some devices of the form shown in Figure 17 were obtained from Motorola, Inc. with the dimensions given in the figure. The depth of the device into the paper was 0.381 cm. If a comparison between Figure 6 and Figure 17 is made; it is noted that if the device of Figure 17 is divided in half as shown by the dashed line the Motorola device can then be analyzed by means of the computer program for the device of Figure 6. A 10 x 10 grid of mesh lines over each base region was used for both turn-on and turn-off calculations.

Base 2, the N_2 region, is the starting material and is about 25 ohm·cm material. The surface concentrations of the P regions are about 5×10^{18} and of the N_1 region is about 5×10^{20} . Using these values of surface concentrations, when the curves by Irvin (10) are used, the average resistivity of base 1 is found to be approximately 0.33 ohm·cm. Emitter 1, the N_1 region, has a resistivity of about 0.0066 ohm·cm while emitter 2 resistivity is about 0.0577 ohm·cm. The capacitances of the junctions of device 2 were found by measurement with a G. R. 1650

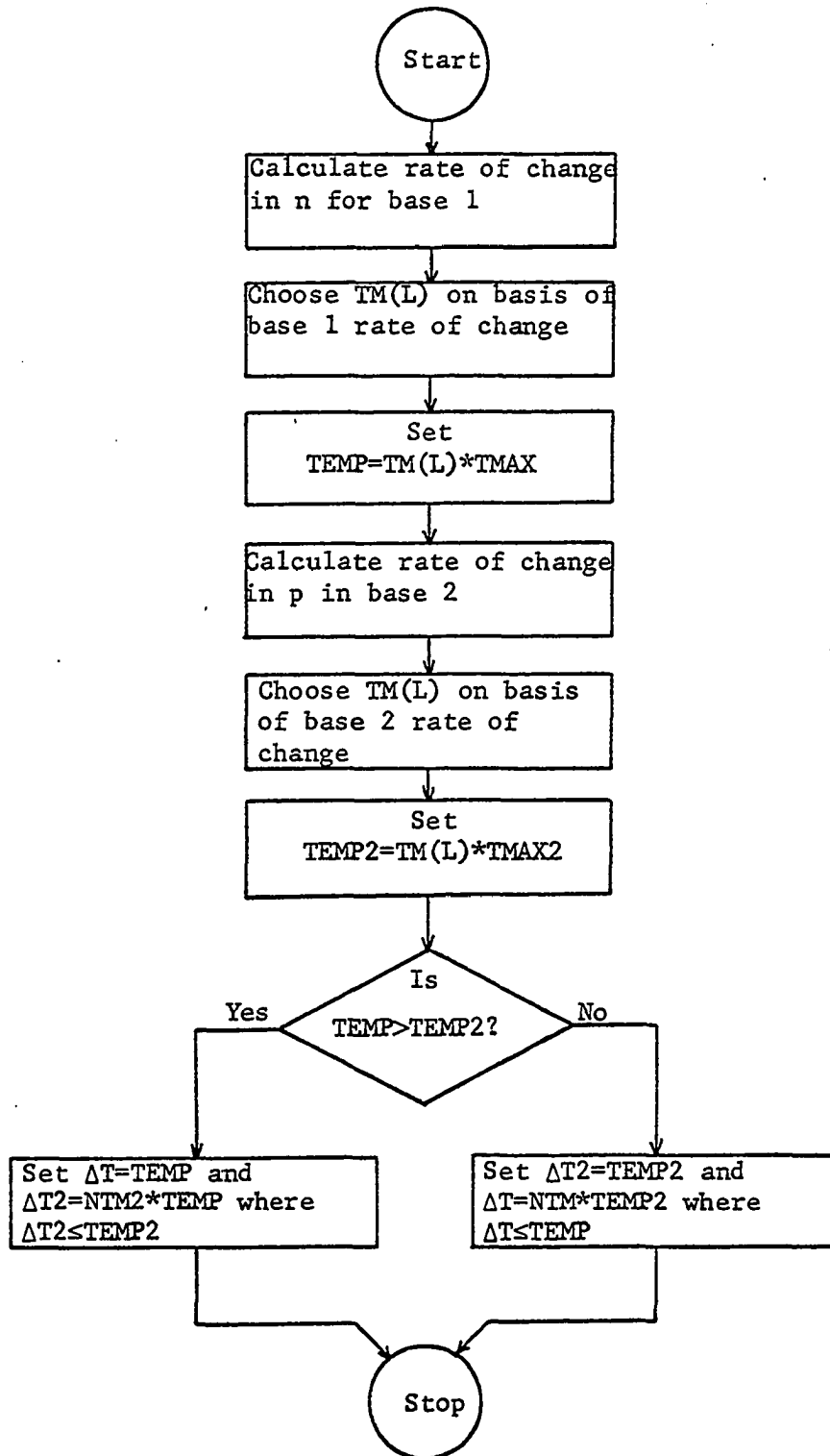


Figure 16. Flow diagram of calculation of time increment program

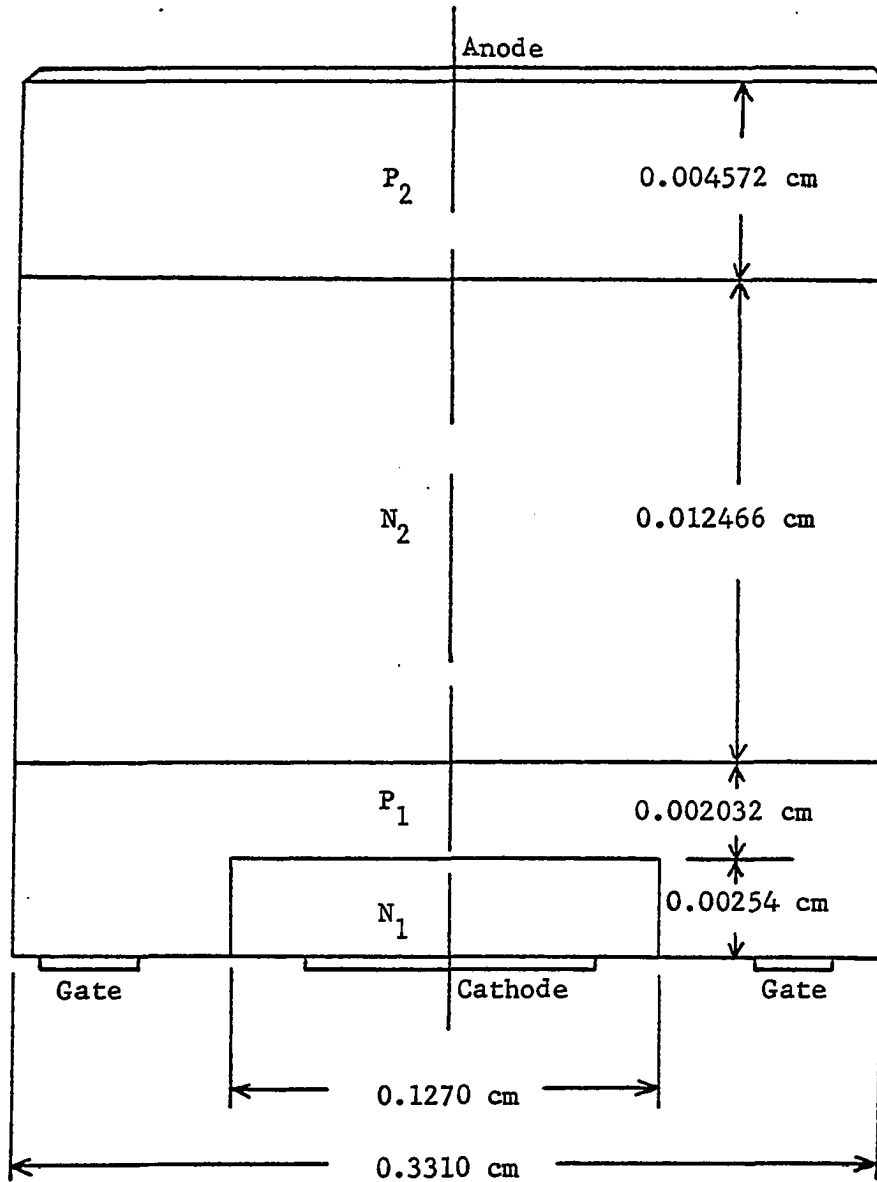


Figure 17. Schematic sketch of the commercial device

impedance bridge to be about $0.1085 \times 10^{-6} \text{ f/cm}^2$ for emitter 1 and about $0.538 \times 10^{-8} \text{ f/cm}^2$ for both the center and emitter 2 junctions, where all these values are for the zero bias case. The values of $\mu_n = 750 \text{ cm}^2/\text{volt}\cdot\text{sec}$, $\mu_p = 500 \text{ cm}^2/\text{volt}\cdot\text{sec}$, $D_n = 19.43 \text{ cm}^2/\text{sec}$, and $D_p = 12.95 \text{ cm}^2/\text{sec}$ were found by use of curves given by Phillips (22a). Since the response of device 2 is the median response of the three devices, the model was set up for comparison to it.

The circuit used for turn-on with reference to Figure 9 had a value R_{EX} of 100 ohms and an E of 20 volts. The model values used were $R_{EX} = 200$ ohms and $E = 20$ volts with the value of R_{EX} doubled to account for the fact that the model would have exactly half as much total current since the actual device is twice as large. The test circuit for turn-on used a pulse for I_g that was 100 ma in magnitude. The value of gate current used to drive the model was 50 ma to account for the fact that the case drive for the model would be only half as much as for the actual device. The response for all of the three devices for turn-on are shown in Figure 18 as solid lines. The model prediction for turn-on is shown as circled dots. The comparison between the curve for device 2 and the model prediction is quite good. The behavior of the voltages $VE(I)$, $VC(I)$, and $CJV(I)$ for turn-on are shown for several values of time as Figure 19. The minority carrier concentration for base 1 along the $I = NIX$ column is shown in Figure 20 and the minority carrier concentration for base 2 along the $I = NIX$ column in Figure 21, both for the turn-on case.

The model was also used to predict the turn-off response of the

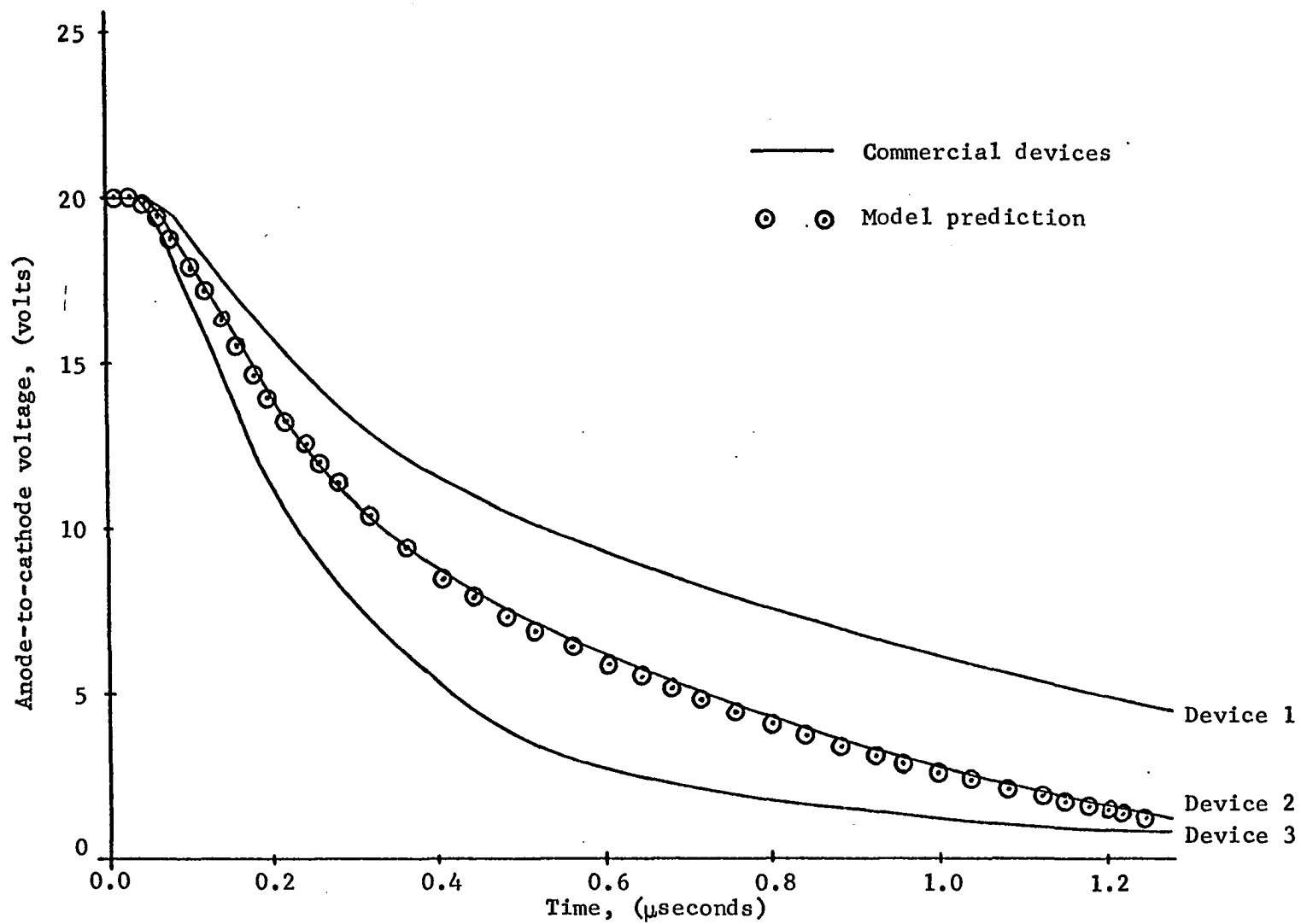


Figure 18. Model prediction and commercial devices turn-on behavior

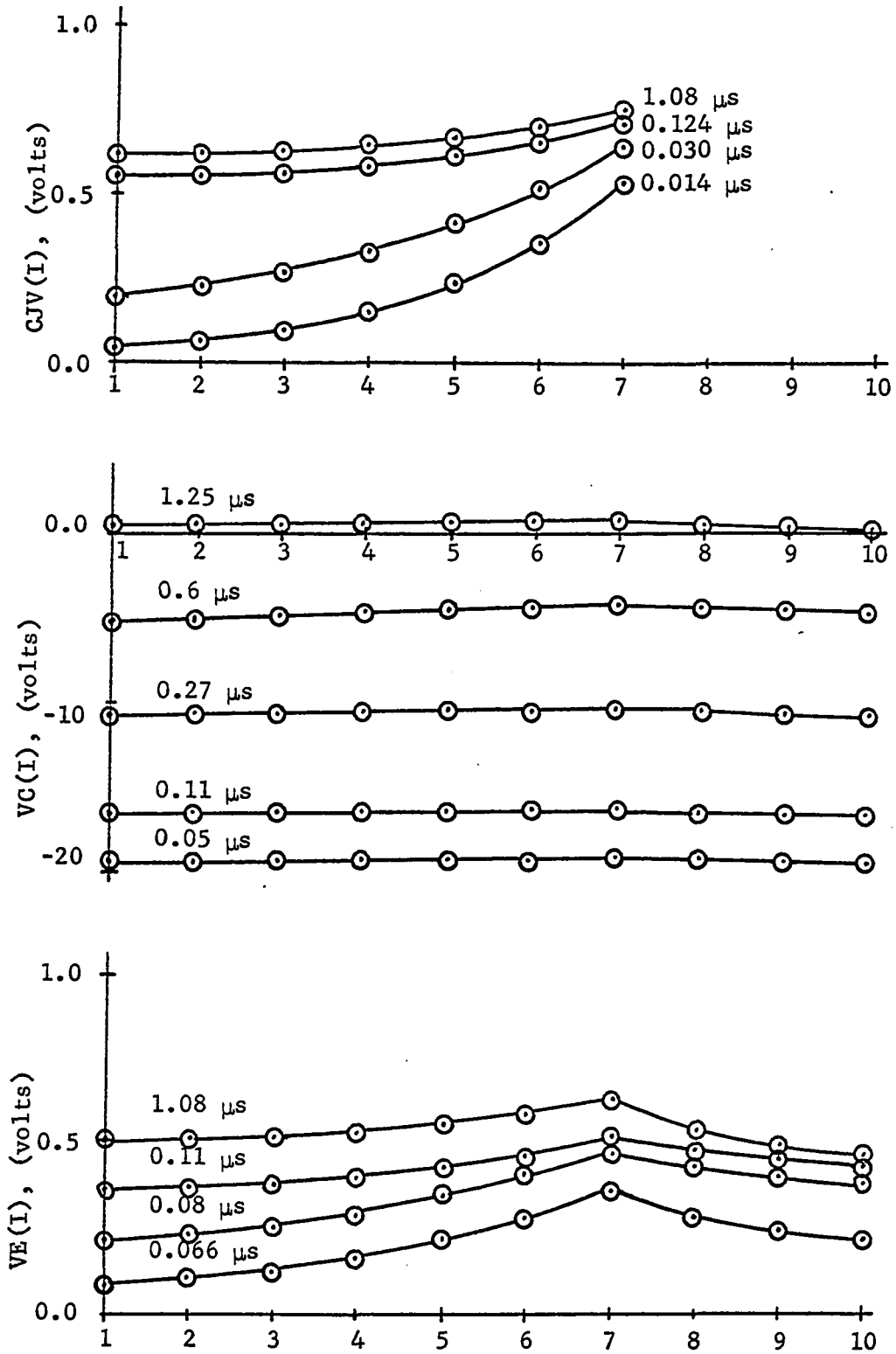


Figure 19. Behavior of junction voltages during turn-on, all versus x-direction mesh lines

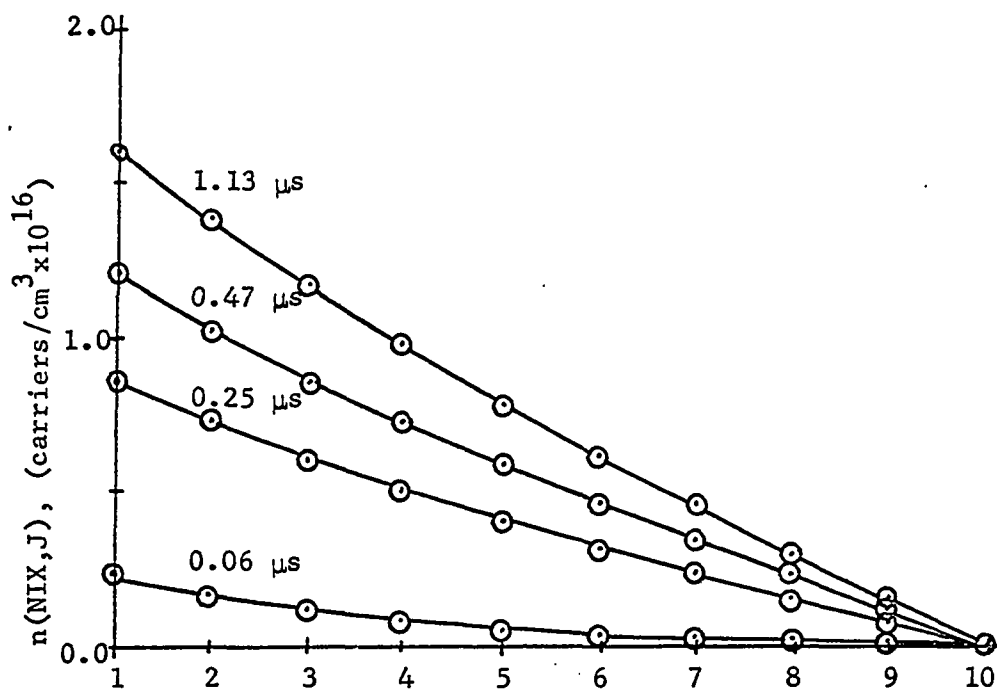


Figure 20. Minority carrier concentration along I=NIX column versus j th row in base 1 for turn-on

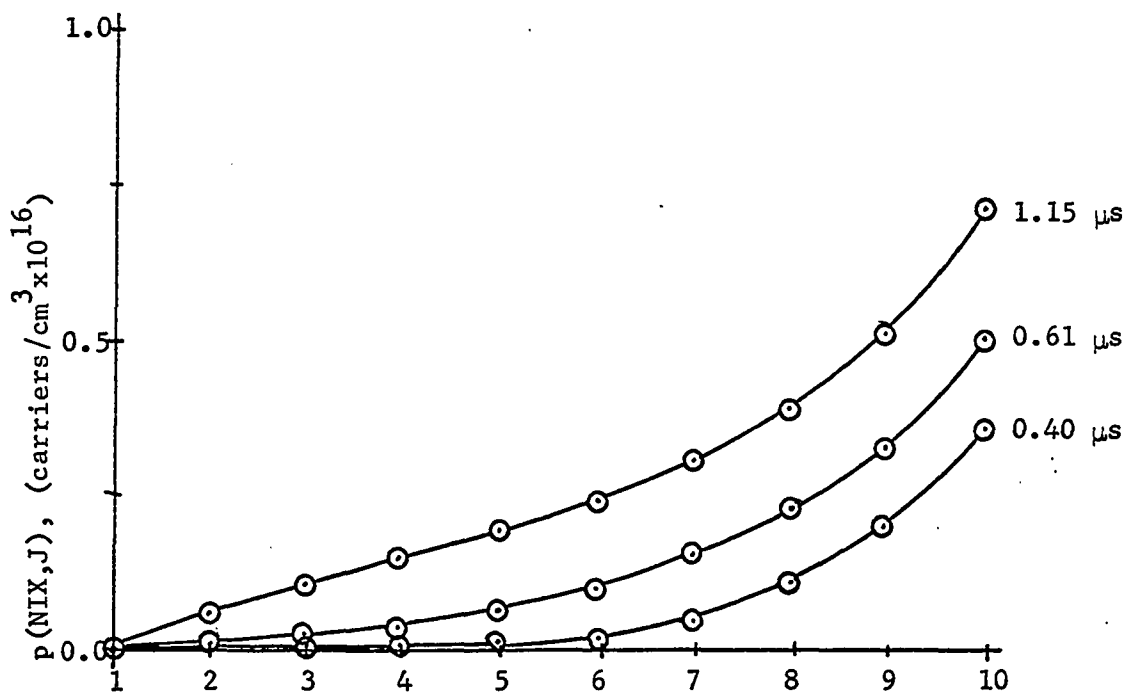


Figure 21. Minority carrier concentration along I=NIX column versus j th row in base 2 for turn-on

same three Motorola devices. The same circuit and external circuit parameters were used with a negative gate pulse of about 70 ma applied to the circuit. The model has a negative gate pulse of about 35 ma to account for the Motorola device being double the model device. The model response and the response of the three devices are all shown in Figure 22. The minority carrier concentration for base 1 along the $I = NIX$ column is shown in Figure 23 and the minority carrier concentration for base 2 along the $I = NIX$ column in Figure 24, both for the turn-off case. The base 2 region caused some difficulty during the early stages of turn-off due to the high resistivity of this base causing very small transverse currents to give a fairly large change in voltage along emitter 2. This problem disappears once the early stage of turn-off is past.

The values of recombination lifetimes for the two base regions were not exactly known, the values used for the model prediction for the response curves shown were $\tau_n = 0.285 \mu s$ for base 1 and $\tau_p = 2.65 \mu s$ for base 2. These values were selected on the basis of getting the best comparison to the response of the commercial devices.

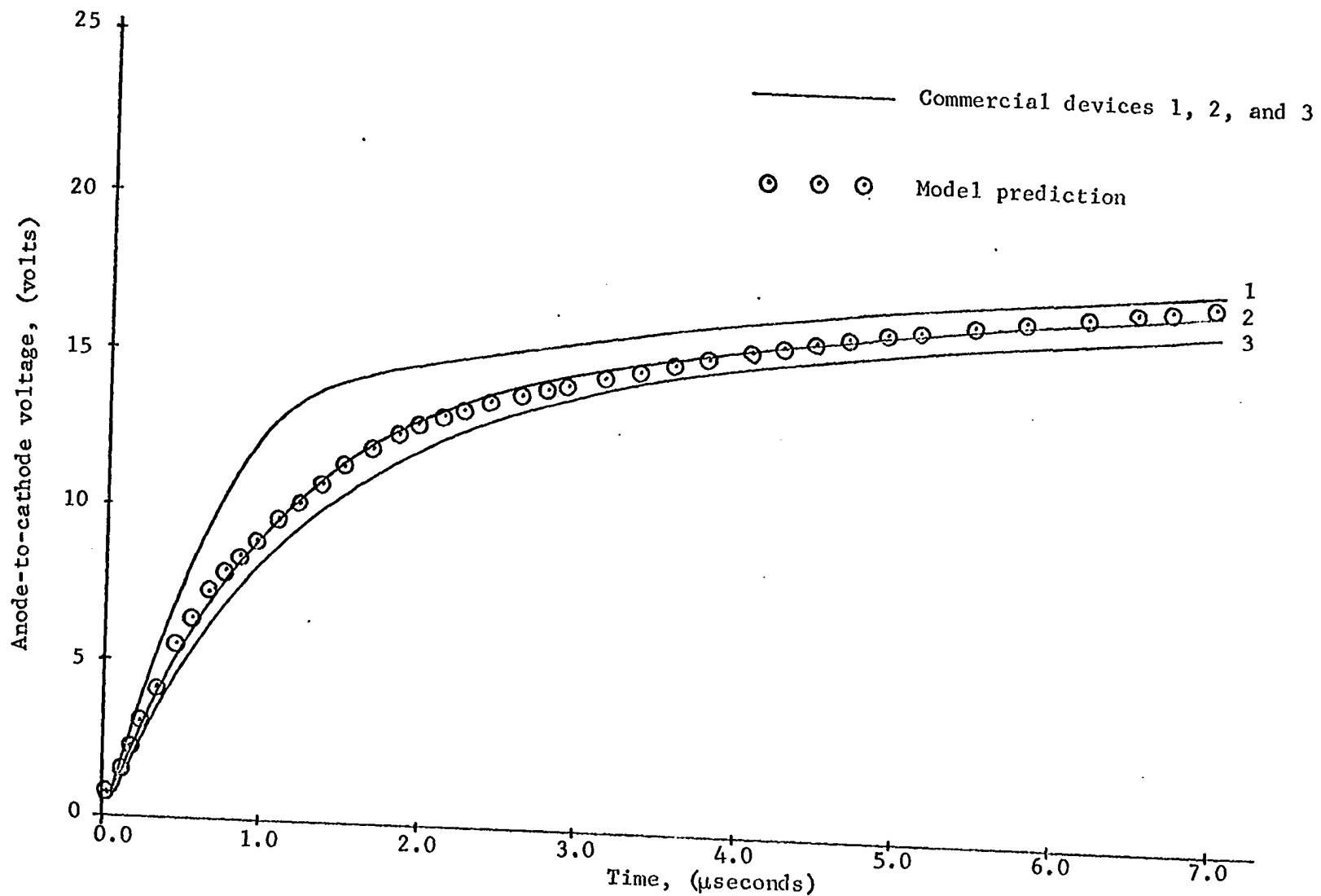


Figure 22. Model prediction and commercial devices turn-off behavior

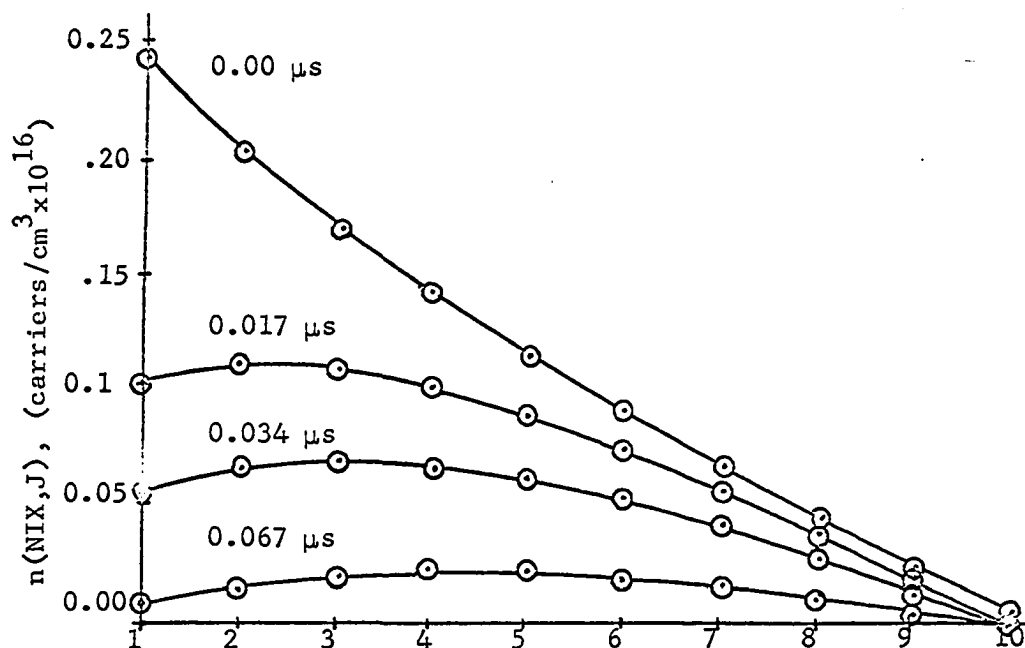


Figure 23. Minority carrier concentration along I = NIX column versus jth row in base 1 for turn-off

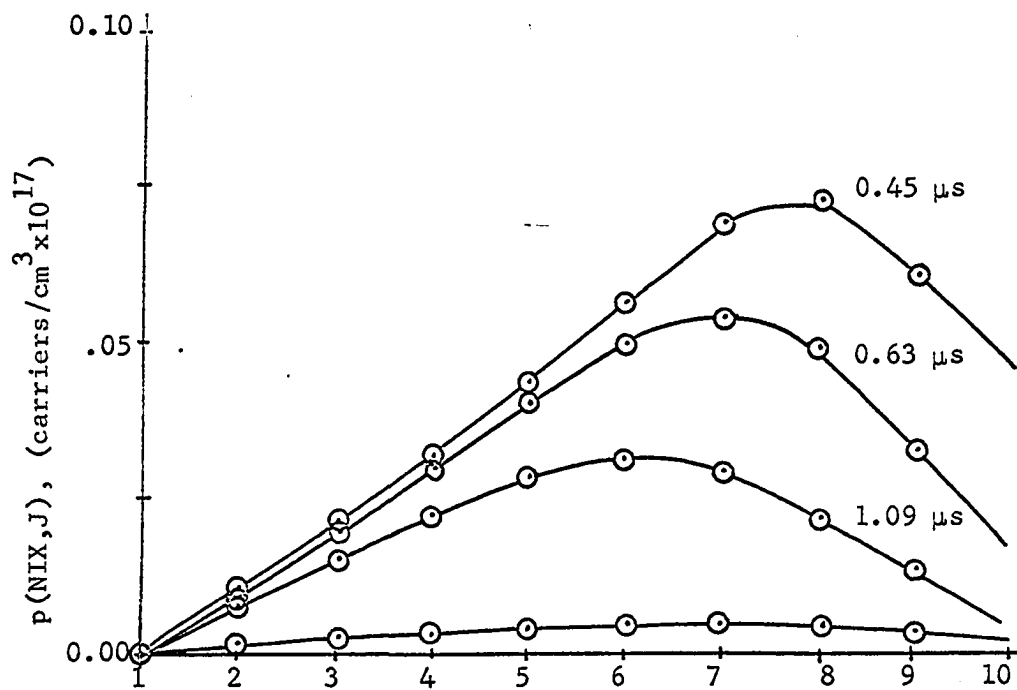


Figure 24. Minority carrier concentration along I = NIX column versus jth row in base 2 for turn-off

SUMMARY AND CONCLUSIONS

The intent of this thesis was to use numerical techniques to model the transient behavior of a three-terminal four-layer p-n-p-n device that is controllable by a gate pulse of current for both turn-on and turn-off. The computer program written for this purpose can be used for the type of device shown as Figure 6 and also for the shorted-emitter type of device shown as Figure 7. The computer program takes into account the transverse variations in voltage and minority carrier concentration in both base 1 and base 2 of both types. It also accounts for conductivity modulation in the base regions as well as electric fields that occur.

The performance of the computer program was tested by comparison to commercial devices obtained from Motorola, Inc. Three devices were tested for both turn-on and turn-off in the circuit of Figure 9 with a d-c voltage of 20 volts and a resistive load of 100 ohms. The computer model prediction and the three device curves are shown on Figure 18 for turn-on. The model prediction compares quite well with the results for device 2 for this case. The results of a turn-off test is shown as Figure 22 where the external circuit source and load are the same values as used for the turn-on test. Again the model prediction compares quite well with the device performance.

The computer program developed in this thesis should be a very useful tool for an aid in the fabrication of devices of this type. By use of the model, an answer could be quickly obtained as to what result the variation of either a dimension or a physical constant of the material would have on the switching behavior of the device. The

relative importance of various physical parameters can also be examined.

The insight that is gained about the functioning of this device is another feature of the use of a model of this type. The allocation of base drive for either base at any point in time is known so that the relative importance of the different junction capacitances, the volume recombination within the base regions, and the supplying of majority carriers to maintain space charge neutrality can easily be seen.

A great deal of time and effort was put into the writing of the computer program used to model this device. There are undoubtedly many improvements that could be made that would allow the program to be faster and more efficient in the calculations that must be gone through, however, the results obtained were good with the program as it stands. The approximate time to go through the bias calculation and the iteration of the finite difference equation for one base for a 10 x 10 spatial mesh on the IBM 360 system was about 1.2 seconds when the center junction was reverse biased. The time required with a forward biased center junction was somewhat higher.

LITERATURE CITED

1. Aldrich, R. W. and N. Holonyak, Jr. Multiterminal p-n-p-n switches. Institute Radio Engineers Proceedings 46: 1236-1239. 1958.
2. Aldrich, R. W. and N. Holonyak, Jr. Two-terminal asymmetrical and symmetrical silicon negative resistance switches. Journal of Applied Physics 30: 1819-1824. 1959.
3. Burley, W. H-104 two-dimensional, transient or steady heat conduction. Hawthorne, N.Y., DP Program Information Dept., International Business Machines. circa 1963.
- 4a. Dodson, W. H. Silicon controlled rectifiers: lateral turn-on velocity, lateral field distribution and lateral skip phenomenon. Unpublished Ph.D. thesis. Pittsburgh, Pennsylvania, Department of Electrical Engineering, Carnegie Institute of Technology. 1965.
- 4b. Douglas, J., Jr. A survey of numerical methods for parabolic differential equations. Advances in Computers 2: 1-54. 1961.
5. Fletcher, N. H. Some aspects of the design of power transistors. Institute Radio Engineers Proceedings 43: 551-559. 1955.
6. Gentry, F. E., F. W. Gutzwiller, N. Holonyak, Jr., and E. E. Von Zastrow. Semiconductor controlled rectifiers: principles and applications of p-n-p-n devices. Englewood Cliffs, N.J., Prentice-Hall, Inc. 1964.
7. Gentry, F. E., R. I. Scace, and J. K. Flowers. Bidirectional triode p-n-p-n switches. Institute of Electrical and Electronic Engineers Proceedings 53: 355-369. 1965.
8. Gibbons, J. F. Semiconductor electronics. New York, N.Y., McGraw-Hill Book Co. 1966.
9. Goldey, J. M., I. M. Mackintosh, and I. M. Ross. Turn-off gain in p-n-p-n triodes. Solid-State Electronics 3: 119-122. 1961.
10. Irvin, J. C. Resistivity of bulk silicon and of diffused layers in silicon. Bell System Technical Journal 41: 387-410. 1962.
- 11a. Jonscher, A. K. Notes on the theory of four-layer semiconductor switches. Solid-State Electronics 2: 143-148. 1961.
- 11b. Lees, M. Alternating direction and semi-explicit difference methods for parabolic partial differential equations. Numerische Mathematik 3: 398-412. 1961.

12. Lesk, I. A. Germanium P-N-P-N switches. Institute of Radio Engineers Transactions on Electron Devices 1, ED-6: 28-34. 1959.
13. Longini, R. L. and J. Melngailis. Gated turn-on of four layer switch. Institute of Electrical and Electronic Engineers Transactions on Electron Devices 3, ED-10: 178-185. 1963.
14. Mackintosh, I. M. The electrical characteristics of silicon p-n-p-n triodes. Institute Radio Engineers Proceedings 46: 1229-1235. 1958.
15. Middlebrook, R. D. An introduction to junction transistor theory. New York, N.Y., John Wiley and Sons, Inc. 1957.
16. Misawa, T. Turn-on transient of p-n-p-n triode. Journal of Electronics and Control 7: 523-533. 1959.
17. Moll, J. L., M. Tanenbaum, J. M. Goldey, and N. Holonyak, Jr. P-n-p-n transistor switches. Institute Radio Engineers Proceedings 44: 1174-1182. 1956.
18. Moyson, J. and J. Petruzella. Investigation of electronically controllable turn-off controlled rectifiers. General Electric Co. Rectifier Components Department Report 4: 1-75. 1961.
19. Mueller, C. W. and J. Hilibrand. The "thyristor": a new high-speed switching transistor. Institute Radio Engineers Transactions on Electron Devices 1, ED-5: 2-5. 1958.
20. O'Brien, G. G., M. A. Hyman, and S. Kaplan. A study of the numerical solution of partial differential equations. Journal of Mathematics and Physics 29: 223-251. 1951.
21. Peaceman, D. W. and H. H. Rachford, Jr. The numerical solutions of parabolic and elliptic differential equations. Journal of the Society for Industrial and Applied Mathematics 3: 28-41. 1955.
- 22a. Phillips, A. B. Transistor engineering and introduction to integrated semiconductor circuits. New York, N.Y., McGraw-Hill Book Co. 1962.
- 22b. Sah, C. T., R. N. Noyce, and W. Shockley. Carrier generation and recombination in p-n junctions and p-n junction characteristics. Institute Radio Engineers Proceedings 45: 1228-1243. 1957.
23. Shockley, W. Electrons and holes in semiconductors. New York, N.Y., D. Van Nostrand Company, Inc. 1950.
24. Varga, R. S. Matrix iterative analysis. Englewood Cliffs, N.J., Prentice-Hall, Inc. 1962.

ACKNOWLEDGMENTS

The author wishes to thank Dr. A. V. Pohm for his very able guidance. The use of the Computer Center facilities of Iowa State University is also appreciated. Thanks are due to Motorola and Texas Instruments for devices and information received. Advice on computer programming by R. A. Sharpe and June Smith was very valuable. Comments from, and discussions with Dr. Joseph M. Brown were also very helpful and much appreciated.

APPENDIX A: DEFINITION OF COMPUTER PROGRAM VARIABLES

The doubly subscripted arrays used in the computer program are listed and defined below.

DNEW(I,J)	Electron concentration in base 1
DPEW(I,J)	Hole concentration in base 2
EYLJ(I,J)	Electric field in y-direction in base 2
IB1(I,J)	Base 1 node identification number
IB2(I,J)	Base 2 node identification number

The arrays SCJL(I,J) and SCJT(I,J) are used in the calculation of the iteration coefficients and are defined in the text material.

The singly subscripted arrays used in the computer program are listed and defined below.

VE(I)	Present value of emitter 1 voltage
VT(I)	Value of VE(I) for prior iteration
VC(I)	Present value of center junction voltage
VCT(I)	Value of VC(I) for prior iteration
CJV(I)	Present value of emitter 2 voltage
CJVT(I)	Value of CJV(I) for prior iteration
EX(I)	Base 2 x-direction electric field
EY(I)	Voltage difference across base 2
CJC(I)	Electron current across center junction
CJC2(I)	Hole current across center junction
E1C(I)	Electron current from emitter 1 into base 1
CCC(I)	Hole current from base 1 into emitter 1
EJC(I)	Hole current from emitter 2 into base 2

AJ(I)	Electron current from base 2 into emitter 2
RB(I)	Base 1 resistivity
RH02(I)	Base 2 resistivity
CEM1(I)	Emitter 1 capacitance (f/cm ²)
CCJ(I)	Center junction capacitance (f/cm ²)
CEM(I)	Emitter 2 capacitance (f/cm ²)
BN(I)	Equilibrium value of base 1 electrons
B1P(I)	Base 1 majority carrier concentration
BP(I)	Equilibrium value of base 2 holes
B2N(I)	Base 2 majority carrier concentration
TEFF(I)	Volume recombination in base 1 or base 2
BULK1(I)	Majority carrier charge to base 1 to maintain space charge equilibrium
BULK2(I)	Majority carrier charge to base 2 to maintain space charge equilibrium
PIC(L)	Values of rate of change of minority carrier concentration
TM(L)	Time multiplier used to calculate time increment size
LC1(J)	Leftmost value of I in the Jth row, base 1
LC2(J)	Rightmost value of I in the Jth row, base 1
LR1(I)	Bottom boundary J value in the Ith column, base 1
LR2(I)	Top boundary J value in the Ith column, base 1
LCC1(J)	Leftmost value of I in the Jth row, base 2
LCC2(J)	Rightmost value of I in the Jth row, base 2
LRR1(I)	Bottom boundary J value in the Ith column, base 2
LRR2(I)	Top boundary J value in the Ith column, base 2
G(I)	Multiplier of the diffusion constant in base 1

All of the singly subscripted arrays A, B, C, A1, B1, C1, BM, B11, A11, and C11 are used as coefficients in the iteration equations for base 1 and base 2 and are defined in the text material. The singly subscripted arrays H, R, and Z are used in the solution of the algorithm defined by Equations 30 through 33. Several other singly subscripted arrays are used temporarily in calculations, but have no permanent definition.

The simple variables used in the computer program are listed and defined below.

B1W,B2W	Base 1 width, base 2 width
E1W,E2W	Emitter 1 width, emitter 2 width
EL,D	Device width, device depth
XN,XI	Number of x-increments, size of x-increments
YN1,YN2	Number of base 1 y-increments, number of base 2 y-increments
Y1I,Y2I	Number of base 1 y-increments, number of base 2 y-increments
Y1I,Y2I	Y-increment size. Base 1, base 2
DT,DT2	Normalized time increment size. Base 1, base 2
TIME,TIMZ	Normalized total time. Base 1, base 2
FREAL,RTIME	Conversion normalized-to-real factor, total real time
TMAX,TMAX2	Maximum time increment. Base 1, base 2
TGATE	Time length of gate pulse
DIFN,DIFP	Electron diffusion constant, hole diffusion constant
TAU,TAUP	Electron average lifetime, hole average lifetime
UN,UP	Electron mobility, hole mobility
DLN,DLP	Electron diffusion length, hole diffusion length
E1EF,E2EF	Emitter 1 efficiency, emitter 2 efficiency

S	Surface recombination velocity
RHO,RH2	Base 1 resistivity, base 2 resistivity
REMI,REM	Emitter 1 resistivity, emitter 2 resistivity
EXM,EYM	Maximum electric field. X-direction, y-direction
REX,E	External circuit resistance, external circuit voltage
BI	Magnitude of gate current pulse
CC1,CC2	Total device electron current, hole current
CC,CGES	Total device current, guessed device current
TRC	Starting variable used in base 2 bias calculation
DUMY	Starting variable used in base 1 bias calculation
DDN1	Base 1 value of n for check on rate of change
DDP2	Base 2 value of p for check on rate of change
CEM1Z	Emitter 1 value of C(0)
CEM2Z	Emitter 2 value of C(0)
CCJZ	Center junction value of C(0)
CZER1	Emitter 1 current density value for junction recombination calculation
CZERO	Emitter 2 current density value for junction recombination calculation
B1CH	Determines accuracy of base 1 bias calculation
B2CH	Determines accuracy of base 2 bias calculation
CFTR	Determines accuracy of base 1 bias calculation for forward biased center junction
CFT2	Determines accuracy of base 2 bias calculation for forward biased center junction
CP2	Determines size of first increment of change for TRC or DUMY
B1CPP,B2CPP	Determines size of first increment of change for CGES for forward biased center junction

There are also many simple variables that are used for temporary calculations and so are not permanently defined.

The integer variables that are used in the computer program are listed and defined below.

IM	Number of column mesh lines
JM1	Number of row mesh lines for base 1
JM2	Number of row mesh lines for base 2
IC,JC	Mesh point of base 1 where DDN1 is taken
IC2,JC2	Mesh point of base 2 where DDP2 is taken
NIX,IS	Rightmost column of emitter 1, NIX 1
JMT	Base 1 row number for center junction
JM2T	Base 2 row number for emitter 2
JJE2	Base 2 shorting contact row number
KK,KKM	Leftmost column number of emitter 2, KK-1
MMLE	Maximum number of iterations for base 1 bias calculation with center junction forward biased
MMLE2	Base 2 counterpart of MMLE
MPC	Maximum number of array PIC and TM entries
MAX	Maximum number of iterations for base 1 or base 2 bias calculations
NTM	Number of base 1 iterations per base 2 iteration
NTM2	Number of base 2 iterations per base 1 iteration
NSE	NSE 0 for device of Figure 6, NSE 1 for device of Figure 7
NSTEP	Number of overall iterations per computer run
NOUT,NOUT2	Gives choice as to how much data is output
LTIME	LTIME 1 calculate DT and DT2, LTIME 0 read in DT and DT2

LINT LINT 0 skip base 2 bias if CCl is smaller than a certain
 value

There are also many other integer variables used as indices or in
temporary calculations that are not permanently defined.

APPENDIX B: COMPUTER PROGRAM

```

/FTC      NOMAP
C      DATA SHOWN IS FOR START OF TURN OFF RUN
        DOUBLE PRECISION E1C(20),CCC(20),VE(20),VT(20),VC(20),VCT(20),
        1TEMP(20),EJC(20),AJ(20),CJV(20),CJVT(20),CJC(20),CJC2(20),
        2TEFF(20),TDN(20),TDP(20),BULK1(20),BULK2(20),B1CH,B2CH,DUMY
        COMMON E1C,CCC,VE,VT,VC,VCT,TEMP,EJC,AJ,CJV,CJVT,CJC,CJC2,TEFF,
        1TDN,TDP,BULK1,BULK2,B1CH,B2CH,DUMY,DNEW(20,20),7PFW(20,20),
        7FYIJ(20,20)
        COMMON G(20),A1(20),B1(20),C1(20),TN1(20),TP2(20),
        1A(20),B(20),C(20),BM(20),BM1(20),H(20),R(20),Z(20),EX(20),FY(20),
        2RR1(20),BP(20),B2N(20),B1P(20),PC(12),PIC(12),
        3TM(12),RHU2(20),CCJ(20),CEM(20),CEM1(20),VDROP(20),
        4BN(20),B1W,B2W,EL,D,XN,YN1,YN2,DIFN,DIFP,S,TAU,TAUP,UN,UP,CLOS2
        COMMON FREAL,CJMI,CJM2,CJM3,CM1,CM3,AR1,AR2,CC,CC1,CC2,CCDR,REX,
        1QU,CLOS,TRC,E,B1,FR2,DT,DT2,TIME,TIM2,RTIME,COLD,CINC,DDN1,DDP2,
        2ALPH,CLN,DLP,EE,E2EF,RHO,RH2,E1EF,E2W,E1W,CFTR,CFT2,CKON,TMAX,
        3TMAX2,CP2,CPP,VNIX,TGATE,EXM,EYM,REM,REM1,QQQQ,RRR,RRR2,EP,E2N,
        4E2P,E1N,XI,Y1I,Y2I,AL,RB1,RTR,CC1D,CGES,B1CPP,B2CPP,CZEM1,CZERO
C      VARIABLE IMMM IS TO BE THE SAME AS IM
        COMMON IMMM,JM1,JM2,IM12,JMI2,IS,JM2T,JMT,NTM2,NNN,KK,KKY,NIX,
        1NSE,NC2,NCJ,NVCNX,IVK,MAX,IC,JC,IC2,JC2,JJE2,MPC,NTM,NDUT,NDUT2,
        2NSTP,NT,NOFF,NSTT,MMAX,LVC,MFIRS,NIT1,NIT2,NCLDS,MCLOS,NRUN,NRUN2,
        3NB2
        DU 2 L=1,1300
        E1C(L)=0.0D+00
        READ (1,1300) IM,JM1,JM2,IC,JC,IC2,JC2,IM12,JMI2,IS,JM2T,JMT,JJE2,
        1KK,KKM,NIX,MMLE,MPC,MAX,NTM2,NSE,NTM,NNN,NSTEP,MMLF2,NDUT,
        2NDUT2,LTIME,LINT,NOFF,NSTT,LVC,NB2
        IMMM=IM
        WRITE (3,1301) IM,JM1,JM2,IC,JC,IC2,JC2,IM12,JMI2,IS,JM2T,JMT,
        1JJE2,KK,KKM,NIX,MMLE,MPC,MAX,NTM2,NSE,NTM,NNN,NSTEP,MMLF2,NDUT,
        2NDUT2,LTIME,LINT,NOFF,NSTT,LVC,NB2
        READ (1,1306) ALPH,DIFN,DIFP,DLN,DLP,EE,E2EF,REX,RHO,RH2,S,XN,YN1,
        1YN2,E,E1EF,B1W,B2W,E2W,E1W,EL,D,UN,UP,CFTR,TAU,TAUP,TMAX,TMAX2,
        2B1,CP2,CPP,VNIX,TGATE,EXM,EYM,CFT2,CZER1,CZERO,CEM1Z,CEM2,CCJZ
        WRITE (3,1307) ALPH,DIFN,DIFP,DLN,DLP,EE,E2EF,REX,RHO,RH2,S,XN,YN1
        1,YN2,E,E1EF,B1W,B2W,E2W,E1W,EL,D,UN,UP,CFTR,TAU,TAUP,TMAX,TMAX2,
        2B1,CP2,CPP,VNIX,TGATE,EXM,EYM,CFT2,CZER1,CZERO,CEM1Z,CEM2,CCJZ
        READ (1,1327) DUMY,B1CH,B2CH
        WRITE (3,1328) DUMY,B1CH,B2CH
        REM=(1.0-E2EF)*E2W*RHO/B2W/E2EF
        REM1=(1.0-E1EF)*E1W*RHO/B1W/E1EF
        QQQQ=2.25F+20*1.601864E-19
        RRR=2.0*11.7*8.85F-14
        RRR2=11.7*8.85E-14
        EP=QQQQ*UN*REM1
        E2N=QQQQ*UP*REM
        E2P=2.25E+20/F2N
        E1N=2.25E+20/EP
        B1HO=1.0/(1.601864E-19*UP*RHO)
        B2EL=1.0/(1.601864E-19*UN*RHO)
        WRITE (3,1353) EP,E2N,REM,REM1,E2P,E1N,B1HO,B2EL
        QU=1.601864E-19/1.38E-23/3CO.0
        READ (1,1314) (PC(L),PIC(L),TM(L),L=1,MPC)
        WRITE (3,1315) (PC(L),PIC(L),TM(L),L=1,MPC)
        XI=EL/XN
        Y1I=B1W/YN1
        Y2I=B2W/YN2
        AK1=XI*D
        AR2=B2W*D

```

```

BYFAC=1.601864E-19*Y2I/TAUP
QQ1=1.601864E-19*DIFN
QQ=1.601864E-19*DIFP
FRZ=1.601864E-19*UP*ARI
FREAL=EL*EL/DIFN
CJM1=QQ1*ARI/Y1I
CJM2=QQ*ARI/Y2I
CJM3=QQ1*ARI/E2W
CM3=CJM3*E2N
CM1=EP*QQ*ARI/E1W
AL=1.0-ALPH
RBI=XI/D/B1W
RTR=XI/D/B2W
WRITE (3,1353) CJM1,CJM2,CJM3,CM3,CM1,RBI,RTR
READ (1,1352) ((DNEW(I,J),I=1,IM),J=1,JMT)
WRITE (3,1337) ((DNEW(I,J),I=1,IM),J=1,JMT)
READ (1,1352) ((DPEW(I,J),I=1,IM),J=1,JM2T)
WRITE (3,1337) ((DPEW(I,J),I=1,IM),J=1,JM2T)
READ (1,1325) (VE(I),VC(I),CJV(I),BULK1(I),BULK2(I),I=1,IM)
WRITE (3,1326) (VE(I),VC(I),CJV(I),BULK1(I),BULK2(I),I=1,IM)
READ (1,1354) (AJ(I),EX(I),EY(I),RB(I),RHO2(I),I=1,IM)
WRITE (3,1355) (AJ(I),EX(I),EY(I),RB(I),RHO2(I),I=1,IM)
READ (1,1300) IVK,NCT2,NCJ,NVCNX,IT1,IT2
WRITE (3,1301) IVK,NCT2,NCJ,NVCNX,IT1,IT2
READ (1,1352) TRC,TIME,TIM2,CC1D,CC2D,CGES,B1CPP,B2CPP,CC,DT,DT2
WRITE (3,1353) TRC,TIME,TIM2,CC1D,CC2D,CGES,B1CPP,B2CPP,CC,DT,DT2
RTIME=FREAL*TIME
NIT1=0
NIT2=0
NRUN=0
NRUN2=0
DO 750 NSTP=1,NSTEP
COLD=CC
IF (NCUT2-NRUN2) 3,3,4
3 NRUN2=0
4 NRUN2=NRUN2+1
WRITE (3,1445)
IF (NCT2) 614,614,615
614 READ (1,1352) DT,DT2
615 IF (TGATE-RTIME) 18,18,19
18 BI=0.0
19 DO 250 NT=1,NTM
IF (NCUT-NRUN) 8,8,7
8 NRUN=0
7 NRUN=NRUN+1
MFIRS=-1
CLOS=0.02*CGES
CLOS2=0.02*CGES
QQQ=ARI*AL
C CALC ELECTRIC FIELDS
DO 461 I=2,IM
EX(I)=(CJV(I)-CJV(I-1))/XI
EXMAG=ABS(EX(I))
IF (EXMAG-EXM) 461,461,462
462 EX(I)=(EXMAG/EX(I))*EXM
461 CONTINUE
EX(I)=0.0
EX(IM)=0.0
DO 470 I=1,IM
EY(I)=0.0
AJDFN=AJ(I)/ARI

```

```

RTEMP=RHO2(I)
DO 465 L=1, JM2T
J=JM2T+1-L
AJDEN=EYFAC*DPEW(I,J)+AJDEN
EYIJ(I,J)=-AJDEN*RTEMP
YMAG=ABS(EYIJ(I,J))
IF (YMAG-EYM) 465,465,463
463 EYIJ(I,J)=(YMAG/EYIJ(I,J))*EYM
465 CONTINUE
DO 454 J=2, JM2T
454 EY(I)=EYIJ(I,J)*Y2I+EY(I)
470 CONTINUE
CC1=0.0
CC2=0.0
C CALC QUANTITIES AFFECTED BY CONDUCTIVITY MODULATION
DO 14 I=1, IM
dN(I)=QQQ*UP*RB(I)
BP(I)=QQQ*UN*RHO2(I)
B1P(I)=2.25E+20/BN(I)
B2N(I)=2.25E+20/BP(I)
Q4=0.0
DO 13 L=2, JM2T
13 Q4=(DPEW(I,L+1)+DPEW(I,L))/YN2+Q4
RHO2(I)=RH2/(Q4/B2N(I)+1.0)
TP2(I)=(Q4/(Q4+B2N(I))+1.0)*TAUP
Q5=0.0
DO 16 L=1, JM1
16 Q5=(DNEW(I,L+1)+DNEW(I,L))/YN1+Q5
RB(I)=RHO/(Q5/B1P(I)+1.0)
TN1(I)=(Q5/(Q5+B1P(I))+1.0)*TAU
QQ=EXP(-QU*VC(I))-1.0
DNEW(I, JMT)=QQ*DN(I)
DPEW(I,1)=QQ*BP(I)
FFCJ=ALOG((B1HO+DNEW(I, JMT))*(B2EL+DPEW(I,1))/2.25E+20)/QU
FEE1=ALOG((B1HO+DNEW(I,1))*E1N/2.25E+20)/CU
FEE2=ALOG((B2EL+DPEW(I, JM2T))*E2P/2.25E+20)/QU
Q1=VC(I)
QQ1=ABS(1.0+Q1/FECJ)
QFIVE=Q5/B1P(I)
IF (QFIVE-0.0005) 702,701,701
7J1 CPRI=CCJZ*SQRT(1.0+QFIVE)
GO TO 703
7J2 CPRI=CCJZ
703 CCJ(I)=CPRI/SQRT(QQ1)
Q1=VE(I)
QQ1=ABS(1.0-Q1/FEE1)
CEM1(I)=CEM1Z/SQRT(QQ1)
Q1=CJV(I)
QQ1=ABS(1.0-Q1/FEE2)
CEM(I)=CEM2/SQRT(QQ1)
CJC2(I)=(DPEW(I,2)-DPEW(I,1))*CJM2
CJC(I)=(DNEW(I, JM1)-DNEW(I, JMT))*CJM1
CC1=CJC(I)+CC1
CC2=CC2+CJC2(I)
VT(I)=VE(I)
14 CJVT(I)=CJV(I)
WRITE (3,1307) TN1(NIX), TP2(NIX)
CC=CC1+CC2
VOLT1=-((CC10+CC2)*REX+E
DO 501 I=1, IM
501 VCT(I)=VOLT1+FY(I)-VE(I)-CJV(I)

```

```

      CALL BIAS1(MMLE)
      IF (MMAX-MAX)6,751,751
      START BASE 1 ITERATION
      C
      C C10=CC1
      CALL ITER1(IT1)
250  CONTINUE
      C TO START SOLUTION,CC1 MUST REACH A CERTAIN VALUE TO DRIVE BASE 2
      IF (LINT) 30,30,33
3J   IF (CC1-0.75E-04) 489,32,32
3Z   TIME=TIME-2.0*DT2
      LINT=1
33   DO 749 NT2=1,NTM2
      CC1=0.0
      CC2=0.0
      DO 402 I=1,IM
      TEMP(I)=0.0D+00
      CJC2(I)=(DPEW(I,2)-DPEW(I,1))*CJM2
      CJC(I)=(DNEW(I,JM1)-DNEW(I,JM2))*CJM1
      CC1=CJC(I)+CC1
402  CC2=CC2+CJC2(I)
      CC=CC1+CC2
      VOLT2=-(CC20+CC1)*REX+E
      DO 401 I=1,IM
401  VCT(I)=VOLT2+EY(I)-VE(I)-CJV(I)
      CLOS=0.02*CGES
      MFTR=-1
      CALL BIAS2(MMLE2)
      IF (MMAX-MAX) 450,751,751
450  CC20=CC2
      IF (NOUT2-NRUN2) 466,466,467
466  WRITE (3,1431)
      WRITE (3,1340) (AJ(I),EJC(I),CJC2(I),CJC(I),VC(I),CJV(I),EX(I),
1EY(I),I=1,IM)
      WRITE (3,1307) EYIJ(NIX,1),EYIJ(NIX,JM2T)
      C
      C START BASE 2 ITERATION
      C
      C CALC NEW VALUE OF B1CPP AND B2CPP
467  IF (NCJ) 468,468,480
480  CINC=ABS(CC-COLD)
      B2CPP=CINC/CGES
      IF (B2CPP-0.01*CFTR) 481,481,482
481  B2CPP=CFTR
482  B1CPP=B2CPP
483  WRITE (3,1307) CINC,B1CPP,B2CPP
484  CALL ITER2(IT2)
485  CONTINUE
486  IF (LTIME) 750,750,490
490  CALL TCALC(NTIME)
1300 FORMAT (17I4)
1301 FORMAT (' ',17I4)
1306 FORMAT (5E13.5)
1307 FORMAT (' ',5E13.5)
1314 FORMAT (3E13.5)
1315 FORMAT (' ',3E13.5)
1325 FORMAT (5D15.8)
1326 FORMAT (' ',5D15.8)
1327 FORMAT (3D15.8)
1328 FORMAT (' ',3D15.8)
1337 FORMAT (' ',6E15.8)
1340 FORMAT (' ',2D13.6,2E13.6,2D13.6,2E13.6)
1352 FORMAT (5E15.8)
1353 FORMAT (' ',5E15.8)

```



```

      IF (NCJ) 14,14,13
13  IF (VC(LVC1+0.375) 18,12,12
12  CGES=TCC
18  CCCR=CGES*REX
      GO TO 16
1+  CCCR=TCC*REX
1+  R1DR=UB+TCC2
      QUB1=TCC2
      IF (BI) 7,7,6
      QUB1=TCC2+BI
  6  MMAX=0
  7  NFIRS=-1
17  OCCR=E-CCDR
      DO 65 MM=1,MAX
      VE(NIX)=DUMY+1.0D+00
      TTDP=DEXP(DU*VE(NIX))-1.0D+00
      TEMP(NIX)=TTDP*RN(NIX)
      GEM1=DNEW(NIX,1)/(BIP(NIX)+DNEW(NIX,1))+1.0
      EIC(NIX)=(TEMP(NIX)-DNEW(NIX,2))*CJM1*GEM1
      CCC(NIX)=TEMP(NIX)*CMI/BN(NIX)
      CE1C=(VE(NIX)-VT(NIX))/DREAL*CEM1(NIX)*AR1
      E1DC=(CABS(EIC(NIX))+CCC(NIX))/AR1
      IF (E1DC-CZER1) 205,206,206
205  T1CD=DSORT(CZER1*E1DC)
      FIRC=(T1CD-E1DC)*AR1
      GO TO 207
206  EIRC=0.0D+00
207  CCC(NIX)=CCC(NIX)+EIRC
      CCJ1=0.0
      COMB=0.0
      DOB1=0.0
      CE1FF=CCC(NIX)
      G1K=08-CF1EF-CE1C
      DO 23 I=NIX,1M
      VC(I)=EY(I)+DCCR-VE(NIX)-CJV(I)
      IF (NCJ) 9,9,8
      TTDP=DEXP(-DU*VC(I))-1.0D+00
      TUP(I)=BP(I)*TTDP
      TDN(I)=BN(I)*TTDP
      TCJ2(I)=(DPEW(I,2)-TDP(I))*CJM2
      TCJ(I)=(DNEW(I,JM1)-TDN(I))*CJM1
  C  TT3=((VCT(I)-VC(I))/DREAL)*CCJ(I)*AR1
      RCB=TFMP(I)*QZ/TN1(I)+TEFF(I)
      COMB=PCB+COMB
      CCJ1=TT3+CCJ1
      TT1=(TEMP(I)-DNEW(I,1))+BULK1(I)*QZZ
      DOB1=TT1+DOB1
23  GIR=GIR-TT1-TT3+TCJ2(I)-RCB
      DO 20 L1=2,NIX
      I=NIX+1-L1
      VE(I)=-RB(I)*RE1*GIP+VE(I+1)
      IF (VE(I)) 26,25,25
25  VC(I)=EY(I)+DCCR-VF(I)-CJV(I)
      IF (VF(I)-1.0D+00) 22,22,21
21  IF(NFIRS) 27,28,28
27  DUMY=1.2D+00*DUMY
      VE(NIX)=DUMY+1.0D+00
      WRITE (3,1500) DUMY,VE(NIX)
  4  IF (NCJ) 65,65,4
  4  IF (MM-1) 65,65,5
  4  CDIF=-0.1E+01

```



```

28  GU TO 120
    NFIRS=1
    CHIP=0.5D+00
    DINC=CHIP*DINC
    DUMY=DUMY-DABS(DINC)
    VE(NIX)=DUMY+1.0D+00
    GO TO 65
22  TTOP=DEXP(DU*VE(I))-1.0D+00
    TEMP(I)=TTOP*BN(I)
    CCC(I)=TTOP*CM1
    IF (NCJ) 81,81,80
80  TTOP=DEXP(-DU*VC(I))-1.0D+00
    TDP(I)=BP(I)*TTOP
    TDN(I)=BN(I)*TTOP
    TCJ2(I)=(DPEW(I,2)-TDP(I))*CJM2
    TCJ(I)=(DNEW(I,JM1)-TDN(I))*CJM1
81  GEM1=DNFW(I,1)/(B1P(I)+DNEW(I,1))+1.0
    EIC(I)=(TEMP(I)-DNEW(I,2))*CJM1*GEM1
    CALCULATE CURRENT FLOW TO SUPPLY JCT RECOMBINATION
    E1DC=(CABS(EIC(I))+CCC(I))/AR1
    IF (E1DC-CZER1) 200,201,201
200 TICD=DSQRT(CZER1*F1DC)
    E1RC=(TICD-E1DC)*AR1
    GO TO 202
201 E1RC=0.0D+00
    LCC(I)=CCC(I)+E1RC
    CE1EF=CCC(I)+CE1EF
    TT1=(TEMP(I)-DNEW(I,1)+BULK1(I))*QZZ
    DQB1=TT1+DQB1
    TT2=((VE(I)-VT(I))/DREAL)*CEM1(I)*AR1
    CE1C=TT2+CE1C
    TT3=((VCT(I)-VC(I))/DREAL)*CCJ(I)*AR1
    CCJ1=TT3+CCJ1
    KCB=TEMP(I)*QZ/TN1(I)+TEFF(I)
    CCMB=RCB+CCMB
    GIR=GIP+TCJ2(I)-TT1-TT2-TT3-CCC(I)-RCB
20  CONTINUE
26  IF (IVK) 35,35,30
30  GDIF=VNIX-VE(NIX)
    GU TO 15
35  GDIF=GIP
    IF (I-1) 10,10,15
10  IF (DABS(GDIF)-BICH*QUR1) 48,48,15
15  IF(NFIRS) 52,54,54
52  NFIRS=0
    CHIP=1.0D+00
    IF(GDIF) 53,63,56
53  CHIP=-1.0D+00
    GO TO 56
54  IF(GORO*GDIF) 57,55,55
55  IF(NFIRS) 58,56,60
56  DINC=CP2*DABS(DUMY)
    GO TO 60
57  NFIRS=1
    CHIP=0.5D+00
    DINC=-DINC
60  IF (DABS(DINC)-0.1D-14*DUMY) 48,51,51
51  DINC=CHIP*DINC
    GORO=GDIF
    DUMY=DUMY+DINC
    VE(NIX)=DUMY+1.0D+00

```

```

65 CONTINUE
48 WRITE (3,1442) MM,GDIF,DINC,DUMY,VE(NIX)
   IF (NOFF) 211,211,63
>11 IF (I-1) 41,41,49
-1 IF (VF(1)-VE(2)) 42,49,49
42 IF (VE(1)) 49,63,63
49 DO 40 N=1,I
   TEMP(N)=0.0
   EIC(N)=(TEMP(N)-DNEW(N,2))*CJM1
   CCC(N)=0.0
40 VE(N)=0.0
   WRITE (3,1300) I
63 DO 111 I=IS,IM
111 VE(I)=VE(NIX)
   IF (NCJ) 108,108,69
108 IF (MFIRS) 68,69,69
68 IF (VC(LVC)) 69,69,145
69 TCC1=0.0D+00
   TCC2=0.0D+00
   DO 140 I=1,IM
   TCC1=TCC1+TCJ(I)
140 TCC2=TCC2+TCJ2(I)
   TCC=TCC1+TCC2
   CDIF=TCC-CGES
   CDIM=ABS(CDIF)
   IF (CCIN-CLOS) 112,114,114
112 CLUS=CDIM
118 CKON=VE(LVC)+CJV(LVC)
114 IF (CDIM-CFTP*CGES) 145,72,72
72 IF (NVCNX) 121,121,120
121 IF (VC(LVC)+0.375) 120,119,119
119 CGES=TCC
   GU TO 142
120 IF (MFIRS) 73,76,76
73 MFIRS=0
   IF (CKON) 117,115,117
115 CKON=VE(LVC)+CJV(LVC)
   CLOS=CDIM
117 DELT=RICPP*CGFS
   IF (CDIF) 74,145,71
74 DELT=-DELT
   GU TO 71
74 IF (CDIO*CDIF) 77,78,78
74 IF (MFIRS) 73,73,75
75 DELT=0.5*DELT
   GU TO 71
77 MFIRS=1
   DELT=-0.50*DELT
71 CGES=CGES+DELT
   CDIO=CDIF
138 QQ=EY(LVC)+E-CKON-CGES*REX
   QQ1=EXP(-QU*QQ)-1.0
   QQ2=(DNEW(LVC,JM1)-8N(LVC)*QQ)*CJM1
   IF (QQ2) 141,141,142
141 IF (MFIRS) 137,137,139
137 IF (DELT) 71,751,139
139 DELT=0.5*DELT
   CGES=CGES-DELT
   WRITE (3,1337) CGES
   MMAX=MMAX+1
   IF (MMAX-MAX) 138,751,751

```

```

751 RETURN
142 CONTINUE
145 NIXL=NIX
      DO 47 I=1,NIX
47  ONEW(I,1)=TEMP(I)
      DO 160 I=1,IM
          CJC(I)=TCJ(I)
          CJC2(I)=TCJ2(I)
          DNEW(I,1)=TUN(I)
160  DPEW(I,1)=TOP(I)
          CC1=TCC1
          CC2=TCC2
          CC=YCC
          NCJ=0
          IF (VC(LVC)) 146,146,149
146  NCJ=1
          NVCNX=0
          IF (VC(LVC)+0.375) 150,151,151
150  NVCNX=1
151  WRITE (3,1443) MLE,CC,CGES,CDIF,CLCS,DELT
          B1DR=B1+CC2
148  WRITE (3,1430) VC(LVC)
149  WRITE (3,1319) CC1,CC2,CC
          TOT=CCJ1+CE1C+CE1EF+DQB1+CCMB
          WRITE (3,1446) CCJ1,CE1C,CE1EF,DQB1,CCMB,TCT,B1DR
456  IF (NOUT-NRUN) 466,466,467
          WRITE (3,1429)
          WRITE (3,1321) (CCC(I),EIC(I),CJC(I),VE(I),VC(I),RR(I),RHQ2(I),
          ICEM(I),CCJ(I),CFM(I),I=1,IM)
1307  FORMAT (17I4)
1319  FORMAT (' ',5H CC)=,E14.6,5H CC2=,E14.6,4H CC=,E14.6)
1321  FORMAT (' ',2D13.6,E13.6,2D13.6,5E11.4)
1337  FORMAT (' ',6F15.8)
1429  FORMAT (' ',4X,6HCCC(I),7X,6HEIC(I),7X,6HCJC(I),8X,5HVE(I),8X,
          15HVC(I),7X,5HRR(I),5X,7HRHQ2(I),4X,6HCEM(I),4X,6HCCJ(I),4X,
          27HCEM(I))
1442  FORMAT (' ',4H MM=,I3,6H GCIF=,D15.8,6H DINC=,D73.14,4H DUMY=,
          1023.16,9H VE(NIX)=,D23.16)
1430  FORMAT (' ', ' VC(NIX) IS NEGATIVE ',D15.8)
1443  FORMAT (' ',5H MLE=,I3,5E14.7)
1446  FORMAT (' ',6H CCJ1=,D15.8,6H CE1C=,D15.8,7H CE1EF=,D15.8,6H DQB1=,
          1,015.8,/, ' BASE 1 RECOMB=,E15.8, ' BASE 1 DRIVL NFFD=,D15.8,
          1 ' SUPPLIED=,E15.8)
1500  FORMAT (' ',?D15.8)
467  RETURN
      END
      SUBROUTINE ITER1(IT1)
          DIMENSION IB1(20,20),LC1(20),LC2(20),LRI(20),LR2(20)
          DOUBLE PRECISION FLC(20),CCC(20),VE(20),VT(20),VC(20),VCT(20),
          1TEMP(20),EJC(20),AJ(20),CJV(20),CJVT(20),CJC(20),CJC2(20),
          2TEFF(20),TDN(20),TDP(20),BULK1(20),BULK2(20),B1CH,B2CH,DUMY
          COMMON EIC,CCC,VE,VT,VC,VCT,TEMP,EJC,AJ,CJV,CJVT,CJC,CJC2,TEFF,
          1TON,TDP,BULK1,BULK2,B1CH,B2CH,DUMY,DNEW(20,20),UPW(2,2),
          2EYIJ(20,20)
          CLMCON G(23),A1(20),B1(20),C1(20),TN1(20),TP2(20),
          1A(20),B(20),C(20),BM(20),BM1(20),H(20),R(20),7(20),EX(20),FY(20),
          2RB(20),BP(20),BPN(20),BIP(20),PC(12),PIC(12),
          3TH(12),RHQ2(20),CCJ(20),CFM(20),CFM1(20),VOROP(20),
          4BN(20),B1W,B2W,EL,D,XN,YN1,YN2,DIFN,DIFP,S,TBJ,TAUP,UN,U?,CLCS>
          COMMON FREAL,CJM1,CJM2,CJM3,CM1,CM3,AP1,AP2,CC,CC1,CC2,CCOR,KEY,
          1QU,CLCS,TRC,E,B1,FB2,DT,DT2,TIME,TIM2,PTIME,COLD,CINC,DJVI,DDP?

```

```

2ALPH,DLN,DLP,FE,E2EF,RHO,RH2,E1EF,E2W,E1W,CFTR,CFT2,CKON,TMAX,
JTMX2,CP2,CPP,VN1X,TGATE,EXM,EYM,REM,REM1,QQQQ,RRR,RR42,EP,E2N,
4E2P,E1N,XI,Y11,Y21,AL,RB1,RTR,CC10,CGES,B1CPP,B2CPP,CZER1,CZER0
COMMON IM,JM1,JM2,INI2,JMI2,IS,JM2T,JMT,NTM2,NNN,KK,KKM,NIX,
INSE,NCT2,NCJ,NVCNX,IVK,MAX,IC,JC,IC2,JC2,JJE2,MPC,NTM,NOJT,NOU2,
ZNS1P,NT,NDFP,NSTT,MMAX,LVC,MFIRS,NIT1,NIT2,NCLDS,MCLOS,NRUN,NRUN7,
3NBZ
IF (NIT1) 1000,1000,1005
1000 NIT1=1
READ (1,1308) ((IB1(I,J),I=1,IM),J=1,JM1)
WRITE (3,1309) ((IE1(I,J),I=1,IM),J=1,JM1)
READ (1,1310) (LC1(J),LC2(J),J=1,JM1)
WRITE (3,1311) (LC1(J),LC2(J),J=1,JM1)
READ (1,1310) (LR1(I),LR2(I),I=1,IM)
WRITE (3,1311) (LR1(I),LR2(I),I=1,IM)
DX=1.0/XN
DY1=B1W/EL/YN1
QQ=0.5*DY1
QQ1=0.5*DX
QA1=QC*QQ1
HA1=2.0*QA1
TA1=2.0*HA1
S1=QQ1*S/DIFN
S2=S1
S3=QQ*S/DIFN
S4=S3
YJX=QQ/DX
XDY=QC1/DY1
AMB=EL*FL/TAU/DIFN
ENN1=AMB*QA1
ENN2=AMB*HA1
ENN3=AMB*TA1
1005 DTI=1.0/DT
EMM1=CTI*QA1
EMM2=CTI*HA1
EMM3=CTI*TA1
TREAL=PREAL*2.0*DT
C REGIN BASE 1 Y-ITERATION
IT1=IT1+1
WRITE (3,1324) IT1
DDN1=DNEW(IC,JC)
DO 1006 I=1,IM
QQ1=0.0
DO 1007 J=2,JM1
1007 QQ1=QQ1-DNEW(I,J)
1006 BULK1(I)=QQ1
DO 1160 I=1,IM
L3=LR1(I)
L4=LR2(I)
IL=I-1
IT=I+1
C CALC VALUES OF G FOR I TH COLUMN
DO 1114 J=L3,L4
1114 G(J)=DNEW(I,J)/(DNFW(I,J)+B1P(I))+1.0
DO 1150 J=L3,L4
JL=J-1
JT=J+1
A1(J)=0.0
B1(J)=0.0
C1(J)=0.0
H(J)=0.0

```

```

      IBB=IR1(I,J)
      GU TO (201,201,201,204,204,206,207,207,210,210,210),IAB
201  QQ1=2.0*G(J)*YCX
      A1(J)=G(J)*XOY
      C1(J)=G(J)*XOY
      QQ4=QQ1-FMM2+S3+S3
      RM1(J)=A1(J)+C1(J)+FMM2+ENN2
      H(J)=-3Q4*DNEW(I,J)+QQ1*DNFW(IT,J)
      IF (IBB-2) 1150,1122,1124
1122 H(J)=C1(J)*DNEW(I,J)+H(J)
      GO TO 1150
1124 H(J)=A1(J)*DNEW(I,JL)+H(J)
      GO TO 1150
204  QQ1=2.0*G(J)*YCX
      A1(J)=G(J)*XOY
      C1(J)=G(J)*XOY
      QQ4=QQ1-FMM2+S3+S3
      RM1(J)=A1(J)+C1(J)+FMM2+ENN2
      H(J)=QQ1*DNEW(IL,J)-QQ4*DNEW(I,J)
      IF (IRB-5) 1150,1127,1150
1127 H(J)=C1(J)*DNEW(I,J)+H(J)
      GU TO 1150
206  QQ1=G(J)*YDX
      C1(J)=G(J)*XOY
      QQ4=QQ1-FMM1+S3
      BM1(J)=C1(J)+FMM1+ENN1+S2
      H(J)=QQ1*DNEW(IL,J)-QQ4*DNEW(I,J)
      GU TO 1150
207  QQ1=G(J)*YDX
      QQ2=QQ1
      C1(J)=2.0*G(J)*XOY
      QQ4=QQ1+QQ2-FMM2
      BM1(J)=C1(J)+FMM2+FNN2+S1+S1
      H(J)=QQ1*DNEW(IL,J)-QQ4*DNEW(I,J)+QQ2*DNEW(IT,J)
      GU TO 1150
210  QQ1=2.0*G(J)*YDX
      QQ2=QQ1
      A1(J)=2.0*G(J)*XOY
      C1(J)=A1(J)
      QQ5=QQ1+QQ2-FMM3
      BM1(J)=A1(J)+C1(J)+ENN3+EMM3
      H(J)=QQ1*DNEW(IL,J)-QQ5*DNFW(I,J)+QQ2*DNEW(IT,J)
      IF (IBB-10) 1130,1150,1132
1130 H(J)=A1(J)*DNEW(I,JL)+H(J)
      GO TO 1150
1132 H(J)=C1(J)*DNEW(I,J)+H(J)
1150 CONTINUE
      KI=L3+1
      QQ=1.0/BM1(L3)
      R(L3)=C1(L3)*QQ
      QQ2=0.0
      Z(L3)=QQ*H(L3)
      DO 1151 K=K1,L4
      QQ=1.0/(-R(K-1)*A1(K)+BM1(K))
      R(K)=C1(K)*QQ
      QQ2=A1(K)*QQ
1151 Z(K)=CC*H(K)+QQ2*7(K-1)
      DNEW(I,L4)=Z(L4)
      JJJ=L4-1
      DO 1157 JJ=L3,JJJ
      J=JJJ+L3-JJ

```

```

1157 DNEW(I,J)=R(I)*DNEW(I,J+1)+Z(J)
1160 CONTINUE
C      END OF Y-ITERATION FOR BASE I
C      START OF X-ITERATION FOR BASE I
      DO 1190 J=1,JM1
        L1=LC1(J)
        L2=LC2(J)
        JL=J-1
        JT=J+1
        DO 1161 I=L1,L2
1161      G(I)=DNEW(I,J)/(R1P(I)+DNEW(I,J))+1.0
          DO 1175 I=L1,L2
            IL=I-1
            IT=I+1
            A(I)=0.0
            B(I)=0.0
            C(I)=0.0
            H(I)=0.0
            IHB=IB1(I,J)
            GO TO (301,301,301,304,304,306,307,307,310,310,310),IHB
301      C(I)=2.0*G(I)*YDX
            QQ2=G(I)*XOY
            QQ3=QQ2
            B(I)=C(I)+FMM2+ENN2+S3+S3
            GO TO 305
304      A(I)=2.0*G(I)*YUX
            QQ2=G(I)*XOY
            QQ3=QQ2
            B(I)=A(I)+EMM2+ENN2+S3+S3
            QQ4=QQ2+QQ3-FMM2
305      H(I)=QQ2*DNEW(I,JL)-QQ4*DNEW(I,J)+QQ3*DNEW(I,JT)
            GO TO 1175
306      A(I)=G(I)*YDX
            QQ3=G(I)*XCY
            B(I)=A(I)+EMM1+ENN1+S3
            QQ4=QQ3-EMM1+S2
            H(I)=-QQ4*DNEW(I,J)+QQ3*DNEW(I,JT)
            GO TO 1175
307      A(I)=G(I)*YDX
            QQ3=2.0*G(I)*XOY
            C(I)=A(I)
            H(I)=A(I)+C(I)+FMM2+ENN2
            QQ4=QQ3-EMM2
            H(I)=-QQ4*DNEW(I,J)+QQ3*DNEW(I,JT)
1171      IF (IHB-7) 1175,1175,1171
            H(I)=A(I)*DNEW(IL,J)+H(I)
            GO TO 1175
310      A(I)=2.0*G(I)*YUX
            QQ2=2.0*G(I)*XOY
            QQ3=QQ2
            C(I)=A(I)
            B(I)=A(I)+C(I)+EMM3+ENN3
            QQ4=QQ2+QQ3-EMM3
            H(I)=QQ2*DNEW(I,JL)-QQ4*DNEW(I,J)+QQ3*DNEW(I,JT)
1175      CONTINUE
            K2=L1+1
            QQ=1.0/B(L1)
            R(L1)=C(L1)*QQ
            QQ2=0.0
            Z(L1)=QQ*H(L1)
            DO 1176 K=K2,L2

```

```

      QQ=1.0/(-R(K-1)*A(K)+B(K))
      R(K)=C(K)*QQ
      QQ2=A(K)*QQ
1174  Z(K)=QQ*M(K)+QQ2*Z(K-1)
      DNEW(L2,J)=Z(I17)
      I11=L2-1
      D11 I11R3 I1=L1,I11
      I=I11+L1-I1
1183  DNEW(I,J)=R(I)*DNEW(I+1,J)+Z(I)
      IF (NCUT-NRUN) 466,466,1190
466   WRITE (3,1336) J,(DNEW(I,J),I=1,IM)
      OUTPUT CTR JCT VALUES
      IF (J-JM1) 1190,1192,1192
1192  WRITE (3,1336) JMT,(DNEW(I,JMT),I=1,IM)
1190  CONTINUE
      END OF X-ITERATION FOR BASF 1
      DO 1194 I=1,IM
      QQ1=0.0
      DO 1193 J=2,JM1
1193  QQ1=DNEW(I,J)+QQ1
1194  BULK1(I)=BULK1(I)+QQ1
      TIME=TIME+2.0*CT
      RTIME=FREAL*TIME
      WRITE (3,1341) DT,TIME,RTIME
1308  FORMAT (10I3)
1309  FORMAT (' ',10I3)
1310  FORMAT (2I3)
1311  FORMAT (' ',2I3)
1334  FORMAT (' ',21HBASF 1 ITERATION NO ,I3)
1336  FORMAT (' ',I3/(' ',5F14.6))
1341  FORMAT (' ',5H DT=,E14.6,13H TOTAL TIME=,E14.6,17H TOTAL REAL TI
      ME=,E15.8)
      RETURN
      END
      SUBROUTINE RIAS2(MMLE2)
      DOUBLE PRECISION F1C(20),CCC(20),VF(20),VT(20),VC(20),VCT(20),
      1TEMP(20),EJC(20),AJ(20),CJV(20),CJVT(20),CJC(20),CJC2(20),
      2TEFF(20),TDP(20),TDP(20),BULK1(20),BULK2(20),B1CH,B2CH,DUMY
      DOUBLE PRECISION DRHO2(20),PEMP(20)
      COMMON F1C,CCC,VE,VT,VC,VCT,TEMP,EJC,AJ,CJV,CJVT,CJC,CJC2,TEFF,
      1TUN,TDP,BULK1,BULK2,B1CH,B2CH,DUMY,DNEW(20,20),DPEW(20,20),
      2EYIJ(20,20)
      COMMON G(20),A1(20),B1(20),C1(20),TNI(20),TP2(20),
      1A1(20),A(20),C(20),AM(20),RM1(20),H(20),R(20),Z(20),EX(20),EY(20),
      2RB(20),BP(20),B2N(20),B1P(20),PC(12),PIC(12),
      3TM(12),RHO2(20),CCJ(20),CEM(20),CEM1(20),VDROP(20),
      4BN(20),B1W,B2W,EL,D,XN,YN1,YN2,DIFF,DIFP,S,TAU,TAUP,IIN,U,CLOS
      COMMON FREAL,CJM1,CJM2,CJM3,CM1,CM3,AP1,AR2,CC,CC1,CC2,CCUR,RF,X,
      1QU,CLGS,TRC,E,RI,FB2,DT,DT2,TIME,TIMP,RTIME,COLD,CTNC,DDN1,DDP?,
      2ALPH,DLN,DLP,EE,E2FF,KHO,RH2,E1FF,E2W,F1W,CFTR,CFT2,CKON,TMAX,
      3TMAX2,CP2,CP,PP,VNIX,TGATE,EXM,FYM,RFM,REM1,QQQQ,RRR,RRR2,FP,F2N,
      4E2P,E1N,X1,Y11,Y21,AL,RB1,RTR,CC10,CGES,B1CPP,B2CPP,CZEK1,C7FR
      COMMON IM,JM1,JM2,IM12,IM12,IS,JM2T,JMT,NTM2,NNN,KK,KKM,NIX,
      1NSE,NCT2,NCJ,NVCNX,IVK,MAX,IC,JC,IC2,JC2,JJE2,MPC,NTM,NUJ1T,NUJ1T?,
      2NSTP,NT,NOFF,NSTT,MMAX,LVC,MFIRS,NIT1,NIT?,NCLCS,MCLCS,NRUN,NRUN2,
      3NB2
      DOUBLE PRECISION CCCJ,CCEM,CAJ,CCQB,DRC,QQ1,QQ2,QQ3,QD,CL E1,
      1RUNT,DELL,OLDP,EDC,TCO,ERC,DEMP,CHUP,QQ5,RCB,COMB2,QZ,QZZ,QQ6,307,
      2OCAP,RZZ,DU
      DU=QU
      QZ=1.6C1864E-19*AR1*Y2I

```

```

TREA2=FREAL*DT2*2.0
DCAP=AR1/TREA2
QZZ=QZ/TREA2
QQ6=-FB2*EYIJ(1,JM2T)+CJM2
QQ7=CJM2*DPEW(1,JM2)
DO 51 I=1,IM
DXXQ2(I)=RTR*RHQ2(I)
PEMP(I)=DPEW(1,JM2T)
TFMP(I)=DPEW(1,JM2T)
QQ=0.0
DN 50 J=2,JM2
50 QJ=UPFW(I,J)+QQ
51 TEFF(I)=QQ*QZ/TP2(I)
DKC=TRC
MFIHS=-1
DO 442 MLE=1,MMLF2
MMAX=0
CJV(KKM)=0.0
NFIPS=-1
IF (NCJ) 73,73,70
70 IF (VC(LVC)+0.375) 72,71,71
71 CGTS=CC
72 CCCR=CGFS*REX
GU TO 74
73 CCCR=CC*REFX
74 QQ5=E-CCDR
DO 100 MM=1,MAX
CJMR2=0.00+00
IF (NSF) 158,159,81
158 TEMP(1)=DRC
CJV(1)=(DL OG(TEMP(1)/BP(1)+1.00+00))/DU
EJC(1)=(TEMP(1)-DPEW(1,JM2T))*CJM2-FB2*EYIJ(1,JM2T)*TFMP(1)
VC(1)=QQ5+EY(1)-VE(1)-CJV(1)
IF (NCJ) 202,202,201
201 QD=DEXP(-QU*VC(1))-1.00+00
DPIW(1,1)=BP(1)*QD
DNEW(1,JM2)=BN(1)*QD
CJC2(1)=(DPEW(1,2)-DPEW(1,1))*CJM2
CJC(1)=(DNEW(1,JM1)-DNEW(1,JM2))*CJM1
202 AJ(1)=CM3*TEMP(1)/BP(1)
EDC=(CABS(EJC(1))+AJ(1))/AR1
IF (ECC-CZER0) 40,41,41
40 DEMP=DABS(EDC)
TCD=DSQRT(CZFFD*DEMP)
ERC=(TCD-EDC)*AR1
GU TO 42
41 ERL=0.00+00
42 CDQB=(TEMP(1)-PEMP(1)+BULK2(1))*QZZ
KK=2
AJ(1)=AJ(1)+ERC
CAJ=AJ(1)
CCCJ=(VCT(1)-VC(1))*DCAP*FCJ(1)
CCEM=(CJV(1)-CJVT(1))*DCAP*CCEM(1)
CDMB2=TEMP(1)*QZ/TP2(1)+TEFF(1)
RUNT=CCCJ+CCEM+CDQB+CAJ+CDMB2-CJC(1)
SCC=0.0
B2DR=0.0
DN 521 I=1,NIX
521 A2DR=CJC(1)+B2DR
GU TO 159
P1 RUNT=DRC

```



```

CDQB=0.0
CCJ=0.0
KR1=0.0
D2 160 I=1,KK
IF (NGJ) 204,204,203
UD=DEXP(-QU*VC(I))-1.0D+00
DPEM(I,1)=RP(I)*QD
DNEM(I,JM1)=BN(I)*QD
CJC2(I)=(DPEM(I,2)-DPEM(I,1))*CJM2
CJC(I)=(DNEM(I,JM1)-DNEM(I,JM1))*CJM1
CUMB2=TEFF(I)*CDB2
R1=CJ(I)+R1-TEFF(I)
Q2=(TEMP(I)-DPEM(I,JM2)+EPEM(I,1)+BULK2(I))*QZ
CDQB=Q2*CDQR
CCJ=(VC(I)-VC(I))*OCAP*CCJ(CJ)+CCJ
SCC=K1-CDQB-CCJ
IF (SCC) 77,77,78
82DR=CC1
GO TO 79
RUNT=DRC-SCC
82DR=CC1-SCC
CJ=0.0
D2 87 I=KK,NB2
IF (NSTT) 518,518,517
CJV(I)=CJV(I-1)
GO TO 519
CJV(I)=CJV(I-1)+RLNT*ORHO2(I)
IF (CJV(I)-1.0D+00) 85,85,82
IF (NFRS) 83,84,84
DRC=0.75D+00*DRC
WRITE (3,1350) DRC
GO TO 100
NFRS=1
R4
CHDP=0.5D+00
DELL=0.5D+00*DELL
DRC=DRC-DA85(DEL)
GU TO 100
QD=DEXP(DU*CJV(I))-1.0D+00
TEMP(I)=BP(I)*QD
AJ(I)=CM3*QD
VC(I)=EV(I)+QD5-VE(I)-CJV(I)
IF (NGJ) 61,61,60
UD=DEXP(-DU*VC(I))-1.0D+00
DPEM(I,1)=RP(I)*QD
DNEM(I,JM1)=BN(I)*QD
CJC2(I)=(DPEM(I,2)-DPEM(I,1))*CJM2
CJC(I)=(DNEM(I,JM1)-DNEM(I,JM1))*CJM1
QJ1=(CJV(I)-CJV(I))*DCAP*CEM(I)
CEM=QJ1+CCEM
EJC(I)=(TEMP(I)-DPEM(I,JM2))*CJM2-FB2*FYJ(I,JM2)*TEMP(I)
CALC CURRENTS FLOW TO SUPPLY JCT RECOMBINATION
ENC=(CABSTEJC(I))*AJ(I)/AR1
IF (EDC-CZBD) 63,69,69
DEMP=DA81(EDC)
TCD=DSO*TCZEPQ*DEMP)
ERC(TCD-EDC)*AR1
GU TO 68
EK=0.0D+00
IF (IS-1) 506,506,508
Q2=0.0D+00

```

506

69

68

63

C

61

60

85

R4

518

519

82

83

159

517

160

77

79

79

203

204

```

GU TO 509
508 QQ2=(TEMP(I)-PEMP(I)+BULK2(I))*QZZ
509 CQQR=CQ2+CQQR
QQ3=(VCT(I)-VC(I))*OCAP*CCJ(I)
CCCJ=CQ3+CCCJ
AJ(I)=AJ(I)+EPC
CAJ=AJ(I)+CAJ
RCB=TEMP(I)*QZ/TP2(I)+TEFF(I)
COMB2=RCB+COMB2
QN=CQ1+QQ2+QQ3+AJ(I)+RCB-CJC(I)
IF (NIX-1) 86,88,86
88 CLE1=RUNT+QD
86 RUNT=RUNT+QD
87 CONTINUE
IF (DABS(RUNT)-B2CH*CC1) 105,105,108
108 IF(NFIRS) 90,92,92
90 NFIRS=0
CHOP=1.0D+00
IF (RUNT) 94,105,91
91 CHOP=-1.0D+00
GO TO 94
92 IF (OLDR=RUNT) 95,93,93
93 IF (NFIRS) 94,94,96
94 DELL=CP2*DRC
GO TO 96
95 NFIRS=1
CHOP=0.5D+00
DELL=-DELL
96 IF (RUNT) 99,89,89
99 IF (DABS(DELL)-0.1D-14*DRC) 105,89,89
89 DELL=CHOP*DELL
OLDR=RUNT
DRC=DELL*DRC
100 CONTINUE
105 WRITE (3,1444) MM,RUNT,CLE1,DRC,DELL,CJV(I)
IF (NOFF) 602,602,600
600 L=NIX-1
IF (CJV(NIX)-CJV(L)) 602,602,601
601 CJV(NIX)=CJV(L)
QD=DEXP(DU*CJV(NIX))-1.0D+00
TEMP(NIX)=BP(NIX)*QD
DO 106 I=1,IM
106 DPEW(I,JM2I)=TEMP(I)
IF (NCJ) 405,405,409
405 IF (MFIRS) 406,409,409
406 IF (VC(LVC)) 409,409,456
409 CC1=0.0
CC2=0.0
DO 440 I=1,IM
440 CC1=CJC(I)+CC1
CC2=CJC2(I)+CC2
CC=CC1+CC2
CDIF=CC-CGES
CDIM=ARS(CDIF)
IF (CDIM-CLOS2) 412,310,310
412 CLOS2=CDIM
CKCN=VE(LVC)+CJV(LVC)
310 IF (CDIM-CFT2*CGES) 456,416,416
416 IF (NVCNX) 417,417,420
417 IF (VC(LVC)+0.375) 420,418,418
418 CGES=CC

```

```

      GU TO 442
420 IF (MFIRS) 421,430,430
421 MFIRS=0
      IF (CKON) 428,426,428
426 CKON=VE(LVC)+CJV(LVC)
      CLOS2=CDIM
428 DELT=B2CPP*CGES
      IF (CCIF) 423,456,436
423 DELT=-DELT
      GO TO 436
430 IF (CDIU=CDIF) 433,431,431
431 IF (MFIRS) 421,421,435
435 DELT=0.5*DELT
      GO TO 436
433 MFIRS=1
      DELT=-0.50*DELT
436 CGES=CGES+DELT
      CDIU=CDIF
438 QQ=EY(LVC)+E-CKUN-CGES*REX
      QQ1=EXP(-QU*QQ)-1.0
      QQ2=(CNEW(LVC,JM1)-BN(LVC)*QQ1)*CJM1
      IF (QQ2) 441,441,442
441 IF (MFIRS) 443,443,445
443 IF (DELT) 436,751,445
445 DELT=0.5*DELT
      WRITE (3,1338) MLE,CGES,DELT
      CGES=CGES-DELT
      WRITE (3,1337) CGES
      MMAX=MMAX+1
      IF (MMAX-MAX) 438,751,751
751 RETURN
442 CONTINUE
456 NCJ=0
      IF (VC(LVC)) 458,458,459
458 NCJ=1
      NVCNX=0
      IF (VC(LVC)+0.375) 475,476,476
475 NVCNX=1
476 WRITE (3,1443) MLE,CC,CGES,CDIF,CLOS2,DELT
      IF (SCC) 480,480,481
480 B?DR=CC1
      GO TO 482
481 B2DR=CC1-SCC
482 WRITE (3,1430) VC(LVC)
489 VDRUP(NIX)=-EY(NIX)+VE(NIX)+CJV(NIX)+VC(NIX)
      WRITE (3,1320) CC1,CC2,CC,VDRUP(NIX)
      IF (NSE) 490,490,491
490 QD=CCCJ+CCEM+CAJ+CDQB+COMR2
      GO TO 492
491 QD=CCCJ+CCEM+CAJ+CDQB+ORC+COMB2
492 TRC=DPC
      WRITE (3,1440) CCCJ,CCFM,CAJ,CDQB,ORC
      WRITE (3,1441) COMB2,QD,B?DR
1350 FORMAT (' ',3D15.8)
1320 FORMAT (' ',5H CC1=,E14.6,5H CC2=,E14.6,4H CC=,E14.6,
122H AN-TQ-CATH VOLT DROP=,E14.6)
1337 FORMAT (' ',6E15.8)
1430 FORMAT (' ', ' VC(NIX) IS NEGATIVE ',D15.8)
1338 FORMAT (' ',14,2E15.8)
1440 FORMAT (' ',6H CCCJ=,D14.6,6H CCEM=,D14.6,5H CAJ=,D14.6,5H CDQB=,D
114.6,5H ORC=,D14.6)

```

```

1441 FORMAT (' ', ' BASE 2 RECDMP=' ,E14.6, ' BASE 2 DRIVE NEEDED=' ,D15.8,
1' SUPPLIED=' ,F15.8)
1442 FORMAT (' ', ' SF MLE=' ,I3, ' SF14.7)
1444 FORMAT (' ', ' MM=' ,I3, ' RUNT=' ,D14.7, ' CLE1=' ,D23.16, ' DRC=' ,
1D73.16, ' DELL=' ,D73.16, /, ' CJV(1)' ,U73.16)
RETURN
END
SUBROUTINE ITER2(IT2)
DIMENSION IB2(20,20),LCC1(20),LCC2(20),LRR1(20),LRR2(20)
DIMENSION A11(20),C11(20),SCJL(20,20),SCJT(20,20)
DOUBLE PRECISION EIC(20),CCC(20),VE(20),VT(20),VC(20),VCT(20),
1TFMP(20),EJC(20),AJ(20),CJV(20),CJVT(20),CJC(20),CJC2(20),
2TEFF(20),TDN(20),TDP(20),BULK1(20),BULK2(20),B1CH,B2CH,DUMY
COMMON EIC,CCC,VE,VT,VC,VCT,TEMP,EJC,AJ,CJV,CJVT,CJC,CJC2,TEFF,
1TDN,TDP,BULK1,BULK2,B1CH,B2CH,DUMY,DNEW(20,20),UPEW(20,20),
2EY1J(20,20)
COMMON G(20),A1(20),H1(20),C1(20),TN1(20),TP2(20),
1A(20),B(20),C(20),RM(20),BM1(20),H(20),R(20),Z(20),EX(20),EY(20),
2RB(20),RP(20),B2N(20),B1P(20),PC(17),PIC(12),
3TM(12),RHO2(20),CCJ(20),CEP(20),CEM1(20),VDROP(20),
4BN(20),B1W,B2W,EL,D,XXN,YN1,YN2,DIFN,DIFP,S,TAU,TAUP,UN,UP,CLOS?
COMMON FREAL,CJM1,CJM2,CJM3,CM1,CM3,AR1,AR2,CC,CC1,CC2,CCDR,REX,
1QU,CLOS,TRC,t,B1,FB2,DT,DT2,TIME,TIM2,RTIME,CDLD,CINC,DDN1,DDP?,
2ALPH,CLN,DLP,FE,E2EF,RHO,RH2,EIEF,E2W,E1W,CFTR,CFT2,CKON,TMAX,
3TMAX2,CP2,CPP,VNIX,TGATE,EXM,EYM,REM,MFM1,QQQQ,RRR,RRR2,t,P,E?N,
4E2P,E1N,XI,Y1I,Y2I,AL,RB1,RTR,CC10,CGES,B1CPP,B2CPP,CZEM,CZEM1
COMMON IN,JM1,JM2,IMI2,JMI2,IS,JM2T,JMT,NTM2,NNN,KN,KKN,NIX,
INSE,NCT2,NCJ,NVCNX,IVK,MAX,IC,JC,IC2,JC2,JJE2,MPC,NTH,NDIT,NUUT?,
2NSTP,NT,NOFF,NSTT,MMAX,LVC,MFIRS,NIT1,NIT2,NCLDS,MCLOS,NRUN,NRUN?,
3NBZ
IF (NIT2) 600,600,605
600) NIT2=1
READ (1,1308) ((IB2(I,J),I=1,IM),J=1,JM2)
WRITE (3,1309) ((IB2(I,J),I=1,IM),J=1,JM2)
READ (1,1310) (LCC1(J),LCC2(J),J=JM12,JM2)
WRITE (3,1311) (LCC1(J),LCC2(J),J=JM12,JM2)
READ (1,1310) (LRR1(I),LRR2(I),I=IMI2,IM)
WRITE (3,1311) (LRR1(I),LRR2(I),I=IMI2,IM)
DX=1.0/XXN
DY2=B2W/EL/YN2
AMB1=EL*EL/TP2(NIX)/DIFP
AMB2=UP*EL/DIFP
QQ=.5*DY2
QQ1=.5*DX
XAM2=QQ1*AMB2
YAM2=QQ*AMB2
XAM4=.05*XAM2
YAM4=.05*YAM2
S21=QQ1*S/DIFP
S22=S21
S23=QQ*S/DIFP
S24=S23
TS23=2.0*S23
YUX2=QQ/DX
XOY2=QQ1/DY2
YOX2=2.0*YOX2
TXOY2=2.0*XOY2
FOX2=4.0*YOX2
FXOY2=4.0*XOY2
QA=QQ1*QQ
HA=2.0*QA

```

```

      TA=2.0*HA
      EN1=AMB1*QA
      EN2=AMB1*HA
      EN3=AMB1*TA
      AT=0IFN/DIFP
605  UTI2=1.0/DT2
      AT1=AT*DTI2
      FM1=AT1*QA
      EM2=AT1*HA
      EM3=AT1*TA
      IT2=IT2+1
      WRITE (3,1335) IT2
      DCP2=DPFH(C2,JC2)
      DO 607 I=1,IM
      Q01=0.0
606  DO 606 J=2,JM2
      Q01=Q01-DPEW(I,J)
607  BULK2(I)=Q01
      IMM=IM-1
      DO 611 I=2,IMM
611  A1(I)=(EX(I-1)+EX(I))*YAM4
      C1(I)=(EX(I)+EX(I+1))*YAM4
      DO 615 J=2,JM2
      DC 614 I=2,IMM
      SCJL(I,J)=(FYIJ(I,J)+FYIJ(I,J-1))*XAM4
614  SCJT(I,J)=(EYIJ(I,J)+EYIJ(I,J+1))*XAM4
615  CONTINUE
      C  BEGIN Y ITERATION AT LEFT MOST COLUMN
610  DO 660 I=IMI2,IM
      L3=LRR1(I)
      L4=LRR2(I)
      IL=I-1
      IT=I+1
      C  INITIALIZE AND CALC COEFF FOR COLUMN I
      DO 650 J=L3,L4
      JL=J-1
      JT=J+1
      A1(J)=0.0
      B*1(J)=0.0
      C1(J)=0.0
      H(J)=0.0
      IBB2=IBB2(I,J)
      GO TO (701,701,701,704,704,704,710,710,710,710,710),IBB2
701  Q01=TYCX2-C1(I)
      A1(J)=0.5*SCJL(I,J)+X0Y2
      C1(J)=-0.5*SCJT(I,J)+X0Y2
      Q04=(SCJT(I,J)-SCJL(I,J))*0.5+TYOX2+TS73-FM2
      BM1(J)=(EX(IT)-EX(IL))*YAM4+TXCY2+EM2+EN2
      H(J)=-Q04*DPEW(I,J)+Q01*DPEW(IT,J)
622  IF(1BB2-2) 650,622,624
      H(J)=C1(J)*DPCW(IT,JT)+H(J)
      GO TO 650
624  H(J)=A1(J)*DPEW(I,JL)+H(J)
      GO TO 650
704  Q01=TYOX2+A1(I)
      A1(J)=0.5*SCJL(I,J)+X0Y2
      C1(J)=-0.5*SCJT(I,J)+X0Y2
      Q04=(SCJT(I,J)-SCJL(I,J))*0.5+TYOX2+TS73-FM2
      BM1(J)=(EX(IT)-EX(IL))*YAM4+TXCY2+EM2+EN2
      H(J)=Q01*DPEW(IL,J)-Q04*DPEW(I,J)
      IF(1BB2-5) 650,627,626

```

```

627 H(J)=C1(J)*DPEW(I,JT)+H(J)
GO TO 650
628 H(J)=A1(J)*DPEW(I,JL)+H(J)
GO TO 650
710 QQ1=TYOX2-C11(I)
GJ2=TYOX2+A11(I)
A1(J)=SCJL(I,J)+TXCY2
C1(J)=-SCJT(I,J)+TXCY2
QQ5=SCJT(I,J)-SCJL(I,J)+FYOX2-EM3
HM1(J)=C11(I)-A11(I)+FXOY2+EM2+EM3
H(J)=QQ2*DPEW(IL,J)-QQ5*DPEW(I,J)+QQ1*DPEW(IT,J)
IF (IBB2-8) 650,635,632
632 IF (IBB2-10) 633,650,635
633 H(J)=A1(J)*DPEW(I,JL)+H(J)
GO TO 650
635 H(J)=C1(J)*DPEW(I,JT)+H(J)
CONTINUE
K1=L3+1
QQ=1.0/BM1(L3)
R(L3)=C1(L3)*QQ
QQ2=0.0
Z(L3)=QQ*H(L3)
DO 651 K=K1,L4
QQ=1.0/(-R(K-1))*A1(K)+BM1(K)
R(K)=C1(K)*QQ
QQ2=A1(K)*QQ
651 Z(K)=QQ*H(K)+QQ2*Z(K-1)
DPEW(I,L4)=Z(L4)
JJJ=L4-1
DO 657 JJ=L3,JJJ
J=JJJ+L3-JJ
657 DPEW(I,J)=R(J)*DPEW(I,J+1)+Z(J)
660 CONTINUE
C END OF Y ITERATION FOR BASE 2
C START OF X ITERATION FOR BASE 2
DO 690 J=JMI2,JM2
L1=LCC1(J)
L2=LCC2(J)
JL=J-1
JT=J+1
C INITIALIZE AND CALC COEFF FOR ROW J
DO 675 I=L1,L2
IL=I-1
IT=I+1
A(I)=0.0
B(I)=0.0
C(I)=0.0
H(I)=0.0
IBB2=IB2(I,J)
GO TO (801,801,801,804,804,804,810,810,810,810,810),IBB2
801 C(I)=TYOX2-C11(I)
QQ2=SCJL(I,J)*0.5+XOY2
QQ3=-SCJT(I,J)*0.5+XOY2
B(I)=(SCJT(I,J)-SCJL(I,J))*0.5+TYOX2+TS23+EM2+EM2
QQ4=(EX(IT)-EX(IL))*YAM4+TXCY2-EM2
GO TO 805
804 A(I)=TYOX2+A11(I)
QQ2=SCJL(I,J)*0.5+XOY2
QQ3=-SCJT(I,J)*0.5+XOY2
B(I)=(SCJT(I,J)-SCJL(I,J))*0.5+TYOX2+TS23+EM2+EM2
QQ4=(EX(I)-EX(IL))*YAM4+TXCY2-EM2

```

```

875 H(I)=CQ2*DPEW(I,JL)-QO4*DPEW(I,J)+QO3*DPEW(I,JT)
GO TO 675
870 A(I)=TYOIX2+A11(I)
C(I)=TYOIX2-C11(I)
QQ3=TXOY2+SCJL(I,J)
QQ4=TXOY2-SCJT(I,J)
B(I)=SCJT(I,J)-SCJL(I,J)+FYOX2+EM3+FN3
QQ5=C11(I)-A11(I)+FXUY2-EM3
671 H(I)=QQ3*DPEW(I,JL)-QQ5*DPEW(I,J)+QQ4*DPEW(I,JT)
IF(18B2-R) 67L,670,675
670 H(I)=C(I)*DPEW(I,J)+H(I)
675 CONTINUE
K?=L1+1
QJ=1.0/H(L1)
R(L1)=C(L1)*QJ
QQ2=0.0
Z(L1)=CQ*H(L1)
DO 674 K=K2,L2
QQ=1.0/(-R(K-1)*A(K)+B(K))
R(K)=C(K)*QQ
QJ2=A(K)*QQ
676 Z(K)=QJ2*H(K)+CC2*Z(K-1)
DPEW(L2,J)=Z(L2)
I1=L2-1
DO 683 I=L1,I11
I=I1+L1-I1
683 DPEW(I,J)=R(I)*DPEW(I+1,J)+Z(I)
IF (NCUT2-NRUN2) 466,466,690
C OUTPUT CTR JCT UPFW VALUES
466 IF(J-?) 672,672,674
672 JJ=1
WRITE (3,1336) JJ,(DPEW(I,1),I=1,IM)
674 WRITE (3,1336) J,(DPEW(I,J),I=1,IM)
C OUTPUT N2P2 OR SHORTING CONTACT DPEW VALUES
682 IF (J-JM2) 690,692,692
692 WRITE (3,1336) JM2T,(DPEW(I,JM2T),I=1,IM)
690 CONTINUE
C END OF X ITERATION FOR BASE 2
DO 1001 I=1,IM
QQ1=0.0
DO 1000 J=2,JM2
1000 QQ1=DPEW(I,J)+QQ1
1001 BULK2(I)=BULK2(I)+QQ1
IF (NCJ) 1203,1203,1195
1203 CSFS=CC
C CALC AND PUNCH TOTAL TIME AND ITERATIONS IN BASE 2
1195 TIM2=TIM2+2.0*CT2
RTIM2=FREAL*TIM2
WRITE (3,1341) DT2,TIM2,RTIM2
1308 FORMAT (10I3)
1309 FORMAT (' ',10I3)
1310 FORMAT (2I3)
1311 FORMAT (' ',2I3)
1335 FORMAT (' ',21+BASE 2 ITERATION NO ,I:)
1336 FORMAT (' ',I3/(' ',5F14.6))
1341 FORMAT (' ',5H DT2=,E14.6,13H TOTAL TIME=,E14.6,17H TOTAL REAL TI
ME=,E15.8)
KFTURN
END
SUBROUTINE TCCALC(NTIME)
DUPLFC PRECISION F1C(20),CCC(20),VE(20),VT(20),VC(20),VCT(20),

```

```

1TFM(20),EJC(20),AJ(20),CJV(20),CJVT(20),CJC(20),CJC2(20),
2TEFF(20),TDN(20),TDP(20),BULK1(20),BULK2(20),B1CH,B2CH,PHMY
3COMMON FIC,CCC,VE,VT,VC,VCT,TFMP,EJC,AJ,CJV,CJVT,CJC,CJC2,TEFF,
1TDN,TDP,BULK1,BULK2,B1CH,B2CH,DUMPY,UNEW(20,20),DPEW(20,20),
2EY1J(20,20)
3COMMON G(20),A1(20),R1(20),C1(20),TN1(20),TP2(20),
1A(20),B(20),C(20),B4(20),B41(20),H(20),R(20),Z(20),FX(20),EY(20),
2RH(20),BP(20),R/N(20),R1P(20),PC(12),PIC(12),
3TM(12),RHU2(20),CCJ(20),CEM(20),CEM1(20),VDRDP(20),
4HN(20),H1W,B2W,FL,E,XN,YN1,YN2,DIFN,DIFP,S,TAU,TAUP,UN,UP,CLOS?
5COMMON FREAL,CJM1,CJM2,CJM3,CM1,CM3,AR1,AR2,CC,CC1,CC2,CCDR,REX,
1JU,CLGS,TRC,E,RI,FB2,OT,OT2,TIME,TIM?,RTIME,CULO,CINC,DDN1,DDP2,
2ALPH,CLN,DLP,EF,E2EF,RHO,RM2,FIEF,E2W,F1W,CFTR,CFT?,CKDN,THAX,
3TMAX2,CP2,CPP,VNIX,TGATE,EXM,EYM,RFM,REM1,QQQU,RRR,RRR2,EP,E2N,
4E2P,E1N,X1,Y1I,Y2I,AL,RB1,RTR,CC1C,CGFS,BICPP,B2CPP,CZER1,CZER?
5COMMON IM,JM1,JM2,IM12,JM12,IS,JM2T,JMT,NTM2,NNN,KK,KKM,VIX,
1NSE,NC T2,NGJ,NVCNX,IVK,MAX,IC,JC,IC2,JC2,JJE2,MPC,NTM,NUMT,NOU T?,
2NSTP,NT,NOFF,NSTT,MAX,LVC,MFIRS,NIT1,NIT2,NCLCS,PCLCS,NRUN,NPUN?,
3N82
4NTIME=0
5TINC=DT
6TTT=TMAX
7TJLD=CCN1
8TNEW=DNEW(IC,JC)
9FIP=(DNEW(IC,1)-DNEW(IC,JMT))/YNI*DNEW(IC,JMT)
1400 IF (TJLD) 1501,1501,1405
1405 POF=TNEW/FIP
PI=ABS((TOLD-TNEW)/TNEW)
DU 1493 LH1=1,MPC
IF (PI-PIC(LH1)) 1493,1493,1494
1493 CONTINUE
LH1=MPC
1494 TINC=TM(LH1)*TTT
1500 WRITE (3,1642) FIP,POF,PI,TINC
1501 IF (NTIME) 1505,1505,1510
1505 DT=TINC
NTIME=1
TINC=DT2
TTT=TMAX2
TOLD=CCP?
TNEW=DPEW(IC2,JC2)
QJ=(DPEW(IC2,JM2T)-DPEW(IC2,1))/YN2
FIP=DPEW(IC2,1)+QJ-FB2*EY1J(IC2,JM2T)*DPEW(IC2,JM2T)/CJM?
GO TO 1400
1510 DT2=TINC
IF (DT-DT2) 1511,1512,1513
1511 TNTM=DT2/DT+1.0E-02
NTM2=1
NTM=INT(TNTM)
DT2=NTM*DT
GO TO 1516
1512 NTM=1
NTM2=1
GO TO 1516
1513 TNTM2=DT/DT2+1.0E-02
NTM=1
NTM2=INT(TNTM2)
DT=NTM2*DT2
1516 WRITE (3,1650) NTM,NTM2,DT,DT2
1642 FORMAT (' ',FIP='E14.6,' POF='E14.6,' PI='E14.6,' TINC='
E14.6)

```



```
1 10 10 10 10 10 10 10 10 4
1 10 10 10 10 10 10 10 10 4
1 10 10 10 10 10 10 10 10 4
1 10 10 10 10 10 10 10 10 4
1 10 10 10 10 10 10 10 10 4
1 10 10 10 10 10 10 10 10 4
1 10 10 10 10 10 10 10 10 4
2 11 11 11 11 11 11 11 11 5
1 10
1 10
1 10
1 10
1 10
1 10
1 10
1 10
1 10
2 9
2 9
2 9
2 9
2 9
2 9
2 9
2 9
2 9
2 9
2 9
2 9
```

END OF INPUT DATA SENSED

6

8

9

8

3

